Fall 2020

Effects of Biomass Loss on the Seasonal Variability in Storage Compounds of Pterygophora Californica

Lindsay M. Cooper

EFFECTS OF BIOMASS LOSS ON THE SEASONAL VARIABILITY IN STORAGE COMPOUNDS OF *PTERYGOPHORA CALIFORNICA*

A Thesis

Presented to the

Faculty of

Moss Landing Marine Laboratories

California State University Monterey Bay

In Partial Fulfillment

of the Requirements for the Degree

Master of Science

in

Marine Science

---

by

Lindsay M. Cooper

Fall 2020

CALIFORNIA STATE UNIVERSITY MONTEREY BAY

The Undersigned Faculty Committee Approves the

Thesis of Lindsay M. Cooper:

EFFECTS OF BIOMASS LOSS ON THE SEASONAL VARIABILITY IN STORAGE COMPOUNDS OF *PTERYGOPHORA CALIFORNICA*

DocuSigned by:
Michael Graham
0AB8FF88D2BC44E...

Michael H. Graham, Chair
Moss Landing Marine Laboratories

DocuSigned by:
Kenneth Coale
0E3F356D708F4AC...

Kenneth Coale
Moss Landing Marine Laboratories

DocuSigned by:
G Jason Smith
CF80BE567786443...

G. Jason Smith
Moss Landing Marine Laboratories

Daniel Shapiro, Interim Dean
Associate VP for Academic Programs and Dean of Undergraduate and Graduate Studies

Dec. 10, 2020
Approval Date

ABSTRACT

Effects of biomass loss on the seasonal variability in storage compounds of *Pterygophora californica*

by
Lindsay M. Cooper
Master of Science in Marine Science
California State University Monterey Bay, 2020

The stalked kelp, *Pterygophora californica*, is an important secondary canopy-forming species of coastal kelp forests from Alaska to Baja. It has long been thought that due to its long-lived, perennial thallus structures, seasonal growth and reproduction, and compound translocation capabilities, *Pterygophora* creates nutrient reserves. However, many aspects of *Pterygophora* have been understudied, including this theorized storage mechanism. This study addressed its storage capabilities by identifying nutrient compartmentalization, monitoring thalli over time, and examining allocation through biomass removals. Compartmentalization was observed among thallus regions of control thalli. All regions of the stipe and the reproductive sori had a higher mean %C than the holdfast, sporophyll, and vegetative blade regions. Isotopic fractionation illustrated that on average, the vegetative blade and sporophylls were more enriched in ^{13}C than the lower stipe, potentially suggesting that the high bulk carbon in the stipe is a reserve that allocates carbohydrates to the blades. However, carbon fractionation due to photosynthesis and respiration was not measured, and therefore it is unknown how much impact those processes have on the ^{13}C enrichment among thallus regions. A pattern of decreasing mean %N was seen from the base to top of the thallus. The holdfast region on average was the region of highest %N, and lowest C:N. A pattern of increasing C:N was seen from the base to the top of the stipe, and the ratio in the sporophylls was more similar to the lower and mid stipe regions than to the other blade tissues. Seasonality of nutrient compartmentalization in the thallus was not seen, meaning time had no effect on the chemical distribution among thallus regions ("compartments"). However, some seasonal variability of chemicals was observed for the thallus as a whole and within thallus regions individually. The only thallus regions that were significantly affected by blade manipulations were the lower, mid, and upper stipe. Changes within these regions were significantly impacted by the removal of sporophylls. Overall, the evident patterns in this study have uncovered a consistent nitrogen reserve in the holdfast, carbon reserve in the stipe, and allocation of carbon to the blades.

TABLE OF CONTENTS

LIST OF FIGURES

LIST OF TABLES

ACKNOWLEDGEMENTS

This work was made possible by funding from MLML Wave Awards, The Bill Watson Memorial Scholarship, The Dr. Earl H. Myers & Ethel M. Myers Oceanographic & Marine Biology Trust, The Signe Lundstrum Memorial Scholarship, The MLML Quilt Guild Scholarship, The Simpkins Fund, The Undergraduate Research Opportunities Center (UROC) at CSU Monterey Bay, and The CSU Council on Ocean Affairs, Science, & Technology (COAST) at CSU Monterey Bay.

First, I would like to thank my thesis committee members Dr. Michael Graham, Dr. Kenneth Coale, and Dr. G. Jason Smith for their invaluable feedback and support while navigating through the program. I was truly fortunate to have such an incredible team of scientists in my corner. I need to give special thanks to Mike Graham for accepting me into his lab, although having little research experience, and constantly challenging me to grow as a scientist. I'm so grateful for the tightly knit family environment that Mike fosters in the Phycology Lab. Over the course of this program, I have felt constantly supported by my lab mates, and they have become some of my closest friends. The BEERPIGs (Benthic Ecology Experimental Research Phycology in General) group has been trained to critically analyze each other's work and to always help a lab member during a time of need. These core values that Mike instilled in us were a huge factor in the completion and success of my study. BEERPIGs for life!!!

Thank you to all of the other members of the MLML community that made my project possible: John Douglas & Brian Ackerman (Marine Operations), Diana Steller (Dive Safety Officer), Kris Machado, James Cochran, Gary Adams, & Billy Cochran (MLML Facilities), Jocelyn Douglas (Environmental Health & Safety Officer), Terra

Eggink (Graduate Program Coordinator), Kathleen Donahue (Assistant to the Director), Katie Lage (Research Librarian), Rhett Frantz & staff (IT). I cannot give enough thanks to my interns Marina Hernandez, Silvia Vasquez, and Natasha Craft who made processing all of my samples possible! Thank you to the rest of the students who helped me while SCUBA diving and processing samples at the lab! These amazing people are why I was able to do the study that I did.

A very special thanks to some of my most loyal, amazing, badass friends Steven Cunningham, Stephan Bitterwolf, Mo Wise, Sarah Jeffries, Cody Dawson, Amber Reichert, Melinda Wheelock, Mina Sattari, & Dan Gossard who were such an amazing support system and always willing to help when I needed them. Moss Landing Marine Labs is a very special place that brings together very special people. I will never forget it for the rest of my life.

Finally, thank you to my family who have proudly supported me throughout my entire academic career. Their unconditional love and support have been a steadfast force throughout my long journey.

INTRODUCTION

Global climate change affects a broad range of organisms with diverse geographical distributions (Hughes 2000; Wuethrich 2000; McCarty 2001; Ottersen 2001; Walther et al. 2002). Due to the complexities of ecosystems, responses to climate change are conveyed through various functional groups. At the organismal level, these responses can be expressed in phenology, physiology, range, and distribution of species (Parmesan et al. 1999; Bairlein & Winkel 2001; Menzel & Estrella 2001). At the habitat level, responses can be expressed in the community composition and interactions, and the structure and dynamics of ecosystems (McCarty 2001, Walther et al. 2002). Tracking the timing of seasonal activities of organisms is a simple and effective way to observe ecological changes in response to climate change (Bairlein & Winkel 2001; Menzel & Estrella 2001). In terrestrial habitats, many studies have shown phenological responses in migratory birds, amphibians, reptiles, insects, and flowering plants (Gatter 1992; Janzen 1994; Parmesan et al. 1999; Sparks et al. 1999; Menzel & Estrella 2001; Menzel et al. 2001). The timing of responses in different species is not always synchronous & can have great consequences (Walther et al. 2002). For example, earlier leaf unfolding in plants can lead to an extended growing season, but also a higher risk of being damaged by a late frost (Walther et al. 2002).

Climate change has overwhelming implications for marine ecosystems. Due to their substantial global importance, an immense amount of research has focused on coastal marine environments and the past, current, and future impacts of climate change (Fields et al. 1993; Lubchenco et al. 1993; Markham 1996; Costanza et al. 1997; Halpin 1997; Harley et al. 2006; Costanza et al. 2014). Changes in global climate have been impacting the marine environment through increasing ocean temperatures, changing ocean chemistry, sea level rise, changing of atmospheric circulation and winds, increasing frequency of storms, and numerous other phenomena (IPCC 2001; Bromirski et al. 2003).

The direct impacts of climate change on an organism's life history can be exhibited physiologically, morphologically, and behaviorally (Andrewartha & Birch 1954; Hughes

2000; Harley et al. 2006). Historically, most marine climate research has focused on increasing temperature as a prominent factor driving future ecological change (Wieser 1973; Woodward 1987; Fields et al. 1993; Lubchenco et al. 1993; Wood & McDonald 1996). Rising ocean temperatures can cause many physiological problems for marine life including protein damage, affecting the fluidity of membranes, and decreasing organ functions (Hochachka & Somero 2002). Many marine organisms already live near their thermal tolerances and will be negatively affected by increases in temperature (Somero 2002; Hughes et al. 2003). A conspicuous example is the bleaching and subsequent mortality of reef-building corals (Hughes et al. 2003; McWilliams et al. 2005).

Increases in dissolved carbon dioxide changes the chemistry of the ocean, which may be more important than changes in ocean temperature for the performance and survival of many organisms (Harley et al. 2006). Although many marine organisms have adapted to temperature fluctuations over the last several million years, predicted changes in pH are higher than any suggested by the last 300 million years of the fossil record (Caldeira & Wickett 2003; Feely et al. 2004). Processes and actions that are commonly affected by increasing CO_2 levels are calcification, respiration, swimming abilities, predator evasion, larval development, photosynthesis, growth, and tissue composition (Hughes 2000). While increasing CO_2 may have positive impacts on photosynthesis in terrestrial plants, most marine algae will not experience enhanced growth. Studies of reef-building corals and calcifying algae such as coralline algae and coccolithophorids have shown that these organisms will be negatively affected by increased levels of CO_2 (Gattuso et al. 1999; Marubini & Thake 1999; Langdon et al. 2000; Leclercq et al. 2000; Riebesell et al. 2000). Due to the widespread collective distribution of these marine organisms, rising CO_2 levels will have drastic biogeochemical and ecological impacts on the global oceans (Gattuso & Buddemeier 2000).

Many physical factors important to marine communities are related to water motion, and one particular stressor predicted to increase with climate change is wave stress (Dayton 1985; Carter & Draper 1988; Bacon & Carter 1991; Elsner et al. 2008; Woolf & Wolf 2013). Physical disturbance from hydrodynamic forces has been found to be instrumental in structuring many subtidal communities (Sousa 1985; 2001; Seymour et al. 1989). Water motion can influence processes such as the feeding rates of herbivores,

movement of sediment, algal propagule dispersal & settlement, nutrient availability & uptake, and intertidal & subtidal zonation of macroalgae and invertebrates (Stephenson & Stephenson 1949; Koehl 1977; 1984; 1986; Denny et al. 1985; Foster & Schiel 1985; Denny 1988; Hurd 2000). Common effects of wave-imposed forces on various species include loss of tissue biomass, weakening of structural integrity, dislodgement, change of shape, and mechanical limitations on size (Dayton 1971; Denny 1985; Denny et al. 1985; Gaylord et al. 1994).

Some marine organisms are more/less able to regulate their physiology than others in order to tolerate environmental changes. Seaweeds (macroalgae) are a specious group of organisms that span the globe as sources of primary production and habitat (Mann 1973; Newell 1984; Dayton 1985). They can be very plastic in their morphology and reproductive adaptations, making them highly adept at surviving changes in their environments (Neushul 1972). The flexibility of algal fronds in both intertidal and subtidal species allows them to contend with hydrodynamic forces in wave-swept coastal environments (Denny & Gaylord 2002). Frond flexibility is influenced by both the shape of the frond and the properties of its materials (Denny & Gaylord 2002). Although many nearshore species may not appear incredibly streamlined, many can reorient their fronds in response to water flow, resulting in an effective streamlined shape. (Koehl 1984; 1986; Koehl & Alberte 1988; Carrington 1990). By utilizing this strategy of flexibility and structural fluidity, coastal algae as a group have managed to withstand the effects of applied forces (Gaylord et al. 1994).

A conspicuous and unique group of coastal seaweeds are the kelps (Laminariales). Kelps are brown macroalgae that grow intertidally and subtidally over a broad geographic range. Their thalli consist of a general pattern of holdfast, stipe, and blade structures. Kelp tissue differentiates internally as epidermis, cortex, and medulla, with the addition of modified medullary cells (Abbott & Hollenberg 1976). Using the specialized medullary tissue, kelps are able to translocate storage products using osmotic diffusion (Parker 1963; Chapman & Craigie 1978). Structures called sieve elements and trumpet hyphae, located in the medulla, allow the conduction of materials throughout the thallus (Schmitz & Srivastava 1976). Schmitz & Lobban (1976) observed translocation of

photoassimilates in 13 genera of the Laminariales; all genera exhibited long-distance transport of 14C-labeled products from their mature source tissue to meristematic sinks (haptera and intercalary growing regions). Kelps transport carbon as sugar compounds produced through photosynthesis, which are used for growth and structural rigidity. Excess sugars from photosynthesis are generally stored as the polysaccharide laminarin, before being converted to mannitol and transported to growth areas (Kremer 1981). Organic nitrogen makes up a large component of photosynthetic pigments, amino acids, and proteins needed for tissue growth (reviewed in Hurd et al. 2014).

It has long been thought that different structures on a kelp thallus perform different functions, such as photosynthesis and storage sinks (Black 1948; Black 1954; Chapman and Craigie 1978; Gagne et al. 1982). Previous study of storage mechanisms in *Macrocystis pyrifera* has shown that the direction of resource translocation relies on the proximity of the storage sink to the tissue acting as the source (Schmitz & Srivastava 1979). Fox (2013) designed his study to quantify the effect of biomass loss on resource translocation to the source region. He observed that for *Macrocystis,* the translocation of stored carbon is essential for productivity and recovery from disturbance. Patterns in $\delta^{13}C$ enrichment in sink versus source regions were found to be directly proportional to biomass loss, and significant connections were seen between the remaining biomass and the type of tissue (Fox 2013). Studies such as these can be used to describe the recovery potential of algal species after natural disturbances.

Storage in kelps is driven, in part, by seasonal variability in the surrounding environment. Early studies of seasonal effects on photosynthesis and respiration of marine algae reported that with increasing temperature, species were respiring more than they were photosynthesizing (Kniep 1914; Harder 1915; Ehrke 1931). This was reflected in higher respiration during summer, with no acquisition of resource surplus, and highest net gain from photosynthesis in the winter and early spring. However, later studies that conducted longer-term measurements of photosynthesis and respiration saw the effects of seasonal adaptations in an assortment of perennial species (Lampe 1935; Montfort 1935). Species were observed producing their highest net gain from photosynthesis during the summer due to stronger underwater irradiances (Lampe 1935; Montfort 1935; Kanwisher

1966). In addition, respiration rates during the summer were only slightly higher than those measured in winter, and therefore were not depleting the resources accumulated during that time. Seasonal fluctuations of growth have been observed in kelp species of the genus *Laminaria* (Parke 1948; Lüning 1971; Mann 1972; Chapman & Craigie 1977). In *Laminaria saccharina*, considerable variation in growth rate of the blade and stipe occurs during different times of year (Parke 1948). Chapman & Craigie (1977; 1978) associated seasonal growth in *Laminaria longicruris* with nutrient availability in seawater and the utilization of carbohydrate and nitrogen reserves. Studies demonstrating a free-running circannual growth rhythm in *Pterygophora californica* and *Laminaria* spp. have contested the conventional ideas that seasonal nitrogen availability directly controls kelp tissue growth (Lüning 1991; tom Dieck 1991; Lüning & Kadel 1993; Schaffelke & Lüning 1994). Many growth and seasonality studies have been conducted for various species of *Laminaria*, however, far less is known about the storage mechanisms of the lone member of the genus *Pterygophora* (Alariaceae).

The subtidal understory kelp, *Pterygophora californica*, is a prime subject for studying storage mechanisms and physiological response due to its long-lived, slow growing perennial thallus, seasonal vegetative tissue, and seasonal reproductive cycle (McKay 1933). It commonly grows in dense, single-species stands, averaging 7 adult thalli per m^2 throughout its range in the northeast Pacific (Dayton et al. 1984; Reed & Foster 1984; De Wreede 1984; 1986; Hymanson et al. 1990; Reed 1990). As a stipitate understory algal species, *Pterygophora* creates a 3-dimensional secondary canopy habitat above the benthos, providing shelter and food for many mobile and sessile invertebrates, fishes, and algal communities (reviewed by Dayton 1985).

Algal species in the understory canopy guild are more adapted to tolerate wave stress than those making up the taller canopy guilds (Dayton et al. 1984). They can exhibit morphology and physiology to help alleviate this stress in several ways including allometric growth patterns and frond flexibility (Gaylord & Denny 1997). Generally speaking, algal blades and stipes are composed of materials that are low in stiffness, and high in extensibility (Koehl 1986; Denny et al. 1989; Hale 2001). Even understory species with erect ‘woody’ stipes, such as *Pterygophora*, are extremely flexible (Koehl

1984; Biedka et al. 1987; Denny et al. 1989). De Wreede et al. (1992) were able to bend intact *Pterygophora* stipes more than 360˚. However, algal materials have a low work of fracture (0.2–3 kJ m^{-2}) and some species may be compromised by very small wounds (Biedka et al. 1987; Denny et al. 1989; Hale 2001). Kelp thalli can obtain cuts and nicks from grazers and from scraping across rocks and large barnacles. Previous experiments have shown the ability of *Pterygophora* to heal wounds by regenerating small cells in the wound gap, and by radially growing larger existing stipe cells inward from the surface layer (De Wreede et al. 1992). Measurements revealed that their stipes healed rapidly, and therefore, deep cuts were merely present for a short period of time. The results seen by De Wreede et al. (1992) do not support the claim by Biedka et al. (1987), that a critical flaw length (CFL) of 0.2 mm is all it takes to compromise the integrity of a *Pterygophora* stipe. The former study saw no catastrophic failure of stipes subjected to cuts that were one-order of magnitude larger than the calculated CFL of the latter. Not only did they recover, but the stipes that had regenerated tissue to heal wounds were able to withstand increased mean forces applied to them during biomechanical tests.

Pterygophora also exhibits seasonal cycles of growth and reproduction (Frye 1918; DeWreede 1984; 1986; Dayton 1984; Lüning 1991). For almost two centuries, we have known of the existence of concentric growth rings in the stipe of this species (Ruprecht 1848). Studies have determined that they are formed during alternating periods of slow (darker tissue) and rapid (lighter tissue) growth associated with light, and that one light and one dark ring were each formed annually (MacMillan 1902; Frye 1918). Researchers are able to use information about the formation of these rings to study the age and structure of *Pterygophora* populations (DeWreede 1984; Hymanson et al. 1990). The growth of various species of marine algae is strongly influenced by the surrounding environment, and therefore expresses patterns of periodicity and seasonality (Kain 1971; Novaczek 1981). Populations of *Pterygophora* in British Columbia undergo their maximum stipe elongation from approximately February or March to June, and have minimal elongation from approximately October to December or January (DeWreede 1984). Seasonal growth in *Pterygophora* has been popularly assumed to be driven by the ability to sustain resource reserves, however previous research has yet to confirm this idea. It is due to their long-lived nature and potential reserve capabilities that

Pterygophora thalli can afford to produce spores only during times most suitable for greatest reproductive success, as they are likely to persist to reproduce in subsequent years (Reed et al. 1996).

My study explores the mechanisms behind the seasonal variations in resource storage and the ability of *Pterygophora* to use this strategy to recover from biotic or abiotic disturbances in the subtidal environment. Through simulated physical disturbance, I will illustrate how this species copes with the stresses of increased hydrodynamic forces that will occur with climate change. More specifically, the questions I have addressed are: 1) Does *Pterygophora californica* exhibit within-thallus compartmentalization? 2) Does *P. californica* exhibit seasonal variability in compartmentalization of resources? 3) Does biomass loss impact the compartmentalization of resources in *P. californica*?

Since it has previously been demonstrated by Schmitz & Lobban (1976) that *Pterygophora* translocate carbon, I did not expect to see homogeneity within its thallus. For this reason, I investigated my first hypothesis that *Pterygophora californica* exhibit a physiological mechanism of compartmentalization by testing for a heterogeneous pattern of nutrients spatially throughout the thallus. The fact that specialized regions of the thallus perform growth, reproduction, photosynthesis, and transport also led me to believe that I would find a distinct difference in the mean values of %C, %N, $\delta^{13}C$, and C:N. My second hypothesis stems from the previous research documenting seasonal patterns of growth and reproduction in various kelps species. I was eager to see if *Pterygophora* would exhibit distinct seasonal variability in compartmentalization of internal resources. Black (1948; 1950a; b) observed variations in carbohydrate content of *Laminaria* spp. in relation to season, depth, current, and wave exposure. This study demonstrated that production of laminarin and mannitol, the two major storage products of kelps, reaches a crest during the summer and fall, with a following decline during the winter. This appears to be the universal trend in several species of brown algae (Craigie 1974). Because wave disturbance is a common and increasing stress to coastal inhabitants, I wanted to examine the effect that it can have on the physiology and recovery potential of one of the most interesting local kelps. Biomass removal can simulate degrees of stress applied to an individual, or in this case a population, inflicted by the natural environment. By

performing this experiment, I intended to build upon the fundamental concepts of this subtidal study, hypothesizing that biomass loss would affect the compartmentalization of resources in *Pterygophora*.

MATERIALS AND METHODS

Study Site

Research was conducted in Stillwater Cove, which is located in Carmel Bay along the central coast of California. The Cove opens to the southwest, and the local kelp forest is fairly protected from large swells by Cypress Point (Storlazzi & Field 2000). These large swells can be attributed to northwesterly winds in the spring and storms in the winter. The kelp forest grows on a hard, moderate-relief substratum of Carmelo Formation sandstone, conglomerate, and lava (Simpson 1972) with depth ranging to approximately 15 meters. Underneath the surface canopy comprised mainly of *Macrocystis pyrifera,* the understory is dominated by *Pterygophora californica* and *Stephanocystis osmundacea*. Stillwater Cove has been well described ecologically and oceanographically, and thus makes for a model location for this study (Reed & Foster 1984; Clark et al. 2004; Donnellan 2004). In addition, kelp tissue chemistry should be largely unaffected by the minimal input of terrestrial nutrients at this site (Carroll 2009).

Experimental Design

In June 2017, a 50-meter-long lead line was laid at approximately 8.5 meters depth and marked at both ends with a surface buoy. A PVC placard was attached to the lead line every 10 meters, marked with the numbers 1-4. The purpose of this was to break up the lead line into manageable sections for sampling purposes and to give divers a sense of direction if disoriented.

Whole *Pterygophora* were tagged as control or experimental thalli. Tags were constructed from DYMO embossing labels depicting the thallus manipulation treatment,

with a hole punched on each end of the label. A single large zip tie was threaded through both holes of the label and cinched down onto the base of the stipe. This design allowed the tags to lay relatively flat against the stipe instead of dangling free at one end. Control thalli were unmanipulated and experimental thalli were subjected to 3 different treatments: (1) removal of the vegetative blade above the meristem; (2) removal of all sporophylls; and (3) removal of both the vegetative blade above the meristem and all sporophylls (Figure 1). At the start of the experiment (time = 0), experimental thalli were manipulated, and a group of control thalli were harvested to represent the starting conditions of the *Pterygophora* population. Blade manipulations were maintained monthly for 15 months, and whole thalli were harvested every three months for 15 months.

In the lab, harvested thalli were cleaned of epiphytes and invertebrate inhabitants, and the following morphometric measurements were recorded for all harvested *Pterygophora* thalli:

- stipe length (cm)
- transition zone length (cm) – (region where the stipe, sporophylls, and base of vegetative blade all converge; this region is less pigmented than the rest of the surrounding tissue).
- vegetative blade length (cm)
- average length of sporophylls (cm) – (an average of the length of a basal, mid and upper sporophyll from each thallus)
- # sporophylls
- reproductivity (presence/absence of sori)
- stipe width at base (cm)
- stipe width at middle (cm)
- stipe width at upper (cm)
- total thallus wet weight
- holdfast wet weight (g)
- stipe wet weight (g)
- total sporophylls wet weight (g) – (combined wet weight of all sporophylls on the thallus)

- vegetative blade wet weight (g)
- control or manipulation treatment

Thalli were then cut into sections using an X-Acto knife, and 3-5 gram samples were taken from 7 different regions: holdfast, lower stipe, mid stipe, upper stipe, vegetative blade, sporophyll with no sorus, and soral tissue (if present) (Figure 2). The uppermost portion of the stipe was considered a "transition zone", due to the fact that it becomes flattened, much lighter in color, and is the area where sporophylls grow out laterally, and the vegetative blade grows apically. In this region, stipe and blades all converge. For this reason, "upper stipe" samples were not taken from this transition zone, but instead were taken from the area just below. Stipe samples were obtained by cross-sectioning through the stipe in order to sample all layers of tissue (epidermis, cortex, and medulla). These tissue samples were dried at 60 °C and ground into a fine powder using the combined efforts of a ball mill and a fabricated steel crushing device for harder pieces. In preparation for chemical analyses, the powdered tissue was weighed into 1-3 mg samples using a microbalance and placed in 5x9 mm tin capsules. A total of 357 individual samples were sent to the SIMS Light Stable Isotope Lab at UC Santa Cruz where they were analyzed for %C, $\delta^{13}C$, %N, $\delta^{15}N$, and C:N. Values of %C and %N were used to describe changes in bulk composition and areas of resource compartmentalization, whereas $\delta^{13}C$ and C:N were used to investigate physiological changes across tissue as a function of the allocation of internal resources. Results for $\delta^{15}N$ are reported in Appendix-A, as they were included with this stable isotope analysis and may be helpful for studies in the future but are not related to the specific hypotheses of this study.

Statistical Analysis

Population Morphometrics

Statistical analysis was performed on morphometric data as well as chemical data. Although morphology did not address hypotheses of this study, these data were used to compliment the data obtained through chemical analysis. Tissue samples from 79 randomly harvested thalli were used for the analyses of this study. For the first two sampling dates, 7/1/2017 and 10/9/2017, 6 thalli were harvested from each treatment. Over the course of the experiment it appeared I had been losing tagged thalli, either to mortality or loss of the tag. I wanted to make sure I had enough of each treatment for the duration of the experiment. For this reason, I reduced my collection size to 3 from each treatment for sampling dates 1/14/2018, 4/21/2018, 7/19/2018, and 11/8/2018. The whole sampled population consisted of 25 unmanipulated controls, 18 that had their vegetative blades removed, 18 that had their sporophylls removed, and 18 that had both their vegetative and sporophylls removed. The sample sizes were used for morphometric data, however, data were standardized to 3 thalli per sampling date, per treatment for analysis of chemical data. For the purpose of this study, any presence of reproductive tissue (sori) depicts the ability of unmanipulated or manipulated thalli to become fertile.

For unmanipulated control thalli, a Pearson's Chi-square (χ^2) test was used to look at the differences in the number of thalli that were reproductive over time. Seasonal changes in regional proportions of the total thallus biomass was analyzed using one-way Analyses of Variance (ANOVAs) and a Tukey HSD post hoc test. The relationships between the average total sporophyll biomass, average number of sporophylls, and average sporophyll length were analyzed with linear regressions, and the seasonal changes of these variables were analyzed with one-way ANOVAs and Tukey HSD post-hoc testing. The relationship between the average vegetative blade biomass and average vegetative blade length was analyzed with a linear regression, and the seasonal changes of these variables were analyzed with one-way ANOVAs and Tukey HSD post-hoc tests. The relationships between the average total sporophyll biomass vs. average vegetative blade biomass and average sporophyll length vs. average vegetative blade length were analyzed using linear regressions.

For manipulated experimental thalli, Pearson's Chi-square tests were used to look at the differences in the number of thalli that were reproductive over time. The

relationships between the average total sporophyll biomass, average number of sporophylls, and average sporophyll length for *Pterygophora* from the minus vegetative blade treatment were analyzed with linear regressions, and the seasonal changes of these variables were analyzed with one-way ANOVAs and Tukey HSD post-hoc testing. The effect of treatment and the interaction of sampling date*treatment on these samples were analyzed with two-way ANOVAs. The relationship between the average vegetative blade biomass and average vegetative blade length was analyzed with a linear regression, and the seasonal changes of these variables were analyzed with one-way ANOVAs. The effect of treatment and the interaction of sampling date*treatment were analyzed with two-way ANOVAs.

Hypothesis Testing

To test the hypothesis that natural populations of *Pterygophora californica* exhibit a physiological storage mechanism of compartmentalization, I tested only the data for the "control" individuals. One-way ANOVAs were used to test the effect of thallus region on the mean amounts of %C, $\delta^{13}C$, %N, $\delta^{15}N$, and C:N. Significant results would reveal different values of these constituents within various regions of the *Pterygophora* thallus, suggesting a mechanism of internal resource compartmentalization. All significant factors were followed by Tukey HSD post-hoc tests to examine the differences among thallus regions.

To test the hypothesis that *Pterygophora californica* exhibit seasonal variability in compartmentalization, I also used only the data for the "control" individuals. Two-way ANOVAs were used to determine if sampling date had an effect on the variability of thallus compartmentalization, and if sampling date and thallus region had an interacting effect on chemical constituents. The data for the "sorus" thallus region was excluded from these tests because it was not present for all sampling dates. All significant factors were followed by Tukey HSD post-hoc tests to examine the differences among each level of sampling date and thallus region. One-way ANOVAs were used to determine if sampling date had an effect on the variability of chemical constituents within each thallus

region individually. All significant factors were followed by a Student's t-test to examine the differences among all sampling dates for each thallus region.

To test the hypothesis that the storage mechanism of *Pterygophora californica* would be affected by biomass loss, I used data from all treatments: the unmanipulated control thalli and the manipulated experimental thalli. The data from 7/1/2017 was excluded from this test because only samples from the "control" treatment were harvested on this date as it was the start of the manipulations for all other treatments. Two-way ANOVAs were used to examine the effects of biomass loss on internal resources and their compartmentalization. All significant factors were followed by Tukey HSD post-hoc tests to examine the differences between each level of sampling date and treatment by thallus region.

RESULTS

Population Morphometrics

Control Thalli (unmanipulated)

Documenting characteristics of control thalli over the course of the study was important for making comparisons to the thalli that were manipulated across the same timeframe. All 6 thalli harvested on 7/1/2017 were controls because this sampling date marked the beginning of all manipulations for experimental treatments. Control thalli harvested on the first date are especially important because they served as the baseline for *Pterygophora* characteristics at the start of the experiment. Significant differences in fertility by sampling date were detected (χ^2 (5, N = 25) = 18.75, p = 0.0021, Figure 3). This clear seasonal pattern illustrates that thalli were partially reproductive (16.7%) during 7/1/2017 sampling, they were 100% reproductive from 10/9/2017 - 1/14/2018, fertility dropped to 0% by 4/21/2018, picked back up again (66.7%) on 7/19/2018, and finally were 100% reproductive on 11/8/2018 (Figure 3). This baseline fertility pattern

was useful in identifying how much of an effect reproduction may have on depleting resource reserves.

The sporophylls consistently made up the majority of the biomass of the thalli throughout the 15 months, followed by the stipe, the holdfast, and lastly the vegetative blade (Figure 4). The only structure for which the percent of the thallus significantly changed by date was that of the vegetative blade (ANOVA: $F_{5,19} = 4.0059$, $p = 0.0119$, Tukey HSD: $p < 0.05$, Table 1A, Figure 4). Both the number of sporophylls (Regression: $R^2 = 0.18$, $F_{1,21} = 4.8865$, $p = 0.0373$, Figure 5) and the average sporophyll length (Regression: $R^2 = 0.47$, $F_{1,21} = 20.4352$, $p = 0.0002$, Figure 5) had a significant positive relationship with the total sporophyll biomass of control thalli. Some seasonal fluctuations in the sporophylls can be seen, however, only the average number of sporophylls per thallus was significantly different based on sampling date (ANOVA: $F_{5,19} = 3.4303$, $p = 0.0224$, Tukey HSD: $p < 0.05$, Table 2A, Figure 6).

Vegetative blade biomass of control thalli had a significant positive relationship with vegetative blade length (Regression: $R^2 = 0.82$, $F_{1,23} = 102.3737$, $p < 0.0001$, Figure 7). Both the average vegetative blade length and average vegetative blade biomass were significantly different among sampling dates (ANOVA: $F_{5,19} = 13.5232$, $p < 0.0001$; $F_{5,19} = 10.3493$, $p < 0.0001$, Tukey HSD: $p < 0.05$, Table 3, Figure 8). Total sporophyll biomass had a significant positive relationship with vegetative blade biomass (Regression: $R^2 = 0.42$, $F_{1,23} = 16.4492$, $p = 0.0005$, Figure 9). Average sporophyll length did not have a significant relationship with vegetative blade length (Regression: $R^2 = 0.12$, $F_{1,23} = 3.1355$, $p = 0.0899$, Figure 10).

Experimental Thalli (manipulated)

Experimental thalli were manipulated with three treatments for 15 months: (1) removal of the vegetative blade above the meristem; (2) removal of all sporophylls; and (3) removal of both the vegetative blade above the meristem and all sporophylls (Figure 1), fundamentally altering the natural patterns of reproduction and blade tissue growth. No experimental thalli were harvested for the 7/1/2017 sampling date because this was

the time of initial manipulations at the start of the experiment, and we assume that controls harvested on this date were representative of the population at the start of the experiment because all thalli were randomly tagged. The first group of experimental thalli were harvested on 10/9/2017. All thalli harvested from the treatment where sporophylls were removed did not develop soral tissue on any sporophyll regrowth regardless of sampling date (Figure 11). Significant differences in fertility by sampling date were only detected for *Pterygophora* from the treatment where the vegetative blade was removed (χ^2 (4, N = 18) = 10.29, p = 0.0359, Figure 11). Like the control group, sampling dates 10/9/2017, 1/14/2018, and 11/8/2018 were 100% reproductive. With this manipulation, however, 33.33% were reproductive on 4/21/2018 and 7/19/2018 (Figure 11). Seasonal changes were seen in fertility of *Pterygophora* from the treatment where both sporophylls and vegetative blade were removed, however, these changes were not deemed significantly different by a Pearson Chi-square test (χ^2 (4, N = 18) = 4.50, p = 0.3425, Figure 11).

By simulating disturbance through biomass loss, I inherently changed the patterns of thallus structure proportions in manipulated thalli compared to the controls. Mirroring the controls, the thalli in the minus vegetative blade treatment showed that sporophylls consistently made up the majority of the biomass, followed by the stipe, the holdfast, and lastly the regrowth of vegetative blade tissue (Figure 12). Vegetative blade regrowth was seen in thalli harvested on 10/9/2017, 1/14/2018, and 11/8/2018. For thalli in the minus sporophylls treatment, the stipe was consistently the majority of the biomass, followed by the holdfast (Figure 12). Thalli harvested on 4/21/2018 exhibited sporophyll regrowth that equated to a higher percentage (5.4%) of the total biomass than the vegetative blade (0.9%) (Figure 12). Thalli harvested on 1/14/2018, 7/19/2018, and 11/8/2018 also exhibited sporophyll regrowth, but not enough to outweigh the average proportion of vegetative blade (Figure 12). For thalli in the minus both sporophylls and vegetative blade treatment, the stipe was consistently the majority of the biomass. The holdfast was the second largest percentage of the biomass for all sampling dates except for 11/8/2018 when the average sporophyll regrowth (15.3%) outweighed the average proportion of holdfast (14.9%) (Figure 12). Regrowth of sporophylls was observed on thalli harvested on 1/14/2018, 4/21/2018, 7/19/2018, and 11/8/2018 (Figure 12). Regrowth of the

vegetative blade was observed on thalli harvested on 7/19/2018 and 11/8/2018 (Figure 12).

The total sporophyll biomass of thalli from the minus vegetative blade treatment had no significant relationship with the number of sporophylls (Regression: $R^2 = 0.05$, $F_{1,15} = 0.7371$, $p = 0.4041$, Figure 13) or the average sporophyll length (Regression: $R^2 = 0.05$, $F_{1,16} = 0.7758$, $p = 0.3915$, Figure 13). Seasonal differences were found in the average number of sporophylls between *Pterygophora* in the minus vegetative blade treatment and those in the controls (ANOVA: $F_{4,26} = 5.2147$, $p = 0.0032$, Tukey HSD: $p < 0.05$, Table 4A, Figure 14). However, there was no difference in the average number of sporophylls by treatment between the controls and minus vegetative blade treatment (ANOVA: $F_{1,26} = 0.0136$, $p = 0.9079$, Table 4A). There was also no effect of the interaction of sampling date*treatment on the average number of sporophylls (ANOVA: $F_{4,26} = 0.5766$, $p = 0.6821$, Table 4A). Seasonal differences were found in the average sporophyll length between *Pterygophora* in the minus vegetative blade treatment and those in the controls (ANOVA: $F_{4,27} = 8.1939$, $p = 0.0002$, Tukey HSD: $p < 0.05$, Table 4B, Figure 14). Treatment also had a significant effect on the average sporophyll length, showing that thalli harvested from the minus vegetative blade treatment had significantly longer sporophylls on average than those from the controls (ANOVA: $F_{1,27} = 5.7415$, $p = 0.0238$, Table 4B, Figure 14). There was no effect of the interaction between sampling date*treatment (ANOVA: $F_{4,27} = 1.9164$, $p = 0.1356$, Table 4B). There was no difference in average total sporophyll biomass among sampling dates (ANOVA: $F_{4,27} = 1.6080$, $p = 0.2010$, Table 4C), treatments (ANOVA: $F_{1,27} = 0.0818$, $p = 0.7771$, Table 4C), or the interaction between sampling date*treatment (ANOVA: $F_{4,27} = 0.1606$, $p = 0.9564$, Table 4C).

Vegetative blade biomass of thalli from the minus sporophylls treatment had a significant positive relationship with vegetative blade length (Regression: $R^2 = 0.79$, $F_{1,16} = 58.4967$, $p < 0.0001$, Figure 15). The data for vegetative blade measurements were not normally distributed due to some values of zero, so a Log [x + 1] transformation was used to normalize these data. Sampling date had no effect on the average vegetative blade biomass (ANOVA: $F_{4,27} = 2.0929$, $p = 0.1095$, Table 5A) or the average vegetative blade

length (ANOVA: $F_{4,27} = 0.7535$, $p = 0.5645$, Table 5B) for *Pterygophora* from the minus sporophylls and control treatments. There was a significant treatment effect for both average vegetative blade biomass (ANOVA: $F_{1,27} = 14.2666$, $p = 0.0008$, Table 5A) and average vegetative blade length (ANOVA: $F_{1,27} = 11.0370$, $p = 0.0026$, Table 5B). Thalli harvested from the minus sporophylls treatment had lower vegetative biomass and shorter vegetative blade length on average than control thalli (Figure 16). This indicates that removing sporophylls significantly decreases vegetative blade production. There was no significant effect of the interaction between sampling date*treatment on the average vegetative blade biomass (ANOVA: $F_{4,27} = 2.2725$, $p = 0.0875$, Table 5A) or average vegetative blade length (ANOVA: $F_{4,27} = 1.2356$, $p = 0.3193$, Table 5B) of these thalli.

Compartmentalization of Internal Resources

To first address the very existence of resource compartmentalization in *Pterygophora*, thallus regions (holdfast, lower stipe, mid stipe, upper stipe, sporophyll, sorus, vegetative blade) were compared to each other for the %C, $\delta^{13}C$, %N, and C:N values obtained from all control samples, for all sampling dates. There were significant differences in %C among thallus regions (ANOVA: $F_{6,112} = 22.2351$, $p < 0.0001$, Table 6A). The %C composition in regions of holdfast, sporophyll, and vegetative blade were significantly lower than all three stipe regions and the sorus (Tukey HSD: $p < 0.05$, Figure 17). There were significant differences in $\delta^{13}C$ among thallus regions (ANOVA: $F_{6,112} = 2.9937$, $p = 0.0095$, Table 6B). The regions of sporophyll and vegetative blade were significantly enriched in ^{13}C relative to the lower stipe region (Tukey HSD: $p < 0.05$, Figure 18). There were significant differences in %N among thallus regions (ANOVA: $F_{6,112} = 24.9665$, $p < 0.0001$, Table 6C). The holdfast region was significantly higher in %N than every other region. In addition, the lower stipe was significantly higher in %N than upper stipe, sporophyll, sorus, & vegetative blade (Tukey HSD: $p < 0.05$, Figure 19). Finally, there were significant differences in C:N among thallus regions (ANOVA: $F_{6,112} = 17.5575$, $p < 0.0001$, Table 6D). The C:N for holdfast region was significantly lower than all other regions. The sporophylls were lower in C:N than the upper stipe, sorus, and vegetative blade regions; the lower stipe also had significantly

lower C:N than the upper stipe region. The mid stipe was only significantly higher than the holdfast region (Tukey HSD: $p < 0.05$, Figure 20).

Seasonal Variability of Internal Resources

To address the seasonal variability of internal storage compounds across the whole thallus and the potential interaction of seasonality and thallus region, sampling date and thallus region factors were used to analyze the %C, $\delta^{13}C$, %N, and C:N values obtained from all control samples. The data for the "sorus" thallus region were excluded from these tests because this structure was not present for all sampling dates.

No significant differences in thallus %C were found among sampling dates (ANOVA: $F_{5,71} = 0.5356$, $p = 0.7486$, Table 7A) or the interaction between sampling date*thallus region (ANOVA: $F_{25,71} = 0.5803$, $p = 0.9354$, Table 7A). However, there were significant differences among thallus regions, which were already confirmed by the analysis for the first question (ANOVA: $F_{5,71} = 22.5332$, $p < 0.0001$; Tukey HSD: $p < 0.05$, Figure 17), indicating that compartmentalization was temporally stable in control thalli.

No significant differences in thallus $\delta^{13}C$ were found for the interaction of sampling date*thallus region (ANOVA: $F_{25,71} = 1.2104$, $p = 0.2616$, Table 7B), however, there were significant differences in thallus $\delta^{13}C$ among sampling dates (ANOVA: $F_{5,71} = 6.0015$, $p = 0.0001$, Tukey HSD: $p < 0.05$, Table 7B, Figure 21) and $\delta^{13}C$ among thallus regions (ANOVA: $F_{5,71} = 4.6385$, $p = 0.0010$, Tukey HSD: $p < 0.05$, Table 7B, Figure 18) independently.

No significant differences in thallus %N were found for the interaction of sampling date*thallus region (ANOVA: $F_{25,71} = 0.7652$, $p = 0.7698$, Table 7C). However, there were significant differences in thallus %N among sampling dates (ANOVA: $F_{5,71} = 5.8356$, $p = 0.0001$, Tukey HSD: $p < 0.05$, Table 7C, Figure 22) and %N among thallus regions (ANOVA: $F_{5,71} = 34.9751$, $p < 0.0001$, Tukey HSD: $p <$

0.05 , Table 7C, Figure 19). Significant differences in mean %N by thallus region were confirmed in the analysis for the first hypothesis (Figure 19).

No significant differences in thallus C:N were found among sampling dates (ANOVA: $F_{5,71} = 1.8383$, $p = 0.1163$, Table 7D) or the interaction between sampling date*thallus region (ANOVA: $F_{25,71} = 1.3082$, $p = 0.1890$, Table 7D). However, there were still significant differences in C:N among thallus regions, which were already confirmed by the analysis for the first question (ANOVA: $F_{5,71} = 23.2633$, $p < 0.0001$, Tukey HSD: $p < 0.05$, Table 7D, Figure 20).

To address the seasonal variability of internal storage compounds in each thallus region individually, sampling date was compared to the %C, $\delta^{13}C$, %N, and C:N values obtained from all control samples in one thallus region at a time. The data for the "sorus" thallus region were excluded from these tests because this structure was not present for all sampling dates.

Results for holdfast region: There were no significant differences in %C (ANOVA: $F_{5,11} = 0.8727$, $p = 0.5296$, Table 8A), $\delta^{13}C$ (ANOVA: $F_{5,11} = 1.0089$, $p = 0.4569$, Table 8B), %N (ANOVA: $F_{5,11} = 1.0666$, $p = 0.4290$, Table 8C), or C:N (ANOVA: $F_{5,11} = 0.1693$, $p = 0.9687$, Table 8D) among sampling dates in the holdfast region.

Results for lower stipe region: No significant differences were found for %C (ANOVA: $F_{5,12} = 0.2531$, $p = 0.9302$, Table 9B), $\delta^{13}C$ (ANOVA: $F_{5,12} = 0.5847$, $p = 0.7118$, Table 9C), or C:N (ANOVA: $F_{5,12} = 1.8256$, $p = 0.1822$, Table 9D) among sampling dates in the lower stipe region. However, there were significant differences in %N among sampling dates in the lower stipe region (ANOVA: $F_{5,12} = 3.2696$, $p = 0.0430$, Tukey HSD: $p < 0.05$, Table 9A, Figure 23).

Results for mid stipe region: No significant differences were found for %C (ANOVA: $F_{5,12} = 2.3984$, $p = 0.0996$, Table 10B), $\delta^{13}C$ (ANOVA: $F_{5,12} = 1.1749$, $p = 0.3765$, Table 10C), or C:N (ANOVA: $F_{5,12} = 0.8880$, $p = 0.5186$, Table 10D) among sampling dates in the mid stipe region. However, there were significant differences in

%N among sampling dates in the mid stipe region (ANOVA: $F_{5,12} = 7.3290$, $p = 0.0023$, Tukey HSD: $p < 0.05$, Table 10A, Figure 24).

Results for upper stipe region: There were no significant differences in %C (ANOVA: $F_{5,12} = 0.7803$, $p = 0.5827$, Table 11A), $\delta^{13}C$ (ANOVA: $F_{5,12} = 0.4725$, $p = 0.7899$, Table 11B), %N (ANOVA: $F_{5,12} = 1.4257$, $p = 0.2838$, Table 11C), or C:N (ANOVA: $F_{5,12} = 0.2377$, $p = 0.9382$, Table 11D) among sampling dates in the upper stipe region.

Results for sporophyll region: There were no significant differences in %C (ANOVA: $F_{5,12} = 0.4639$, $p = 0.7959$, Table 12A), $\delta^{13}C$ (ANOVA: $F_{5,12} = 2.6573$, $p = 0.0768$, Table 12B), %N (ANOVA: $F_{5,12} = 0.4579$, $p = 0.8001$, Table 12C), or C:N (ANOVA: $F_{5,12} = 1.9375$, $p = 0.1614$, Table 12D) among sampling dates in the sporophyll region.

Results for vegetative blade region: No significant differences were found for %C (ANOVA: $F_{5,12} = 0.4302$, $p = 0.8191$, Table 13B), %N (ANOVA: $F_{5,12} = 2.7330$, $p = 0.0713$, Table 13C), or C:N (ANOVA: $F_{5,12} = 1.8282$, $p = 0.1817$, Table 13D) among sampling dates in the vegetative blade region. However, there were significant differences in $\delta^{13}C$ among sampling dates in the vegetative blade region (ANOVA: $F_{5,12} = 3.4369$, $p = 0.0370$, Student's t: $p < 0.05$, Table 13A, Figure 25).

Effects of Biomass Loss on Internal Resources

To address the effects of biomass loss on internal storage compounds and compartmentalization in *Pterygophora* and the potential interaction of seasonality and treatment, sampling date and treatment were tested among thallus regions for the %C, $\delta^{13}C$, %N, and C:N values obtained from all control and experimental samples. The data from the 7/1/2017 sampling date were excluded from this test because only samples from the "control" treatment were harvested, as it was the start of the manipulations for all other treatments.

Results for holdfast region: No significant differences were found for %C (ANOVA: $F_{4,39} = 0.6496$, $p = 0.6306$; $F_{3,39} = 0.4055$, $p = 0.7499$; $F_{12,39} = 0.4441$, $p = 0.9344$, Table 14A), %N (ANOVA: $F_{4,39} = 0.5416$, $p = 0.7061$; $F_{3,39} = 1.4798$, $p = 0.2350$; $F_{12,39} = 0.7186$, $p = 0.7244$, Table 14C), or C:N (ANOVA: $F_{4,39} = 1.3191$, $p = 0.2799$; $F_{3,39} = 2.4373$, $p = 0.0791$; $F_{12,39} = 0.3689$, $p = 0.9669$, Table 14D) among sampling dates, treatments, or the interaction between sampling date*treatment. No significant differences in $\delta^{13}C$ were found among treatments or the interaction between sampling date*treatment (ANOVA: $F_{3,39} = 0.6392$, $p = 0.5943$; $F_{12,39} = 0.5447$, $p = 0.8714$, Table 14B). However, there were significant differences in $\delta^{13}C$ among sampling dates (ANOVA: $F_{4,39} = 3.2695$, $p = 0.0210$, Tukey HSD: $p < 0.05$, Table 14B, Figure 26).

Results for lower stipe region: No significant differences in %C were found among sampling dates or the interaction between sampling date*treatment (ANOVA: $F_{4,40} = 0.2463$, $p = 0.9102$; $F_{12,40} = 0.1840$, $p = 0.9985$, Table 15A). No significant differences in %N were found among treatments or the interaction between sampling date*treatment (ANOVA: $F_{3,40} = 0.5531$, $p = 0.6491$; $F_{12,40} = 0.4191$, $p = 0.9469$, Table 15C). No significant differences were found for $\delta^{13}C$ (ANOVA: $F_{4,40} = 1.8923$, $p = 0.1307$; $F_{3,40} = 0.7339$, $p = 0.5379$; $F_{12,40} = 0.7999$, $p = 0.6483$, Table 15B) or C:N (ANOVA: $F_{4,40} = 1.8170$, $p = 0.1445$; $F_{3,40} = 0.3186$, $p = 0.8119$; $F_{12,40} = 0.4645$, $p = 0.9236$, Table 15D) among sampling dates, treatments, or the interaction between sampling date*treatment. However, there were significant differences in %C among treatments (ANOVA: $F_{3,40} = 4.1432$, $p = 0.0120$, Tukey HSD: $p < 0.05$, Table 15A, Figure 27). There were also significant differences in %N among sampling dates (ANOVA: $F_{4,40} = 3.1023$, $p = 0.0258$, Tukey HSD: $p < 0.05$, Table 15B, Figure 28).

Results for mid stipe region: No significant differences in %C were found among sampling dates or the interaction between sampling date*treatment (ANOVA: $F_{4,40} = 1.7445$, $p = 0.1593$; $F_{12,40} = 1.7933$, $p = 0.0829$, Table 16A). No significant differences were found for $\delta^{13}C$ (ANOVA: $F_{4,40} = 1.8253$, $p = 0.1429$; $F_{3,40} = 0.8222$, $p = 0.4894$; $F_{12,40} = 0.4332$, $p = 0.9402$, Table 16B), %N (ANOVA: $F_{4,40} = 1.810$, $p = 0.3338$; $F_{3,40} = 0.3412$, $p = 0.7956$; $F_{12,40} = 0.9950$, $p = 0.4707$, Table 16C), or C:N (ANOVA: $F_{4,40} =$

1.1954, p = 0.3277; $F_{3,40}$ = 1.1137, p = 0.3549; $F_{12,40}$ = 0.3209, p = 0.9812, Table 16D) among sampling dates, treatments, or the interaction between sampling date*treatment. However, there were significant differences in %C among treatments (ANOVA: $F_{3,40}$ = 9.2957, p < 0.0001, Tukey HSD: p < 0.05, Table 16A, Figure 29).

Results for upper stipe region: No significant differences in %C were found among sampling dates or the interaction between sampling date*treatment (ANOVA: $F_{4,39}$ = 1.0953, p = 0.3724; $F_{12,39}$ = 0.7259, p = 0.7177, Table 17A). No significant differences in $\delta^{13}C$ were found among treatments or the interaction between sampling date*treatment (ANOVA: $F_{3,39}$ = 1.8711, p = 0.1504; $F_{12,39}$ = 0.4846, p = 0.9115, Table 17B). No significant differences were found for %N (ANOVA: $F_{4,39}$ = 2.3677, p = 0.0693; $F_{3,39}$ = 0.9844, p = 0.4101; $F_{12,39}$ = 0.9986, p = 0.4681, Table 17C) or C:N (ANOVA: $F_{4,39}$ = 1.1168, p = 0.3625; $F_{3,39}$ = 0.2277, p = 0.8765; $F_{12,39}$ = 0.5430, p = 0.8726, Table 17D) among sampling dates, treatments, or the interaction between sampling date*treatment. However, there were significant differences in %C among treatments (ANOVA: $F_{3,39}$ = 6.7230, p = 0.0009, Tukey HSD: p < 0.05, Table 17A, Figure 30). There were also significant differences in $\delta^{13}C$ among sampling dates (ANOVA: $F_{4,39}$ = 3.4090, p = 0.0175, Tukey HSD: p < 0.05, Table 17B, Figure 31).

Results for sporophyll, sorus, and vegetative blade regions: Due to the biomass removal experiment, there was not enough sporophyll, sorus, or vegetative blade tissue present for all sampling dates and/or treatments to analyze the chemistry statistically. Mean values of %C, %N, $\delta^{13}C$, and C:N for each of these regions can be seen in Appendix- B.

DISCUSSION

Previous work on various kelp species has revealed that different thallus structures perform different physiological and ecological functions including growth, photosynthesis, structural integrity, translocation, and storage (Black 1948; Black 1954; Lüning et al. 1973; Chapman & Craigie 1978; Küppers & Kremer 1978; Gagne et al.

1982). *Pterygophora californica* is a kelp species that possesses both perennial and annual thallus structures on the same individual, which can perform different functions (McKay 1933). It has been popularly assumed that the ability of *Pterygophora* to sustain resource reserves allows for their seasonal growth patterns and presence of specialized structures. The primary objective of this study was to document the presence of *Pterygophora*'s storage ability by targeting resource compartmentalization and its changes over time and during manipulations.

After testing for compartmentalization in a population of controls, I can confidently report that for all response variables measured (%C, $\delta^{13}C$, %N, and C:N), significant results confirmed the existence of compartmentalization of storage compounds. The results of the carbon data were interesting in that the values of %C in the holdfast were more similar to those of the sporophylls and vegetative blade regions than of the entire stipe and the soral tissue, indicating C enrichment (=storage, accumulation) in the stipe and reproductive tissues. I had assumed that the primary function of the holdfast was attachment, and that because of its proximity to the lower stipe, it would be most similar to that region. It seems intuitive that the stipe would have higher carbon on average because of its perennial presence, but surprising that the holdfast does not as well. The data shows that on average, the holdfast also contains slightly more carbon biomass than the sporophylls (Figure 17). Seeing as they historically make up at least 44% of the biomass of the entire thallus (De Wreede 1984) and were consistently the largest proportion of control thallus biomass throughout my study, it's logical to think that they might've steadily contained the bulk of the carbon.

Many organisms put huge amounts of energy into reproduction, so it seems intuitive that because of spore production, the sporophyll and sorus regions would have high carbon values. However, previous kelp research suggests that the energy cost of producing spores may be quite low (De Wreede & Klinger 1988; Pfister 1992). Unlike flowering plants, macroalgae do not form large, complex structures to produce their spores, and the structures that do encapsulate them can photosynthesize (De Wreede & Klinger 1988; Amsler & Neushul 1991; Reed et al. 1992). Since the sporophylls can photosynthesize in addition to producing sites of spore production, this concept adds

more complexity to the sporophyll story. This region may be performing the bulk of the photosynthesis and continuously transporting those photosynthates down to the stipe reserves. This mechanism could explain why the main sporophyll tissue could be more deplete in carbon, while retaining a higher concentration of carbon in the sori. Further analysis of the carbon in these regions such as sugar analysis and stable carbon isotope feeding experiments would help to illustrate this data in greater detail.

When looking at the results for $\delta^{13}C$, it appears that the vegetative blade and sporophylls on average had more positive values of $\delta^{13}C$ than the lower stipe. This means that compared to the lower stipe, those blades were more enriched in ^{13}C, or the heavier carbon isotope. Vascular plant research has discovered that carbon allocation can drive isotopic gradients in different types of tissue (Hobbie and Werner 2004, Gessler et al. 2009, Werner and Gessler 2011). It has been observed that heterotrophic (sink) tissues such as roots and stems are generally ^{13}C-enriched relative to autotrophic (source) tissue such as the leaves (Cernusak et al. 2009). Fox (2013) illustrated with his experiment that similar to plants, *Macrocystis pyrifera* frond initials (dominant sinks) were consistently ^{13}C-enriched relative to canopy blades (sources). *Macrocystis* was observed translocating ^{13}C-enriched compounds from mature blades to frond initials, aiding in translocation-mediated recovery. A comprehensive study of translocation in numerous species of the Laminariales confirmed that not only can *Pterygophora* perform long-distance transport of carbon, but the pattern of translocation is consistently from source to sink (Schmitz and Lobban 1976). That study was conducted from May-June and identified the transition zones between stipe and lamina and growing haptera as sinks. However, they recognized that there could be a different translocation pattern in fall. So, it appears that although mean %C data shows that the vegetative blade and sporophylls contain less overall carbon than the lower stipe, it is possible that more ^{13}C-enriched compounds are likely being allocated to the former regions for tissue growth. Carbon fractionation also takes place during photosynthesis and respiration, so it is very likely that these processes are altering the values for ^{13}C-enrichement in these regions. Additional carbon analyses are required to provide explanations of allocation.

My findings for the compartmentalization of %N are quite interesting. The values of %N decreased from the base to the top of the thallus. Since photosynthetic pigments contain lots of nitrogen, naturally I would expect to see higher amounts of nitrogen in the blades. However, the holdfast region on average contained the highest %N, significantly different from all others. Lower stipe was similar to mid stipe, but different from all other upper regions as well. It is possible that the dark epidermal layer of cells on the stipe and holdfast contains a high amount of pigment, and consequently, a high number of pigment-proteins. However, this dark epidermal layer covers the entirety of the stipe, which if this were the reason, would mean the holdfast and all 3 designated stipe regions would be similar. Several past studies have looked into the details of seasonal growth rings present in the stipes of *Pterygophora* (MacMillan 1902; Frye 1918; DeWreede 1984; Hymanson et al. 1990). These rings, consisting of alternating dark and light tissue, hypothetically could contain more nitrogen-rich pigments combined than internal cell layers of the blades. More in-depth microscopy to look at the types of cell tissue and pigments in the layers of the stipe and the transition area would be a great addition. A likely explanation for greater nitrogen in the lower regions is the fully perennial nature of the holdfast and stipe, continually serving as sites for nitrogen storage, allowing for nutrient allocation unaffected by nitrogen levels in the surrounding environment. Previous research described that adult kelp thalli invest a trivial amount of nitrogen into spores compared to the amount they invest in vegetative tissue (Reed et al. 1996). My results did not produce a significant difference in the amount of bulk nitrogen contained in the general blade tissues vs. the soral tissue. Since soral tissue is part of the sporophyll blade tissue, this finding suggests that nitrogen that was allocated beyond the normal amount found in blade tissue was so little that it was undetectable.

Results for C:N values corresponded well with the results for %N and %C, showing a lower value for C:N in the holdfast region than all other regions. Across the control samples, the holdfast region has stood out as an area with highest nitrogen concentration and lower carbon concentration. This holdfast pattern seems to be the most intriguing of the study. The holdfast is at the base of the thallus, receiving the least light, and yet is the most nitrogen rich. This phenomenon suggests that nutrients are being transported to and collected in the holdfast. It’s highly unlikely that the amount of

nitrogen available to the holdfast would be any greater than that available to the rest of the thallus, let alone the lower stipe which is connected to it and therefore in extremely close proximity. Cunningham (2019) argued that the water column in kelp beds is well mixed due to turbulence caused by wave orbitals shearing off of the stipes of *Macrocystis pyrifera*. In addition, De Wreede (1984) found that rapid growth of *Pterygophora* did not coincide with periods of high levels of nitrogen availability in the surrounding water. Further chemical investigations such as protein and pigment analyses could be done to determine in what form the nitrogen is accumulated within the holdfast region. In addition, an pattern of increasing C:N was seen from the base to top of the stipe, and the ratio in the sporophylls was more similar to the lower and mid stipe than to the sorus and vegetative blade regions.

I harvested unmanipulated *Pterygophora californica* thalli for 15 months, in an attempt to characterize seasonal fluctuations of chemical compartmentalization. Kelps normally display robust seasonality in growth, exhibiting elongation in the winter and early spring. Even in darkness, kelps initiate winter growth. By restricting *Laminaria hyperborea* thalli to darkness from January to June, Lüning (1971) revealed they were able to form a new blade. This is made possible by the storage of carbohydrates produced the previous summer season, allowing for seasonal growth that is not solely driven by nitrogen availability in the water (Lüning 1971; Mann 1973; Chapman & Craigie 1978; Chapman & Lindley 1980). A multi-year study of *Macrocystis pyrifera* and *Pterygophora* in southern California confirmed that resource availability and other environmental conditions had a greater impact on the fecundity of species that produce all year (*Macrocystis*), than on those with stringent seasonal reproductive cycles (*Pterygophora*) (Reed et al. 1996).

Analyses of the interaction between sampling date and thallus region on the internal constituents revealed that time had no significant effect on the compartmentalization. However, chemical differences were seen within thallus region "compartments" when analyzed individually. Holdfast, upper stipe, and sporophyll tissue chemistry did not significantly change according to sampling date. Mean %N significantly differed seasonally in the lower stipe and mid stipe. In the lower stipe, mean

%N was significantly higher on 1/14/2018 than it was on 7/1/2017 (Figure 23). In the mid stipe, mean %N was significantly higher on 1/14/2018 than it was on 7/1/2017, 4/21/2018, 7/19/2018, and 11/8/2018 (Figure 24). Results for these two stipe regions reflect the whole thallus mean %N values relative to sampling date (Figure 22). The enriched nitrogen levels in the winter and fall are likely the concentration of pigments for better light harnessing during the shorter photoperiod. Since the typical Monterey Bay upwelling season is March-July, it is very unlikely that this pattern is reliant on nitrogen availability in the water. In addition, 100% of thalli harvested on 1/14/2018 had reproductive sori present. This suggests that fertility has negligible to no effect on the internal nitrogen content of the other regions of the thallus, consistent with previous research detailing how little nitrogen is invested in spores at any given time (Reed et al. 1996).

The vegetative blade region varied significantly in $\delta^{13}C$ among sampling dates. Values for mean ^{13}C were higher on 7/1/2017 and 10/9/2017 than on 7/19/2018 and 11/8/2018. Morphometric measurements throughout the study confirmed that thalli harvested on 7/1/2017 and 10/9/2017 also had higher mean vegetative blade biomass and longer mean vegetative blade length than thalli from 7/19/2018 and 11/8/2018. The seasonal patterns in these data are disjointed, and it is unclear why I am seeing a different pattern of ^{13}C enrichment from one summer and fall season to another, other than the simple fact that there was more blade tissue in the summer and fall of 2017. In theory, the vegetative blade would act as a sink in winter and early spring (highest ^{13}C), and a source in summer and fall (lowest ^{13}C), but this pattern is only expressed with summer and fall 2017. It is possible that inconsistencies in sampling may have had an effect. Because the vegetative blade tissue was so variable and a minimum amount of tissue was needed for chemical analysis, sometimes only a piece of the blade was sampled, and sometimes it required the entire blade. It is possible that by sampling an entire blade, more mature blade tissue could have diluted a signal of enriched new growth, and vice versa. Of course, there is a possibility that this pattern is accurate and could be explored further.

Starting on 7/1/2017, I manipulated experimental thalli to mimic natural wave disturbance removing blade biomass. Over the course of the 15-month experiment, I

maintained these blade removals in an attempt to detect differences in internal chemical composition and compartmentalization over time. Stored reserves have been demonstrated to be vital to autotrophs when recovering from disturbance. As vascular plants have been studied in much detail, the results of this study can provide further understanding of this mechanism in our coastal marine macrophytes. Due to my findings of compartmentalization of thallus regions in controls, each region for this question was analyzed individually for the effects of seasonality and experimental treatment as its own "compartment". It seemed appropriate to observe the thallus regions in this way since they have proven to be chemically and functionally unique.

The holdfast region exhibited significant differences in $\delta^{13}C$ only among sampling dates. Holdfast samples from thalli harvested on 7/19/2018 had significantly higher mean ^{13}C than those harvested on 1/14/2018, regardless of treatment. The internal pattern of $\delta^{13}C$ in the holdfast region shows a slightly greater enrichment in the controls, and the least enrichment for samples from the minus veg. blade + sporophylls treatment. However, this pattern is not significant by treatment, and so what makes it significant by sampling date? The perennial regions such as the stipe and holdfast are likely able to photosynthesize just enough on their own in summer to enrich, and any uncut or re-grown blade tissue that is present could allocate whatever extra assimilates is possible. In addition, vascular plant research has observed enrichment of stored carbohydrates in comparison to newly assimilated ones. It is possible that similar physiological processes in kelps may be able to drive fractionation within a storage reserve (Tcherkez et al. 2004).

The lower stipe region exhibited significant differences in %C among treatments and %N among sampling dates. Lower stipe samples from thalli in the minus vegetative blade treatment had a higher mean %C than those in the minus sporophylls and minus veg. blade + sporophylls treatments, regardless of sampling date. This clearly illustrates that removing the sporophylls has a greater impact on the bulk carbon in the lower stipe than removing the vegetative blade. Lower stipe samples from thalli harvested on 1/14/2018 had higher mean %N than those harvested on 4/21/2018, regardless of treatment. The mechanism behind this difference in nitrogen of all experimental thalli is

difficult to pin down. Since nitrogen is a major component of chlorophyll, amino acids, energy transporting compounds, and nucleic acids, further analysis is required to categorize these values in more detail. Pigment and protein analysis on these samples would add more clarity.

The mid stipe region exhibited significant differences in %C only among treatments. Mid stipe samples from control thalli and from thalli in the minus vegetative blade treatment had a higher mean %C than those in the minus sporophylls and minus veg. blade + sporophylls treatments, regardless of sampling date. Like what was seen in the lower stipe region, it appears that the vegetative blade has very little, if any, effect on the carbon content in the mid stipe. The sporophylls seem to drive the carbon changes.

The upper stipe region exhibited differences in %C among treatments and $\delta^{13}C$ among sampling dates. Upper stipe samples from control thalli and from thalli in the minus vegetative blade treatment had a higher mean %C than those in the minus sporophylls and minus veg. blade + sporophylls treatments, regardless of sampling date. Like the results for the other stipe regions, it appears that removal of the sporophylls has a much greater effect on the bulk carbon in the stipe than removal of the vegetative blade. Thalli harvested on 4/21/2018 had higher mean $\delta^{13}C$ than those harvested on 1/14/2018, regardless of treatment. Like the holdfast, the stipe is likely able to photosynthesize just enough on its own in summer to enrich, and any uncut or re-grown blade tissue that is present could allocate whatever extra assimilates is possible. In addition, vascular plant research has observed enrichment of stored carbohydrates in comparison to newly assimilated ones. It is possible that similar physiological processes in kelps may be able to drive fractionation within a storage reserve (Tcherkez et al. 2004). Winter storms remove a large majority of *Macrocystis pyrifera* surface canopy, leaving them to start replenishing biomass in the spring, and reaching a maximum canopy size in summer (Foster 1982; Reed & Foster 1984). Benthic light levels can increase 4- to 5-fold from thinning or removing a giant kelp surface canopy (Watanabe et al. 1992). With the presence of *Macrocystis* canopy, the greatest amount of light intensity for *Pterygophora* may very well be in April before the surface canopy thickens. It's likely that *Pterygophora* perennial regions are able to access more light at this time, and could likely

explain why the highest amount of carbon allocation to the upper stipe region was detected on 4/21/2018 compared to all other sampling dates (Figure 31).

CONCLUSIONS

While some aspects of this study remain unexplained, it seems several overarching patterns were uncovered. Compartmentalization of internal compounds in *Pterygophora californica* exists, suggesting regions of nutrient storage. All regions of the stipe and the reproductive sori had a higher mean %C than the holdfast, sporophylls, and vegetative blade. Isotopic fractionation illustrated that on average, the vegetative blade and sporophylls were more enriched in ^{13}C than the lower stipe, potentially suggesting that the high bulk carbon in the stipe is a reserve that allocates carbohydrates to the blades. However, carbon fractionation due to photosynthesis and respiration was not measured, and therefore it is unknown how much impact those processes have on the ^{13}C enrichment among thallus regions. A pattern of decreasing mean %N was seen from the base to top of the thallus. The holdfast region on average was the region of highest %N, and lowest C:N. This is perhaps the most intriguing development of the study. However, without further analyses of nitrogen-based compounds, the explanation for this occurrence is purely conjecture. Carbon to nitrogen ratio increased from the base to the top of the stipe, and the ratio in the sporophylls was more similar to the lower and mid stipe regions than to the other blade tissues. Seasonality of nutrient compartmentalization in the thallus was not seen, meaning time had no effect on the chemical distribution among thallus regions ("compartments"). However, some seasonal variability of chemicals was observed for the thallus as a whole and within thallus regions individually. The only thallus regions that were significantly affected by blade manipulations were the lower, mid, and upper stipe. Changes within these regions were significantly impacted by the removal of sporophylls. Overall, the evident patterns in this study have uncovered a consistent nitrogen reserve in the holdfast, carbon reserve in the stipe, and allocation of carbon to the blades.

This study provides the first empirical evidence of compartmentalization of resources in *Pterygophora californica*. Much research has been done on the chemical composition of other kelp species, but *Pterygophora* morphology and longevity is so unique that this information does not fully translate to the understanding of this species. To further the understanding of the patterns of chemical distribution and seasonal variability of these resources, future research should include a wider range of chemical analyses such as sugar, pigment, and protein analyses. The development of compound-specific stable isotope values for laminarin and mannitol would tremendously benefit the use of isotopic fractionation as a method of examining kelp physiology. An additional laboratory experiment using radioactive ^{14}C would also help to illuminate some of the more elusive concepts of this study.

LITERATURE CITED

Abbott, I. A., & Hollenberg, G. J. (1976). *Marine algae of California*. Stanford, CA: Stanford University Press, 827 pp.

Amsler, C. D., & Neushul, M. (1991). Photosynthetic physiology and chemical composition of spores of the kelps *Macrocystis pyrifera*, *Nereocystis luetkeana*, *Laminaria farlowii*, and *Pterygophora californica* (Phaeophyceae). *Journal of Phycology*, *27*(1), 26–34.

Andrewartha, H. G., & L. C. Birch. (1954). *The distribution and abundance of animals*. Chicago: University of Chicago Press.

Bacon, S., & Carter, D. J. T. (1991). Wave climate changes in the North Atlantic and North Sea. *International Journal of Climatology*, *11*(5), 545–558.

Bairlein, F., & Winkel W. (2001). Changes and risks. In: Lozan, J.L., Graûl, H., Hupfer, P. (eds) *Climate of the 21st century*. Wissenschaftliche Auswertungen, Hamburg, 278–282.

Biedka, R. F., Gosline, J. M., & De Wreede, R. E. (1987). Biomechanical analysis of wave-induced mortality in the marine alga *Pterygophora californica*. *Marine Ecology Progress Series*, *36*, 163–170.

Black, W. A. P. (1948). Seasonal variation in chemical constitution of some common British Laminariales. *Nature*, *161*, 174.

Black, W. A. P. (1950). The seasonal variation in weight and chemical composition of the common British Laminariaceae. *Scottish Seaweed Research Association UK*, *29*(1), 45–72.

Black, W. A. P. (1954). Concentration gradients and their significance in *Laminaria saccharina* (L.) Lamour. *Journal of the Marine Biological Association of the United Kingdom*, *33*(1), 49–60.

Bromirski, P. D., Flick, R. E. & Cayan, D. R. (2003). Storminess variability along the California coast: 1858–2000. *J. Climate*, *16*, 982–993.

Caldeira, K., & Wickett, M. E. (2003). Anthropogenic carbon and ocean pH. *Nature*, *425*, 365–367.

Carrington, E. (1990). Drag and dislodgment of an intertidal macroalga: consequences of morphological variation in *Mastocarpus papillatus* Kützing. *J. Exp. Mar. Biol. Ecol*., *139*, 185–200.

Carroll, D. (2009). *Carmel Bay: Oceanographic dynamics and nutrient transport in a small embayment of the central California coast* (MS thesis, California State University, Monterey Bay).

Carter, D. J. T., & Draper, L. (1988). Has the north-east Atlantic become rougher? *Nature*, *332*(6164), 494–494.

Cernusak, L. A., Tcherkez, G., Keitel, C., Cornwell, W. K., Santiago, L. S., Knohl, A., Barbour, M. M., Williams, D. G., Reich, P. B., Ellsworth, D. S., Dawson, T. E., Griffiths, H. G., Farquhar, G. D., & Wright, I. J. (2009). Why are non-photosynthetic tissues generally ^{13}C enriched compared with leaves in C_3 plants? Review and synthesis of current hypotheses. *Functional Plant Biology*, *36*(3), 199–213.

Chapman, A. R. O., & Craigie, J. S. (1977). Seasonal growth in *Laminaria longicruris*: Relations with dissolved inorganic nutrients and internal reserves of nitrogen. *Marine Biology*, *40*, 197–205.

Chapman, A. R. O., & Craigie, J. S. (1978). Seasonal growth in *Laminaria longicruris*: Relations with reserve carbohydrate storage and production. *Marine Biology*, *46*, 209–213.

Chapman, A. R. O., & Lindley, J. E. (1980). Seasonal growth of *Laminaria solidungula* in the Canadian high Arctic in relation to irradiance and dissolved nutrient concentrations. *Marine Biology*, *57*, 1–5.

Clark, R., Edwards, M., & Foster, M. (2004). Effects of shade from multiple kelp canopies on an understory algal assemblage. *Marine Ecology Progress Series*, *267*, 107–119.

Costanza, R., D'Arge, R., de Groot, R., Farber, S., Grasso, M., Hannon, B., Limburg, K., Naeem, S., O'Neill, R. V., Paruelo, J., Raskin, R. G., Sutton, P., & van den Belt, M. (1997). The value of the world's ecosystem services and natural capital. *Nature*, *387*(6630), 253–260.

Costanza, R., de Groot, R., Sutton, P., van der Ploeg, S., Anderson, S. J., Kubiszewski, I., Farber, S., & Turner, R. K. (2014). Changes in the global value of ecosystem services. *Global Environmental Change*, *26*(1), 152–158.

Craigie, J. S. (1974). Storage products. In: *Algal physiology and biochemistry*. Oxford: Blackwell, *10*, 206-237.

Cunningham, S. R. (2019). *Physical and biological consequences of giant kelp (Macrocystis pyrifera) removals within a central California kelp forest* (MS thesis, California State University, Monterey Bay).

Dayton, P. K. (1971). Competition, disturbance, and community organization: The provision and subsequent utilization of space in a rocky intertidal community. *Ecological Monographs, 41*(4), 351–389.

Dayton, P. K. (1985). Ecology of kelp communities. *Annual Review of Ecology and Systematics*, *16*, 215–245.

Dayton, P. K., Currie, V., Gerrodette, T., Keller, B. D., Rosenthal, R., & Ven Tresca, D. (1984). Patch dynamics and stability of some California kelp communities. *Ecological Society of America*, *54*(3), 253–289.

De Wreede, R. E. (1984). Growth and age class distribution of *Pterygophora californica* (Phaeophyta). *Marine Ecology*, *19*, 93–100.

De Wreede, R. E. (1986). Demographic characteristics of *Pterygophora californica* (Laminariales, Phaeophyta). *Phycologia*, *25*(1), 11–17.

De Wreede, R. E., Ewanchuk, P., & Shaughnessy, F. (1992). Wounding, healing and survivorship in three kelp species. *Marine Ecology Progress Series*, *82*, 259–266.

De Wreede, R. E., and T. Klinger. 1988. Reproductive strategies in algae. In: Doust, J. L. & Doust, L. L. (eds), *Plant reproductive ecology: patterns and strategies*. New York: Oxford University Press, 267-284.

Denny, M. W. (1985). Wave forces on intertidal: A case study. *Limnology and Oceanography*, *30*(6), 1171–1187.

Denny, M. W. (1988). *Biology and the mechanics of the wave-swept environment*. Princeton, NJ: Princeton University Press.

Denny, M., Brown, V., Carrington, E., Kraemer, G., Miller, A. (1989). Fracture mechanics and the survival of wave-swept macroalgae. *J. exp. mar Biol. Ecol., 127*: 211-228.

Denny, M. W., & Gaylord, B. P. (2002). The mechanics of wave-swept algae. *The Journal of Experimental Biology*, *205*, 1355–1362.

Denny, M. W., Daniel, T. L., & Koehl, M. A. R. (1985). Mechanical limits to size in wave-swept organisms. *Ecological Monographs*, *55*, 69–102.

Donnellan, M. (2004). *Spatial and temporal patterns of kelp canopies in central California* (MS thesis, San Jose State University).

Ehrke, G. (1931). Über die Wirkung der Temperatur und des Lichtes auf die Atmung und Assimilation einiger Meeres-und Süßwasseralgen. *Zeitschrift für wissenschaftliche Biologie. Abteilung E. Planta*, *13*(2/3), 221-310.

Elsner, J. B., Kossin, J. P., & Jagger, T. H. (2008). The increasing intensity of the strongest tropical cyclones. *Nature*, *455*(7209), 92–95.

Feely, R. A., Sabine, C. L., Lee, K., Berelson, W., Kleypas, J., Fabry, V. J. et al. (2004). Impact of anthropogenic CO_2 on the $CaCO_3$ system in the oceans. *Science, 305*, 362–366.

Fields, P. A., Graham, J. B., Rosenblatt, R. H., & Somero, G. N. (1993). Effects of expected global climate change on marine faunas. *Trends in Ecology & Evolution, 8*(10), 361-367.

Foster, M. S., & Schiel, D. R. (1985). The ecology of giant kelp forests in California: A community profile. *U.S. Fish and Wildlife Service Biological Report*, *85*(7.2).

Fox, M. D. (2013). Resource translocation drives $\delta^{13}C$ fractionation during recovery from disturbance in giant kelp, *Macrocystis pyrifera*. *Journal of Phycology*, 1–5.

Frye, T. C. (1918). *The age of Pterygophora californica*. University of Washington.

Gagné, J. A., Mann, K. H., & Chapman, A. R. O. (1982). Seasonal patterns of growth and storage in *Laminaria longicruris* in relation to different patterns of availability of nitrogen in the water. *Marine Biology*, *69*, 91–101.

Gatter, W. (1992). Timing and patterns of visible autumn migration-can effects of global warming be detected. *Journal fur Ornithologie, 133*(4), 427-436.

Gattuso, J. P., Allemand, D., & Frankignoulle, M. (1999). Photosynthesis and calcification at cellular, organismal and community levels in coral reefs: A review on interactions and control by carbonate chemistry. *American Zoologist*, *39*(1), 160–183.

Gattuso, J. P., & Buddemeier, R. W. (2000). Calcification and CO_2. *Nature, 407*(6802), 311–313.

Gaylord, B., Blanchette, A., & Denny, M. W. (1994). Mechanical consequences of size in wave-swept algae. *Ecological Society of America*, *64*(3), 287–313.

Gaylord, B., & Denny, M. W. (1997). Flow and flexibility. *Journal of Experimental Biology*, *200*, 3141–3164.

Gessler, A., Brandes, E., Buchmann, N., Helle, G., Rennenberg, H. & Barnard, R. L. (2009). Tracing carbon and oxygen isotope signals from newly assimilated sugars in the leaves to the tree-ring archive. *Plant Cell Environ., 32*, 780–95.

Hale, B. B. (2001). *Materials properties of marine algae and their role in the survival of plants in flow* (PhD thesis, Stanford University).

Halpin, P. N. (1997). Global climate change and natural-area protection: Management responses and research directions. *Ecological Applications*, *7*, 828–843.

Harder, R. (1915). Beiträge zur Kenntnis des Gaswechsels der Meeresalgen. *Jb. wiss. Bot.*, *56*, 254-98.

Harley, C. D. G., Hughes, A. R., Kristin, M., Miner, B. G., Sorte, C. J. B., Carol, S., Randall Hughes, A., Hultgren, K. M., Thornber, C. S., Rodriguez, L. F., Tomanek, L., & Williams, S. L. (2006). The impacts of climate change in coastal marine systems. *Ecology Letters*, *9*, 228–241.

Hobbie, E. A., & Werner, R. A. (2004). Bulk carbon isotope patterns in C_3 and C_4 plants: a review and synthesis. *New Phytologist*, *161*, 371–385.

Hochachka, P. W. & Somero, G. N. (2002). *Biochemical adaptation: Mechanism and process in physiological evolution*. New York: Oxford University Press.

Hughes, L. (2000). Biological consequences of global warming: Is the signal already apparent? *Trends in Ecology & Evolution, 15*(2), 56–61.

Hughes, T. P., Baird, A. H., Bellwood, D. R., Card, M., Connolly, S. R., Folke, C. et al. (2003). Climate change, human impacts, and the resilience of coral reefs. *Science, 301*, 929–933.

Hurd, C. L. (2000). Water motion, marine macroalgal physiology, and production. *Journal of Phycology*, *36*(3), 453–472.

Hurd, C. L., Harrison, P. J., Bischof, K., & Lobban, C. S. (2014). *Seaweed ecology and physiology*. Cambridge University Press.

Hymanson, Z. P., Reed, D. C., Foster, M. S., & Carter, J. W. (1990). The validity of using morphological characteristics as predictors of age in the kelp *Pterygophora californica* (Laminariales, Phaeophyta). *Marine Ecology Progress Series*, *59*, 295–304.

IPCC (2001). *Climate Change 2001, Synthesis Report. A contribution of working groups I, II, and III to the Third Assessment Report of the Intergovernmental Panel on Climate Change*. Cambridge, UK: Cambridge University Press.

Janzen, F. J. (1994). Climate change and temperature-dependent sex determination in reptiles. *Proceedings of the National Academy of Sciences, 91*(16), 7487-7490.

Kain, J. M. (1971). *Synopsis of biological data on Laminaria hyperborea* (No. 87). Food and Agriculture Organization of the United Nations.

Kanwisher, J. W. (1966). Photosynthesis and respiration in some seaweeds. In: Barnes, H. (ed.), *Some Contemporary Studies in Marine Science*. London: George Allen and Unwin Ltd., 407-420.

Kniep, H. (1914). Über die Assimilation und Atmung der Meeresalgen. *Internationale Revue der gesamten Hydrobiologie und Hydrographie, 7*(1), 1-38.

Koehl, M. A. R. (1977). Effects of sea anemones on the flow forces they encounter. *Journal of Experimental Biology*, *69*, 87–105.

Koehl, M. A. R. (1984). How do benthic organisms withstand moving water? *American Zoologist*, *24*, 57–70.

Koehl, M. A. R. (1986). Seaweeds in moving water: Form and mechanical function. In: Givnish, T. J. (ed), *On the economy of plant form and function.* Cambridge, England: Cambridge University Press, 603-634.

Koehl, M. A. R. & Alberte, R. S. (1988). Flow, flapping, and photosynthesis of *Nereocystis luetkeana*: a functional comparison of undulate and flat blade morphologies. *Marine Biology*, *99*, 435–44.

Kremer, B. P. (1981). Metabolic implications of non-photosynthetic carbon fixation in brown macroalgae. *Phycologia*, *20*(3), 242–250.

Küppers, U., Kremer, B. P. (1978). Longitudinal profiles of CO_2-fixation capacities in marine macroalgae. *Pl. Physiol*., *62*, 49-54.

Lampe, H. (1935). Die Temperatureinstellung des Stoffgewinns bei Meeresalgen als plasmatische Anpassung. *Protoplasma*, *23*(1), 534-578.

Langdon, C., Takahashi, T., Sweeney, C., Chipman, D., Goddard, J., Marubini, F., Aceves, H., Barnett, H., & Atkinson, M. J. (2000). Effect of calcium carbonate saturation state on the calcification rate of an experimental coral reef. *Global Biogeochemical Cycles*, *14*(2), 639–654.

Leclercq, N., Gattuso, J. P., & Jaubert, J. (2000). CO_2 partial pressure controls the calcification rate of a coral community. *Global Change Biology*, *6*(3), 329–334.

Lubchenco, J., Navarrete, S. A., Tissot, B. N. & Castilla, J. C. (1993). Possible ecological responses to global climate change: Near-shore benthic biota of Northeastern Pacific coastal ecosystems. In: Mooney, H.A., Fuentes, E.R. & Kronberg, B.I. (eds), *Earth System Responses to Global Climate Change: Contrasts between North and South America*. San Diego, CA: Academic Press, 147–166.

Lüning, K. (1971). Seasonal growth of Laminaria hyperborea under recorded underwater light conditions near Helgoland. *Fourth European Marine Biology Symposium*, *4*, 347–361.

Lüning, K. (1991). Circannual growth rhythm in a brown alga, *Pterygophora californica*. *Bot. Acta*, *104*, 157–162.

Lüning, K., & Kadel, P. (1993). Daylength range for circannual rhythmicity in *Pterygophora californica* (Alariaceae, Phaeophyta) and synchronization of seasonal growth by daylength cycles in several other brown algae. *Phycologia*, *32*(5), 379–387.

Lüning, K., Schmitz, K., & Willenbrink, J. (1973). CO_2 fixation and translocation in benthic marine algae. III. Rates and ecological significance of translocation in *Laminaria hyperborea* and *L. saccharina*. *Marine Biology*, *23*, 275–281.

MacMillan, C. (1902). *Observations on Pterygophora*.

Mann, K. H. (1972). Ecological energetics of the seaweed zone in a marine bay on the Atlantic coast of Canada. II. Productivity of the seaweeds. *Marine Biology*, *14*, 199–209.

Mann, K. H. (1973). Seaweeds: Their productivity and strategy for growth. *Science*, *182*(4116), 975–981.

Markham, A. (1996). Potential impacts of climate change on ecosystems: A review of implications for policymakers and conservation biologists. *Climate Research*, *6*, 179–191.

Marubini, F., & Thake, B. (1999). Bicarbonate addition promotes coral growth. *Limnology and Oceanography*, *44*(3), 716–720.

McCarty, J. P. (2001). Ecological consequences of recent climate change. *Conservation Biology*, *15*(2), 320–331.

McKay, H. H. (1933). The life-history of *Pterygophora californica* Ruprecht. *University of California Publications in Botany*, *17*(1932–1934), 111–148.

McWilliams, J. P., Côté, I. M., Gill, J. A., Sutherland, W. J. & Watkinson, A. R. (2005). Accelerating impacts of temperature-induced coral bleaching in the Caribbean. *Ecology*, *86*, 2055– 2060.

Menzel, A., & Estrella, N. (2001). Plant phenological changes. In: *"Fingerprints" of climate change*. Boston, MA: Springer, 123-137.

Menzel, A., Estrella, N., & Fabian, P. (2001). Spatial and temporal variability of the phenological seasons in Germany from 1951 to 1996. *Global Change Biology, 7*(6), 657–666.

Montfort, C. (1935). Zeitphasen der Temperatur-Einstellung und jahreszeitliche Umstellungen bei Meeresalgen. *Ber. dt. bot. Ges*. *53*, 651-74.

Neushul, M. (1972). Functional interpretation of benthic marine algal morphology. In: Abbott, I. A. & Kurogi, M. (eds), *Contributions to the systematics of benthic marine algae of the North Pacific*. Kobe. Japanese Soc. Phycol., 47-74.

Newell, R. C. (1984). The biological role of detritus in the marine environment. In: Fasham, M. J. R. (ed), *Flows of energy and materials in marine ecosystems*. New York: Plenum Press, 317-343.

Novaczek, I. (1981). Stipe growth rings in *Ecklonia radiata* (C.Ag.) J.Ag. (Laminariales). *British Phycological Journal*, *16*(4), 363–371.

Ottersen, G., Planque, B., Belgrano, A., Post, E., Reid, P. C., & Stenseth, N. C. (2001). Ecological effects of the North Atlantic Oscillation. *Oecologia*, *128*(1), 1–14.

Parke, M. (1948). Studies on British Laminariaceae. I. Growth in Laminaria Saccharina (L.) Lamour. *Journal of Marine Biology Ass. U.K.*, *27*, 651–709.

Parker, B.C. (1963). Translocation in the giant kelp *Macrocystis*. *Science, 140*, 891-2.

Parmesan, C., Ryrholm, N., Stefanescu, C., Hill, J. K., Thomas, C. D., Descimon, H., Huntley, B., Kaila, L., Kullberg, J., Tammaru, T., Tennent, W. J., Thomas, J. A., & Warren, M. (1999). Poleward shift in geographical ranges of butterfly species associated with regional warming. *Nature*, *399*, 579–583.

Pfister, C. A. (1992). Costs of reproduction in an intertidal kelp: Patterns of allocation and life history consequences. *Ecology*, *73*(5), 1586–1596.

Reed, D. C. (1990). An experimental evaluation of density dependence in a subtidal algal population. *Ecological Society of America*, *71*(6), 2286–2296.

Reed, D. C., Amsler, C. D., Ebeling, A. W. (1992). Dispersal in kelps: Factors affecting spore swimming and competency. *Ecological Society of America*, *73*(5), 1577–1585.

Reed, D. C., Ebeling, A. W., Anderson, T. W., & Anghera, M. (1996). Differential reproductive responses to fluctuating resources in two seaweeds with different reproductive strategies. *Ecological Society of America*, *77*(1), 300–316.

Reed, D. C., & Foster, M. S. (1984). The effects of canopy shadings on algal recruitment and growth in a giant kelp forest. *Ecological Society of America*, *65*(3), 937–948.

Riebesell, U., Zondervan, I., Rost, B., Tortell, P. D., Zeebe, R. E., & Morel, F. M. M. (2000). Reduced calcification of marine plankton in response to increased atmospheric CO_2. *Nature, 407*(6802), 364–367.

Schaffelke, B., & Lüning, K. (1994). A circannual rhythm controls seasonal growth in the kelps *Laminaria hyperborea* and *L. digitata* from Helgoland (North Sea). *European Journal of Phycology*, *29*(1), 49-56.

Schmitz, K., & Lobban, C. (1976). A survey of translocation in Laminariales (Phaeophyceae). *Marine Biology*, *36*, 207–216.

Schmitz, K., Srivastava, L. M. (1976). The fine structure of sieve elements of *Nereocystis luetkeana*. *American Journal of Botany*, *63*(5), 679–693.

Schmitz, K., & Srivastava, L. M. (1979). Long Distance Transport in Macrocystis integrifolia. *Plant Physiology*, *63*, 995–1002.

Seymour, R. J., Tegner, M. J., Dayton, P. K., & Parnell, P. E. (1989). Storm wave induced mortality of giant kelp, *Macrocystis pyrifera*, in southern California. *Estuarine, Coastal and Shelf Science*, *28*, 277–292.

Simpson, J. P. (1972). *The geology of Carmel Bay, California* (MS thesis, Naval Postgraduate School).

Somero, G.N. (2002). Thermal physiology and vertical zonation of intertidal animals: optima, limits, and costs of living. *Integ. and Comp. Biol.*, *42*, 780–789.

Sousa, W. P. (1985). Disturbance and patch dynamics on rocky intertidal shores. In: Pickett, S. T. A., White, P.S. (eds) *The ecology of natural disturbance and patch dynamics*. Orlando: Academic Press, 101-124.

Sousa, W. P. (2001). Natural disturbance and the dynamics of marine benthic communities. In: M. D. Bertness, S. D. Gaines, and M. E. Hay, (eds) *Marine Community Ecology.* Sunderland, MA: Sinauer Associates, 85–130.

Sparks, T., Heyen, H., Braslavska, O., & Lehikoinen, E. (1999). Are European birds migrating earlier. *bto News, 223*(8), 82-87.

Stephenson, T. A., & Stephenson, A. (1949). The universal features of zonation between tide-marks on rocky coasts. *Journal of Ecology, 37*(2), 289–305.

Storlazzi, C. D., & Field, M. E. (2000). Sediment distribution and transport along a rocky, embayed coast: Monterey Peninsula and Carmel Bay, California. *Marine Geology*, *170*, 289–316.

Tcherkez, G., Farquhar, G., Badeck, F., & Ghashghaie, J. (2004). Theoretical considerations about carbon isotope distribution in glucose of C_3 plants. *Functional Plant Biology*, *31*, 857–877.

tom Dieck, I. (1991). Circannual growth rhythm and photoperiodic sorus induction in the kelp *Laminaria setchellii* (Phaeophyta). *Journal of Phycology*, *27*, 341–350.

Walther, G., Post, E., Convey, P., Menzel, A., Parmesan, C., Beebee, T. J. C., Fromentin, J., I, O. H., & Bairlein, F. (2002). Ecological responses to recent climate change. *Nature*, *416*, 389–395.

Werner, C., & Gessler, A. (2011). Diel variations in the carbon isotope composition of respired CO_2 and associated carbon sources: A review of dynamics and mechanisms. *Biogeosciences*, *8*(9), 2437–2459.

Wieser, W. (ed). (1973). *Effects of temperature on ectothermic organisms*. New York: Springer-Verlag.

Wood, C. M., and D. G. McDonald, editors. (1996). *Global warming: implications for freshwater and marine fish*. New York: Cambridge University Press.

Woodward, F. I. (1987). *Climate and plant distribution*. New York: Cambridge University Press.

Woolf, D., & Wolf, J. (2013). Impacts of climate change on storms and waves. *MCCIP Science Review*, *2013*, 20–26.

Wuethrich, B. (2000). How climate change alters rhythms of the wild. *Science, 287*(5454), 793–795.

FIGURES

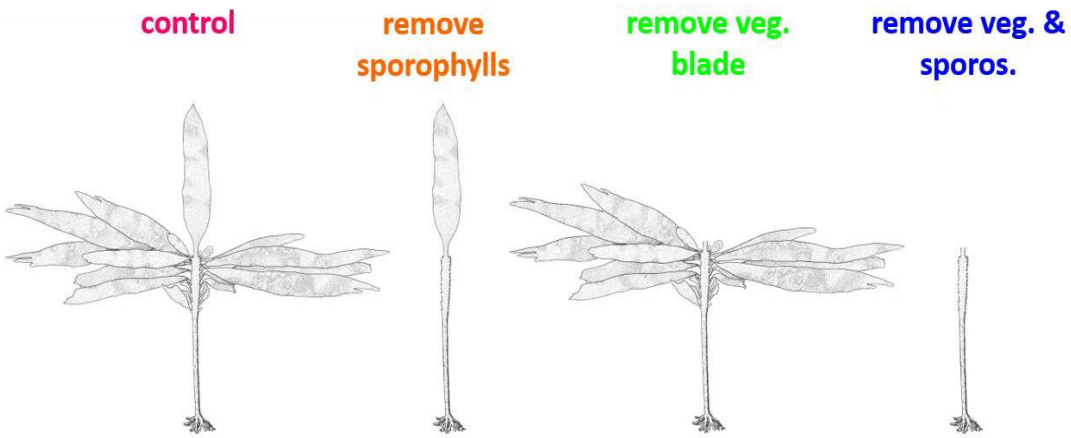

Figure 1: Manipulation treatments performed on experimental *Pterygophora californica* thalli

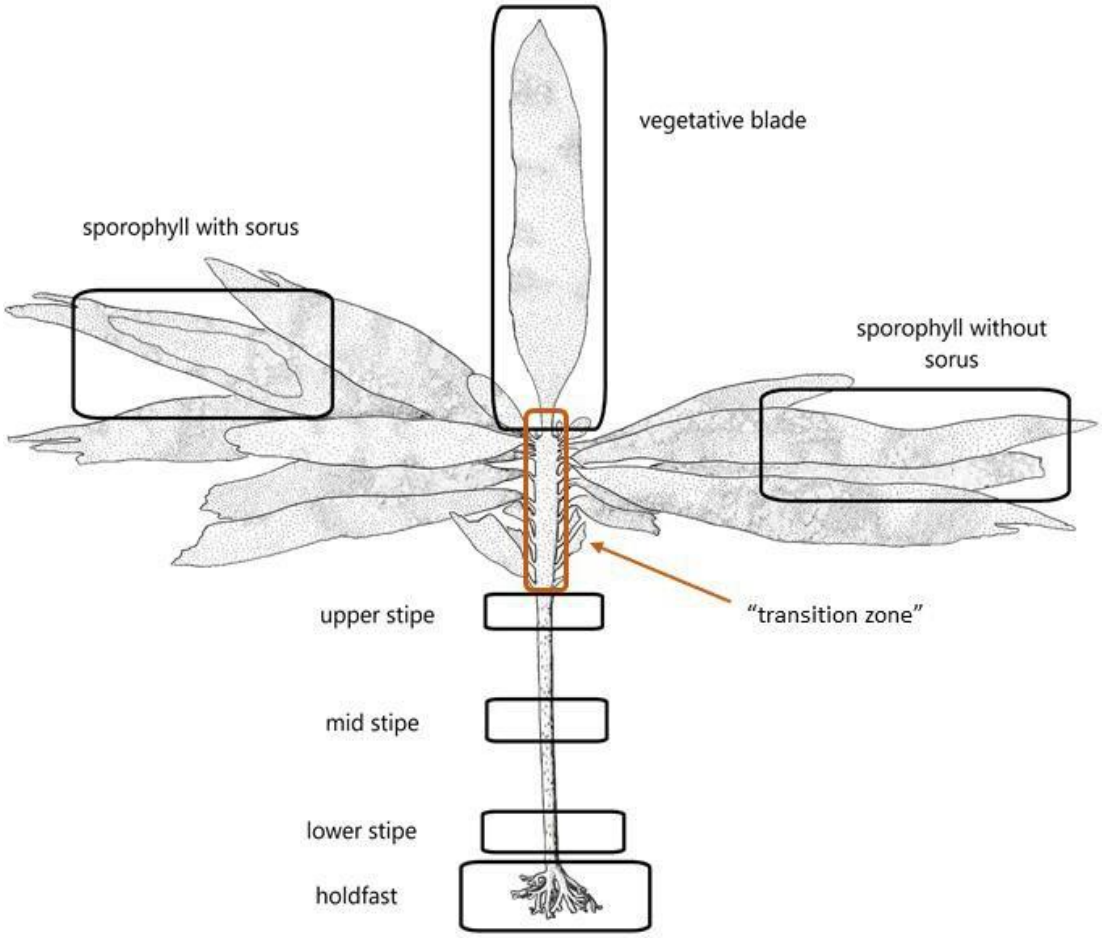

Figure 2: Section designations for samples taken from harvested *Pterygophora* thalli. Upper stipe samples were taken below the "transition zone" as indicated. Samples were used for the chemical analyses.

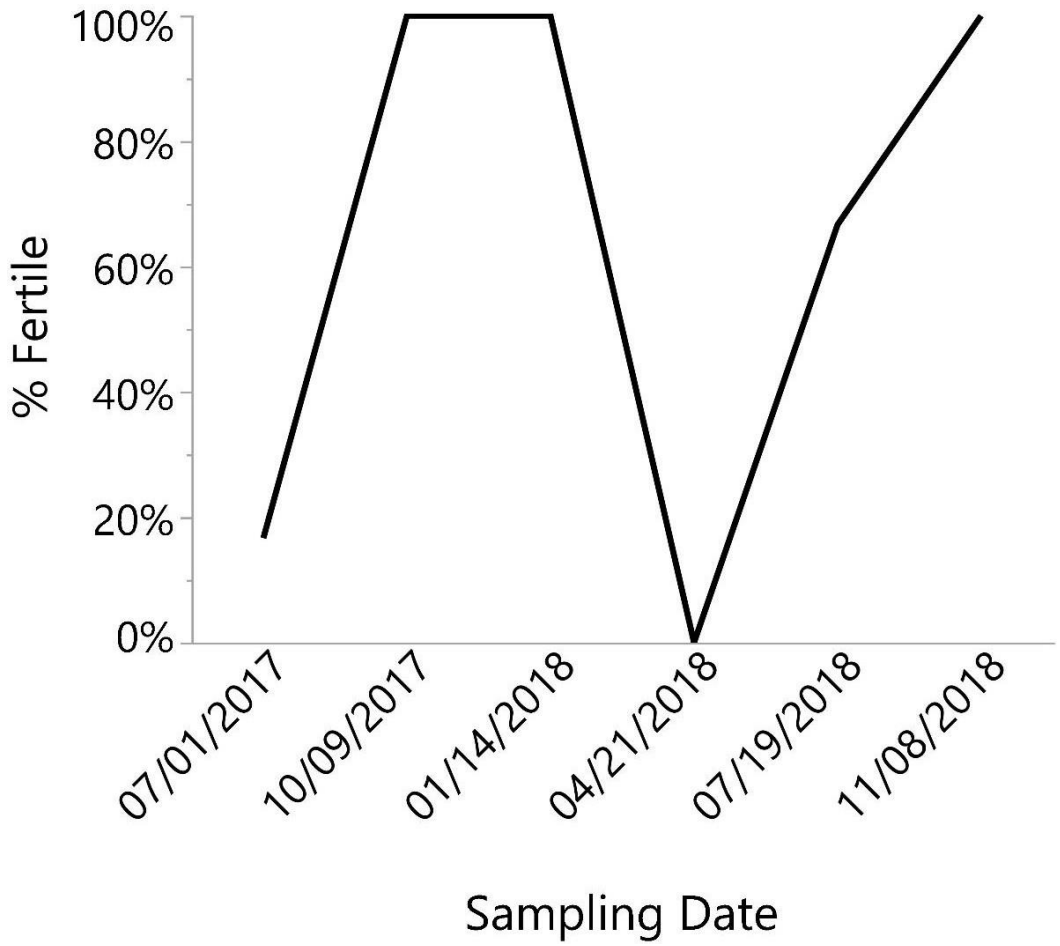

Figure 3: Percent of harvested control thalli that were reproductive on each sampling date (n = 6, n = 6, n = 3, n = 4, n = 3, n = 3) respectively.

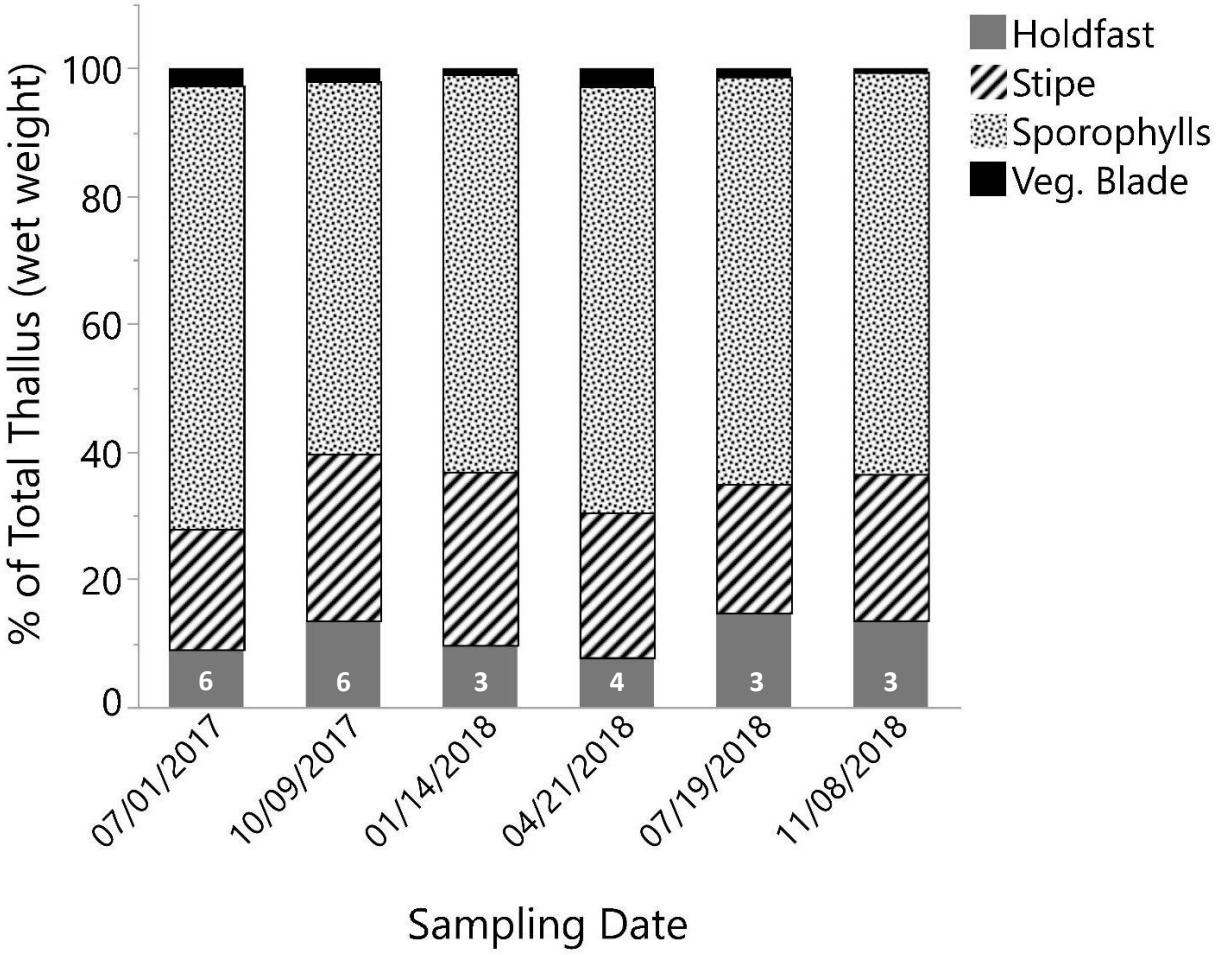

Figure 4: Wet weight of thallus regions as the % of total thallus biomass for control thalli harvested among sampling dates. Sample sizes are indicated by the number at the base of each bar.

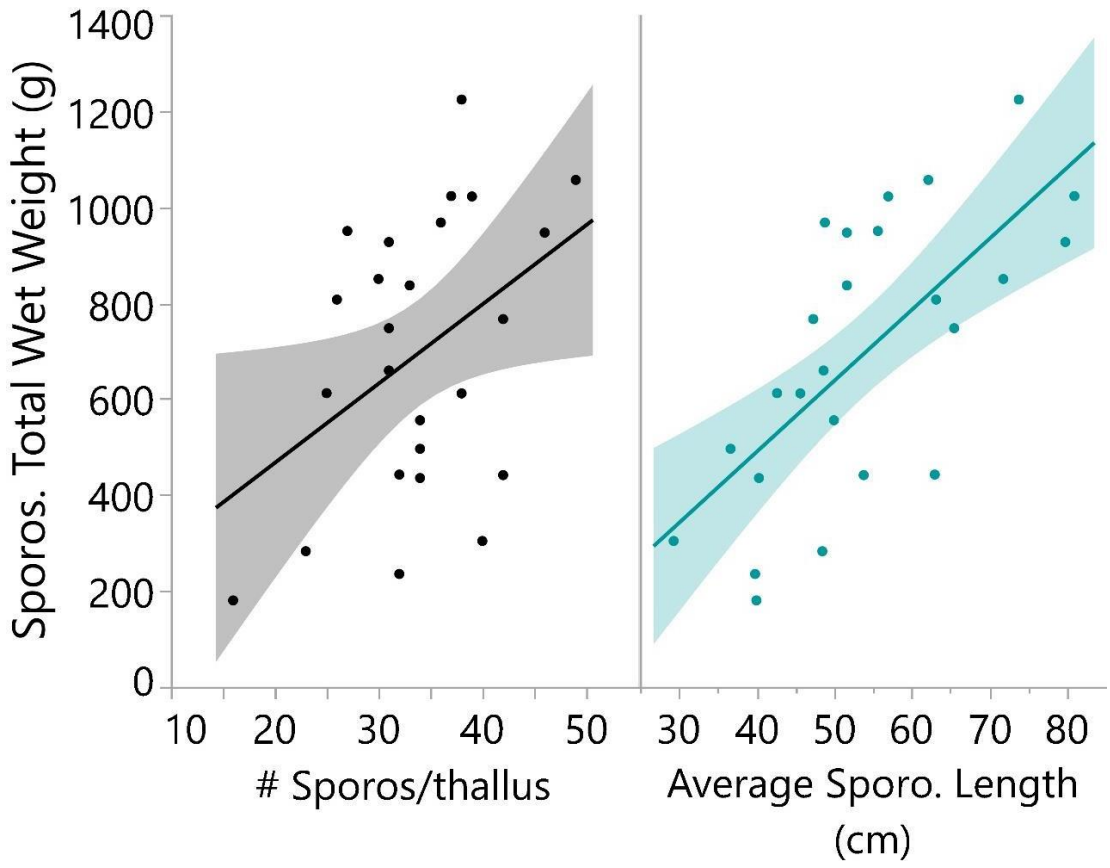

Figure 5: Regression analysis of the relationship of total wet weight of sporophylls (g) to the number of sporophylls per thallus (n = 25, y = 135.9 + 16.53*x) and the average sporophyll length (cm) (n = 25, y = -102.8 + 14.8*x) for harvested control thalli. Shaded region is 95% confidence interval.

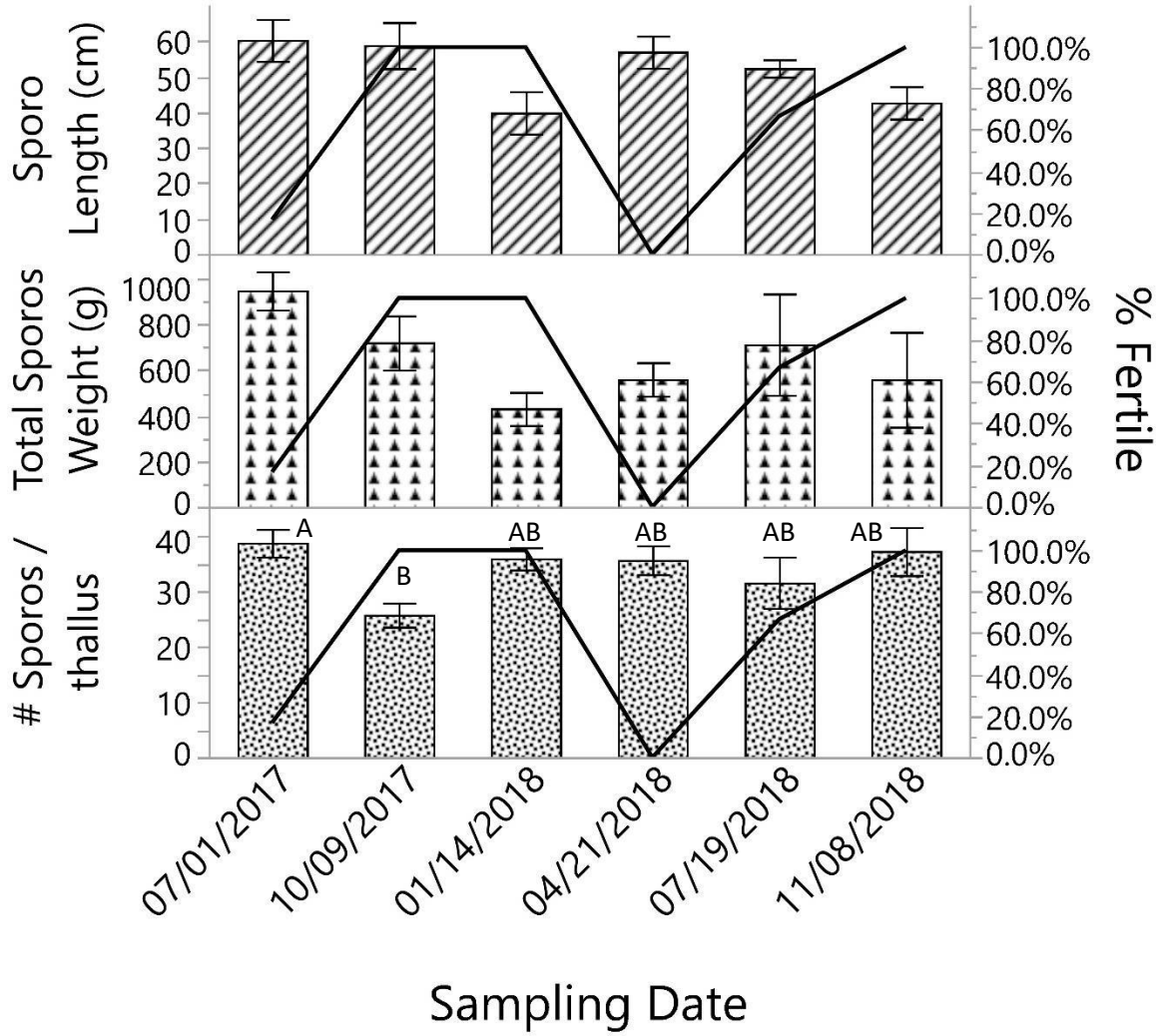

Figure 6: Mean sporophyll length (cm), total wet weight of sporophylls (g), and number of sporophylls of harvested control thalli among sampling dates (n = 6, n = 6, n = 3, n = 4, n = 3, n = 3) respectively. Letters indicate significant differences among sampling dates; sampling dates not connected by the same letter are significantly different. Line graph overlay is percent of fertile thalli in the sampled control population (%). Error bars are ±SE.

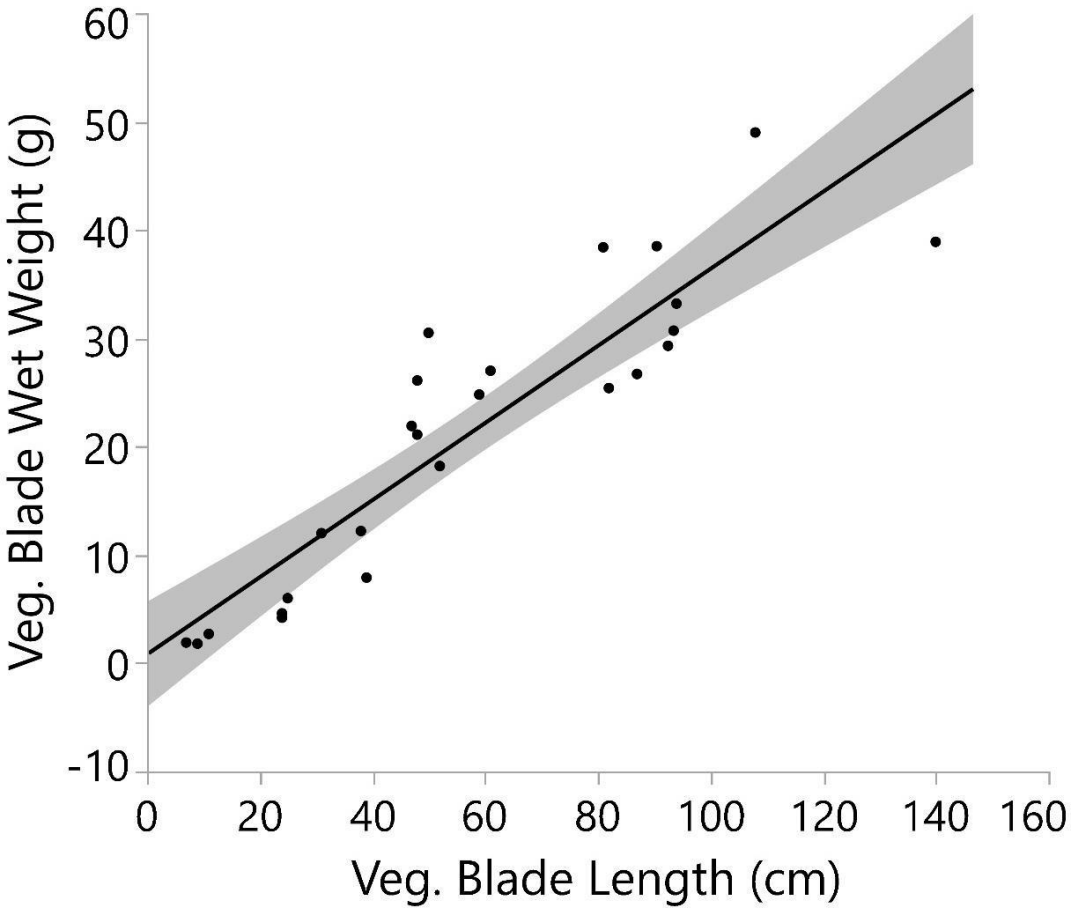

Figure 7: Regression analysis of the relationship between wet weight of the vegetative blade (g) and the vegetative blade length (cm) for harvested control thalli (n = 25, y = 0.7917 + 0.356*x). Shaded region is 95% confidence interval.

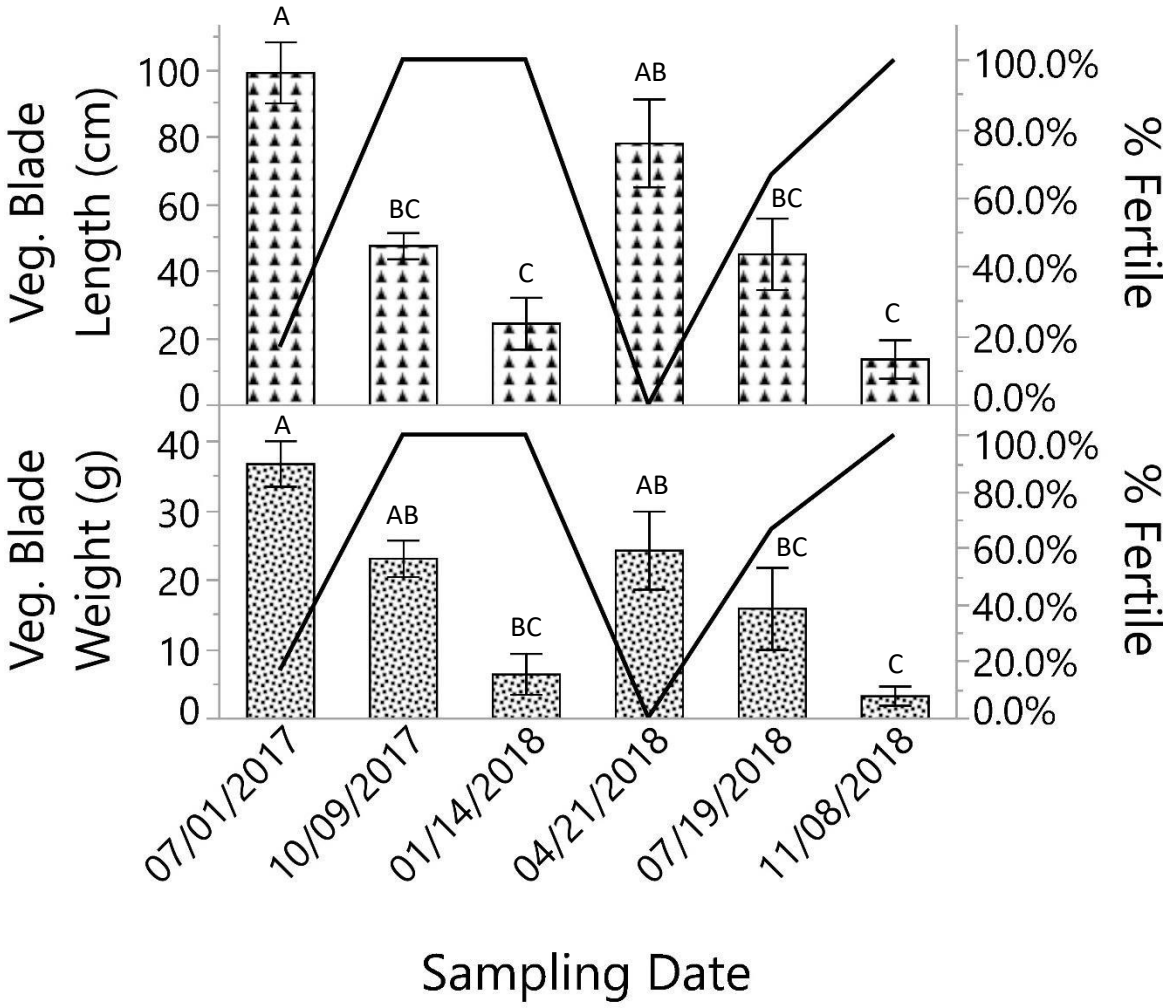

Figure 8: Mean wet weight of the vegetative blade (g) and vegetative blade length (cm) of harvested control thalli among sampling dates (n = 6, n = 6, n = 3, n = 4, n = 3, n = 3) respectively. Letters indicate significant differences among sampling dates; sampling dates not connected by the same letter are significantly different. Line graph overlay is percent of fertile thalli in the sampled control population (%). Error bars are ±SE.

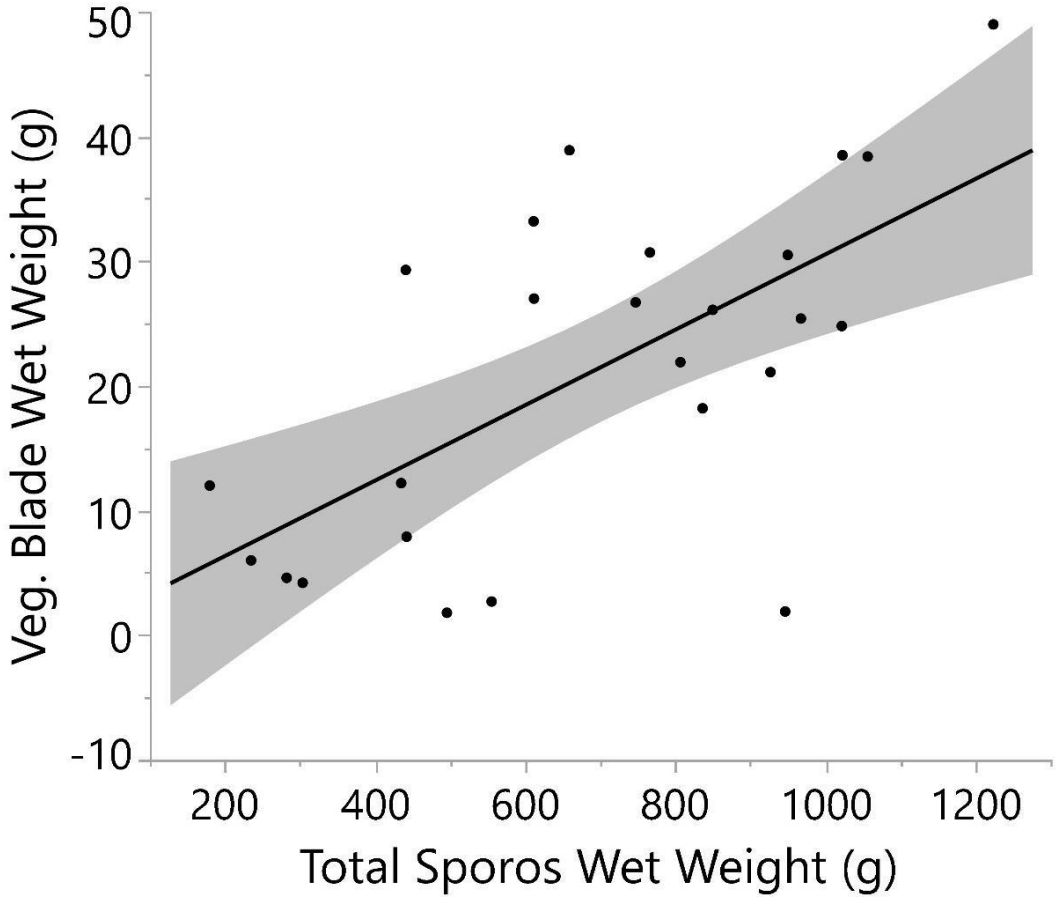

Figure 9: Regression analysis of the relationship between total wet weight of sporophylls (g) and the wet weight of the vegetative blade (g) for harvested control thalli (n = 25, y = 0.2899 + 0.03025*x). Shaded region is 95% confidence interval.

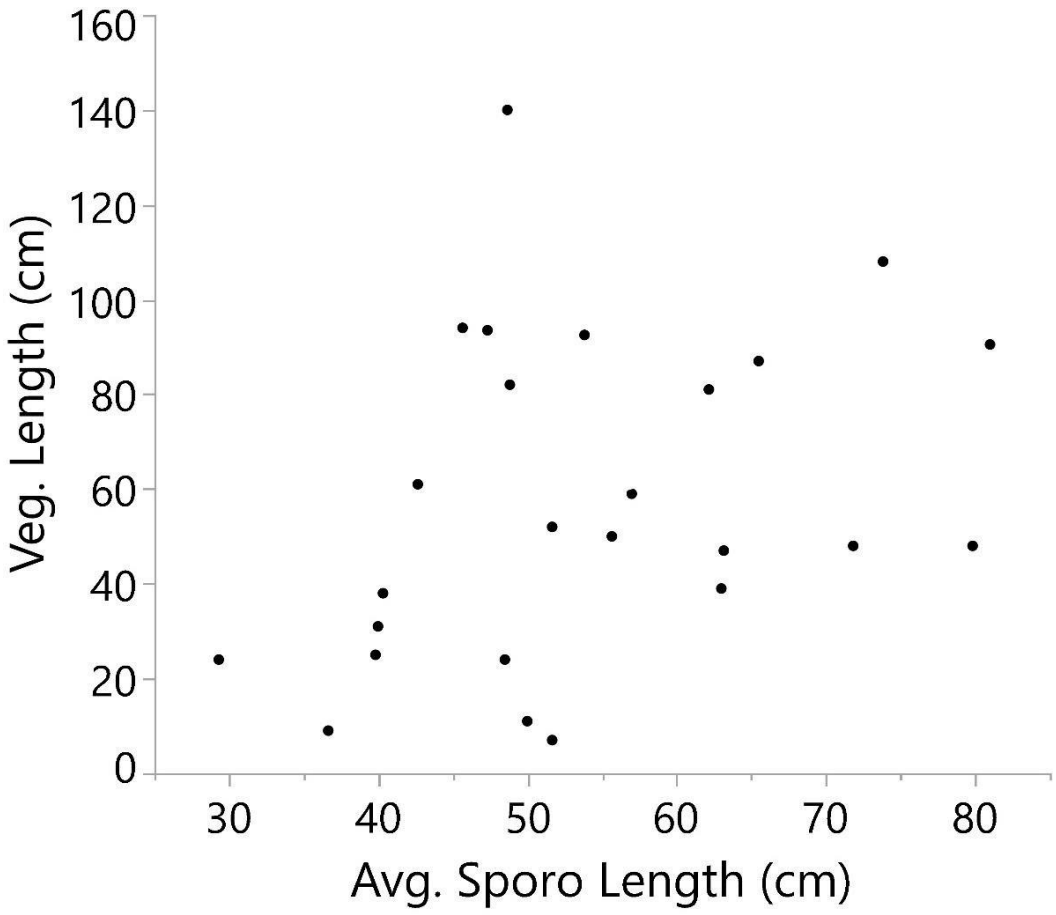

Figure 10: Regression analysis of the relationship between average sporophyll length (cm) and vegetative blade length (cm) for harvested control thalli from all sampling dates (n = 25).

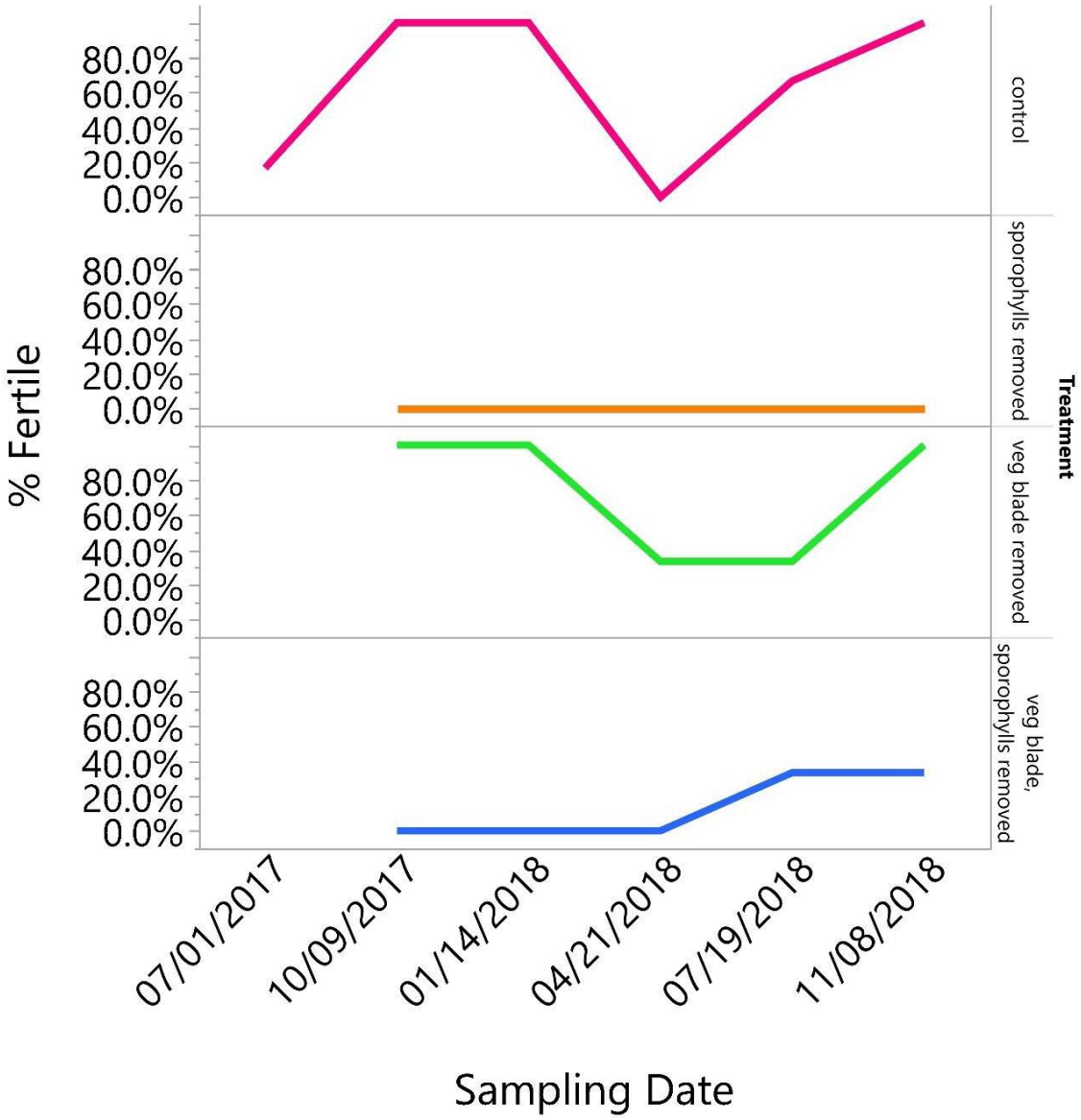

Figure 11: Percent of harvested control & manipulated thalli that were reproductive on each sampling date among treatments. On 7/1/2017, only control thalli were harvested as it was the start of experimental manipulations. Control thalli and experimental thalli were harvested on all other sampling dates. Sample sizes among treatments and sampling dates are as follows: control (n = 6, n = 6, n = 3, n = 4, n = 3, n = 3, respectively); minus sporophylls (n = 0, n = 6, n = 3, n = 3, n = 3, n = 3, respectively); minus vegetative blade (n = 0, n = 6, n = 3, n = 3, n = 3, n = 3, respectively); minus vegetative blade and sporophylls (n = 0, n = 6, n = 3, n = 3, n = 3, n = 3, respectively).

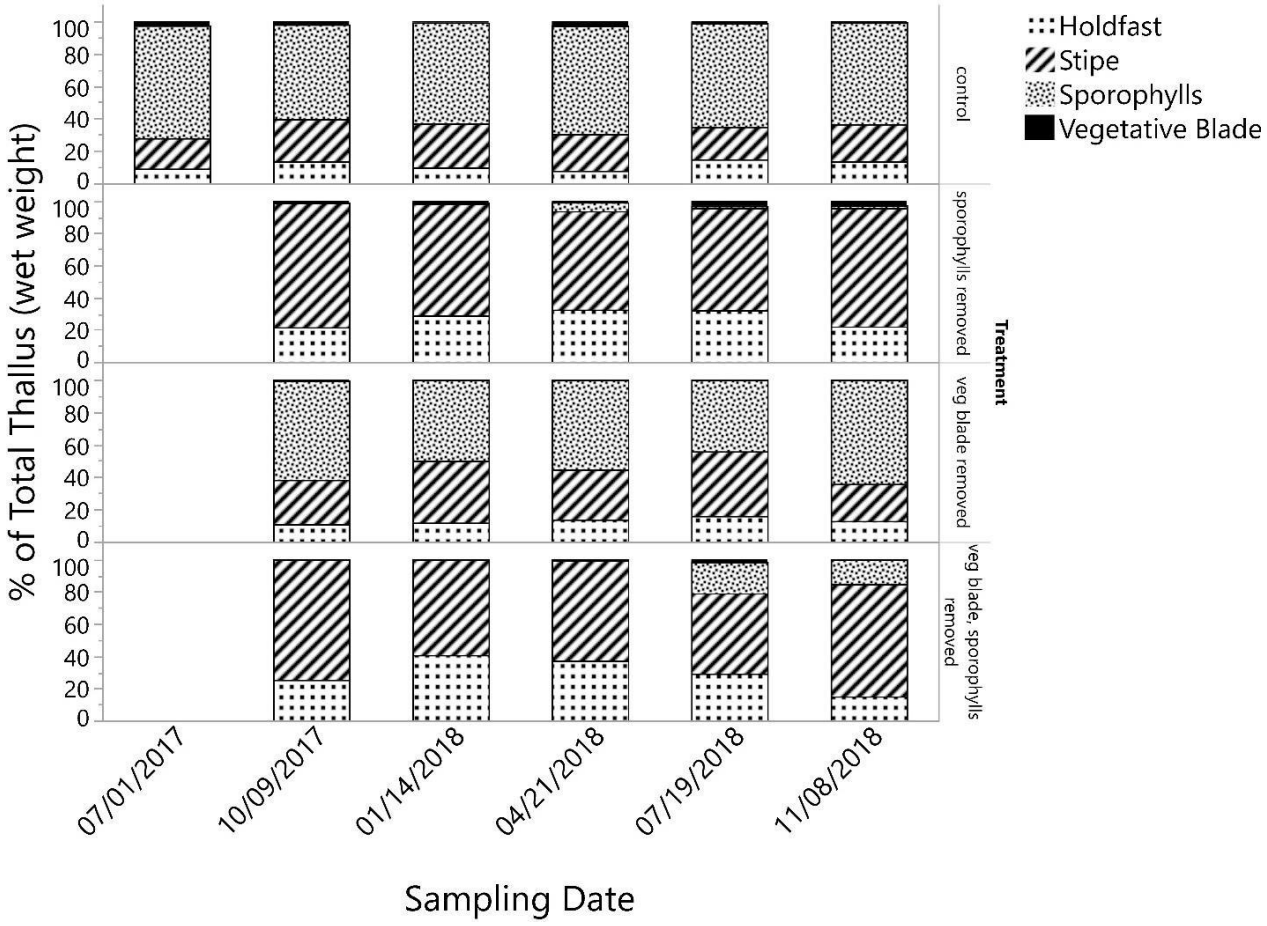

Figure 12: Wet weight of thallus regions as the % of total thallus biomass for control & manipulated thalli harvested among sampling dates and treatments. On 7/1/2017, only control thalli were harvested as it was the start of experimental manipulations. Control thalli and experimental thalli were harvested on all other sampling dates. Sample sizes among treatments and sampling dates are as follows: control (n = 6, n = 6, n = 3, n = 4, n = 3, n = 3, respectively); minus sporophylls (n = 0, n = 6, n = 3, n = 3, n = 3, n = 3, respectively); minus vegetative blade (n = 0, n = 6, n = 3, n = 3, n = 3, n = 3, respectively); minus vegetative blade and sporophylls (n = 0, n = 6, n = 3, n = 3, n = 3, n = 3, respectively).

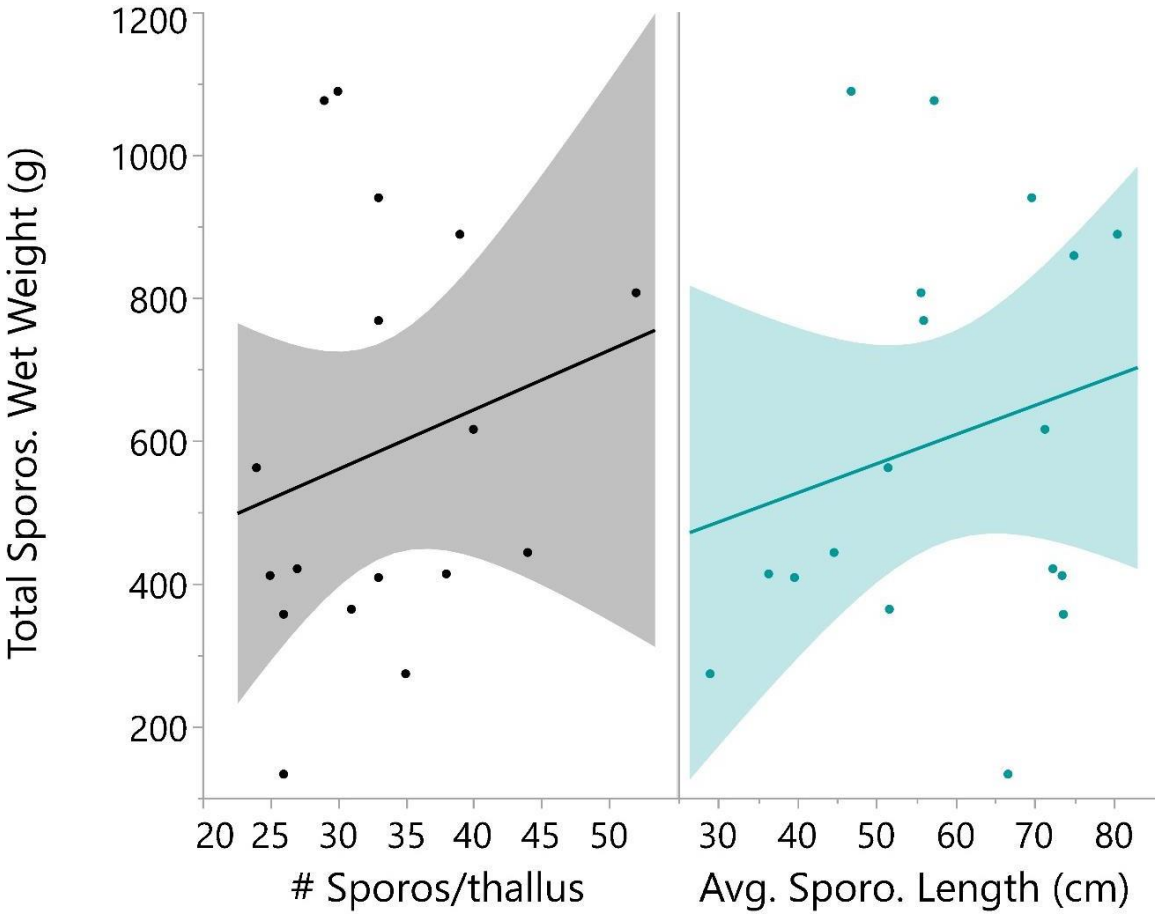

Figure 13: Regression analysis of the relationship of total wet weight of sporophylls (g) to the number of sporophylls per thallus (n = 18, y = 309.6 + 8.33*x) and the average sporophyll length (cm) (n = 18, y = 363.3 + 4.08*x) for harvested thalli from the minus vegetative blade treatment. Shaded region is 95% confidence interval.

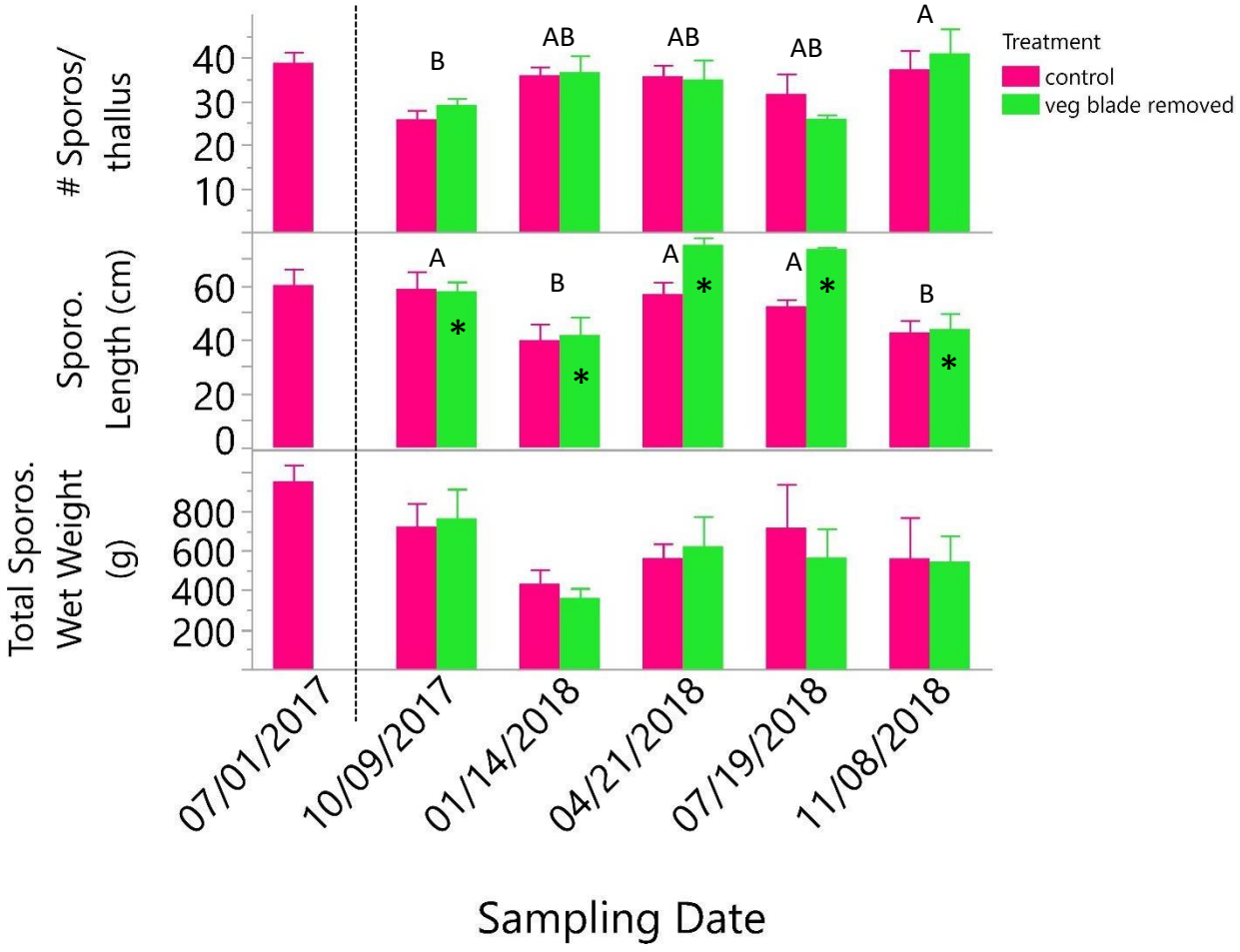

Figure 14: Mean number of sporophylls, total wet weight of sporophylls (g), and sporophyll length (cm) of harvested control & minus veg. blade treatment thalli among sampling dates. On 7/1/2017, only control thalli were harvested as it was the start of experimental manipulations. Data to the right of the dotted line were included in the analysis of variance. Letters indicate significant differences among sampling dates; sampling dates not connected by the same letter are significantly different. Asterisks indicate a significant difference between treatments. Sample sizes among treatments and sampling dates are as follows: control (n = 6, n = 6, n = 3, n = 4, n = 3, n = 3, respectively); minus vegetative blade (n = 0, n = 6, n = 3, n = 3, n = 3, n = 3, respectively). Error bars are ±SE.

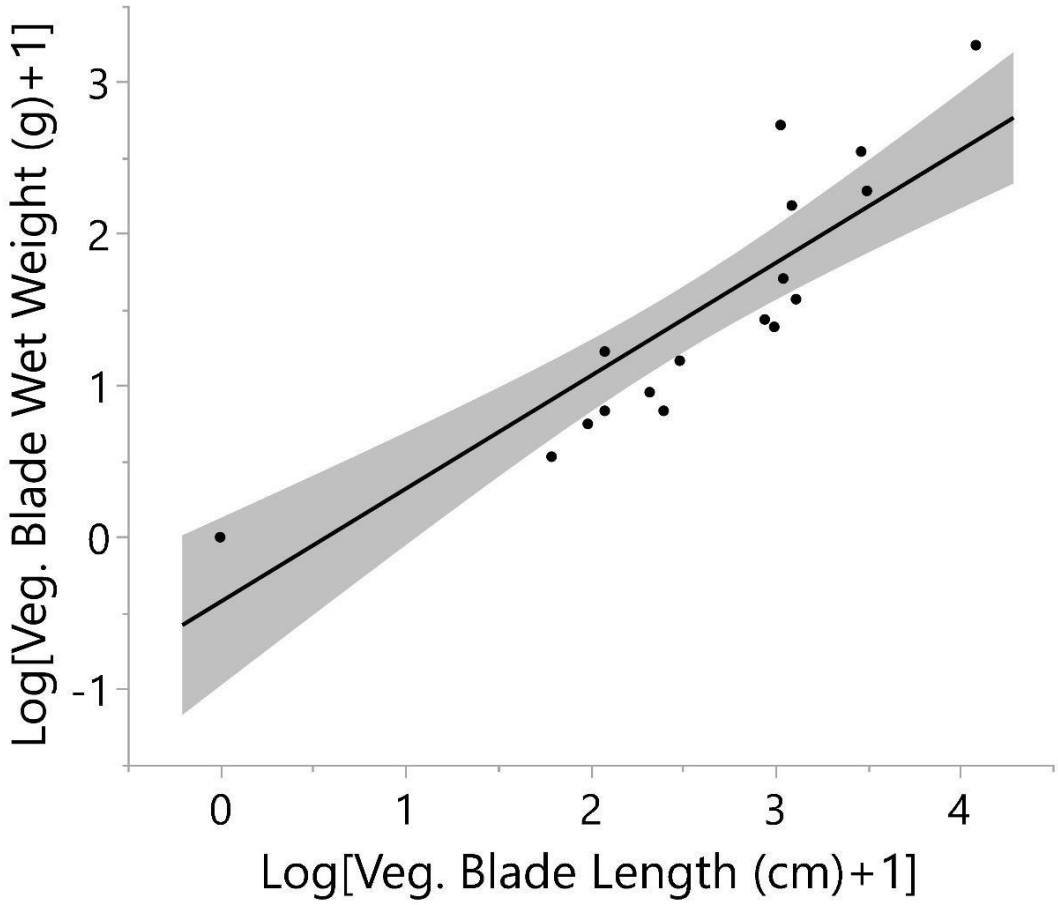

Figure 15: Regression analysis of the relationship between the vegetative blade wet weight (g) and the vegetative blade length (cm) for harvested thalli from the minus sporophylls treatment (n = 18, y = -0.4275 + 0.744*x). Data was Log [x+1] transformed to satisfy the assumption of normal distribution. Shaded region is 95% confidence interval.

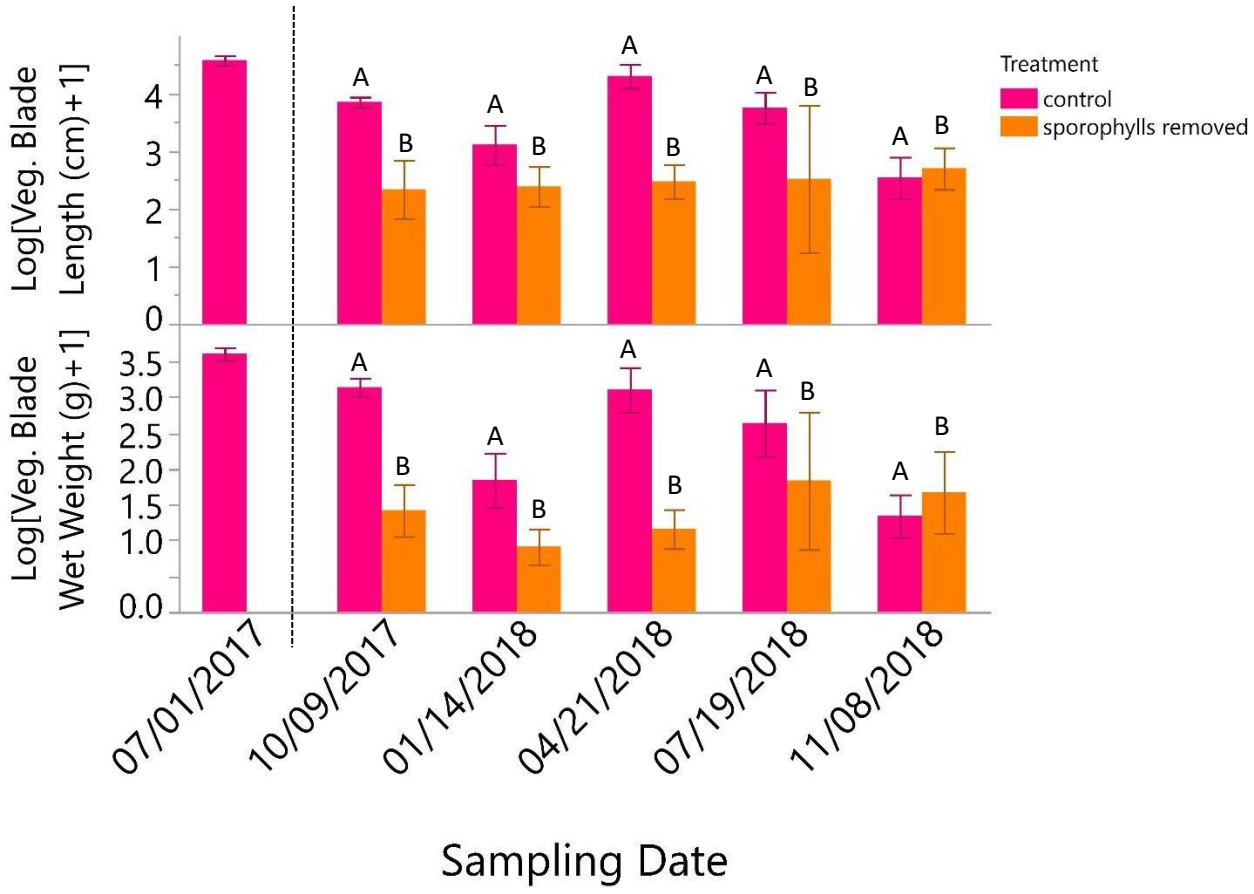

Figure 16: Mean vegetative blade length (cm) and wet weight (g) of harvested control & minus sporophylls treatment thalli among sampling dates. Data was Log [x+1] transformed to satisfy the assumption of normal distribution. On 7/1/2017, only control thalli were harvested as it was the start of experimental manipulations. Data to the right of the dotted line were included in the analysis of variance. Letters indicate significant differences among treatments; treatments not connected by the same letter are significantly different. Sample sizes among treatments and sampling dates are as follows: control (n = 6, n = 6, n = 3, n = 4, n = 3, n = 3, respectively); minus vegetative blade (n = 0, n = 6, n = 3, n = 3, n = 3, n = 3, respectively). Error bars are ±SE.

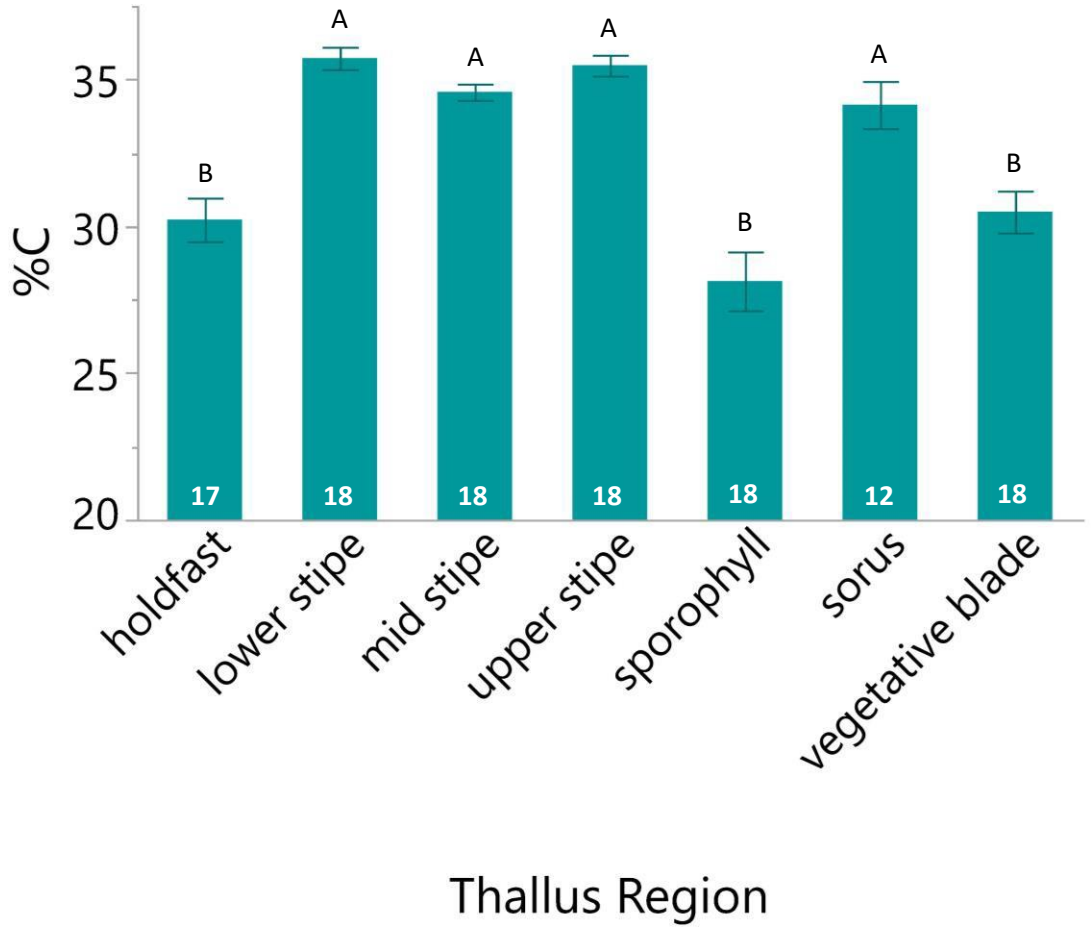

Figure 17: Mean %C among thallus regions of harvested control thalli for all sampling dates. Sample sizes are indicated by the number at the base of each bar. Letters indicate significant differences among thallus regions; thallus regions not connected by the same letter are significantly different. Error bars are ±SE.

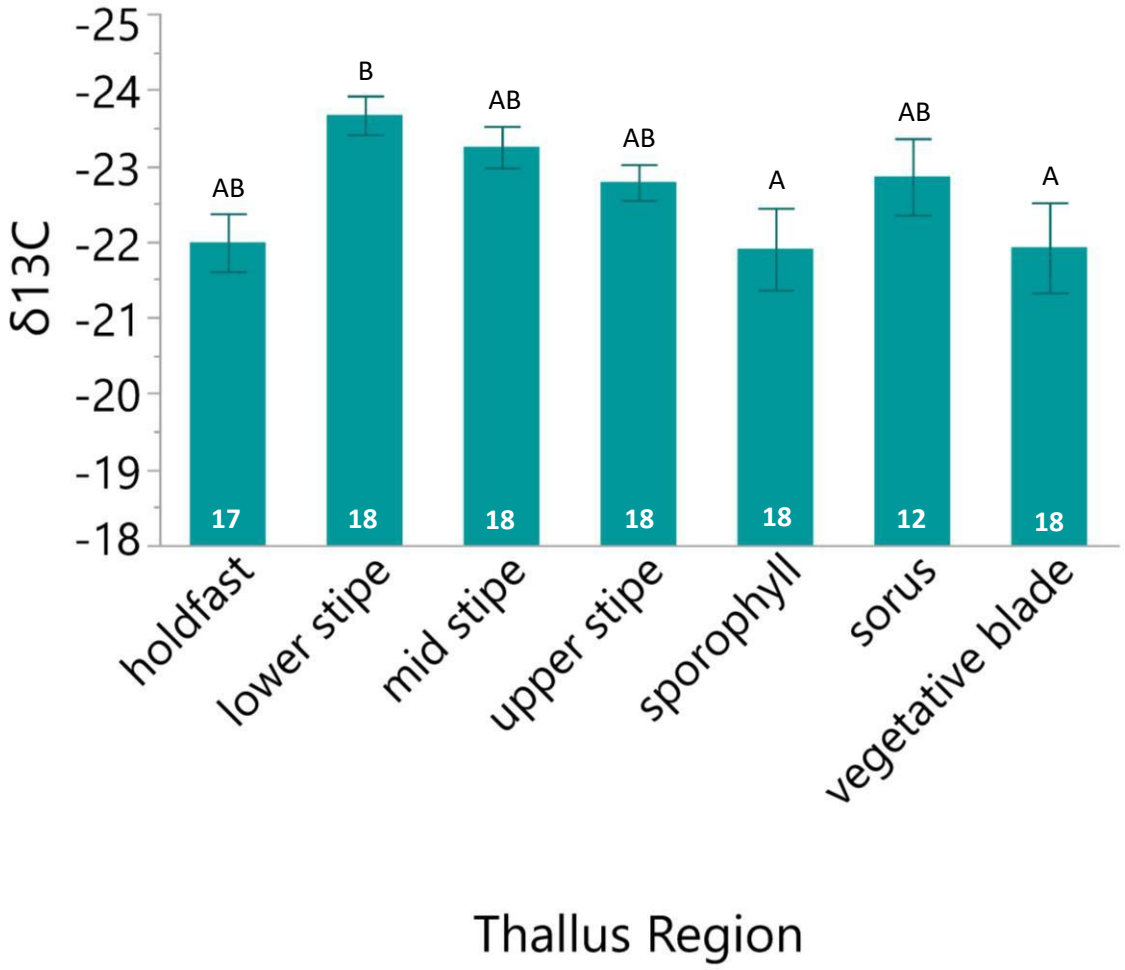

Figure 18: Mean $\delta^{13}C$ among thallus regions of harvested control thalli for all sampling dates. Sample sizes are indicated by the number at the base of each bar. Letters indicate significant differences among thallus regions; thallus regions not connected by the same letter are significantly different. Error bars are ±SE.

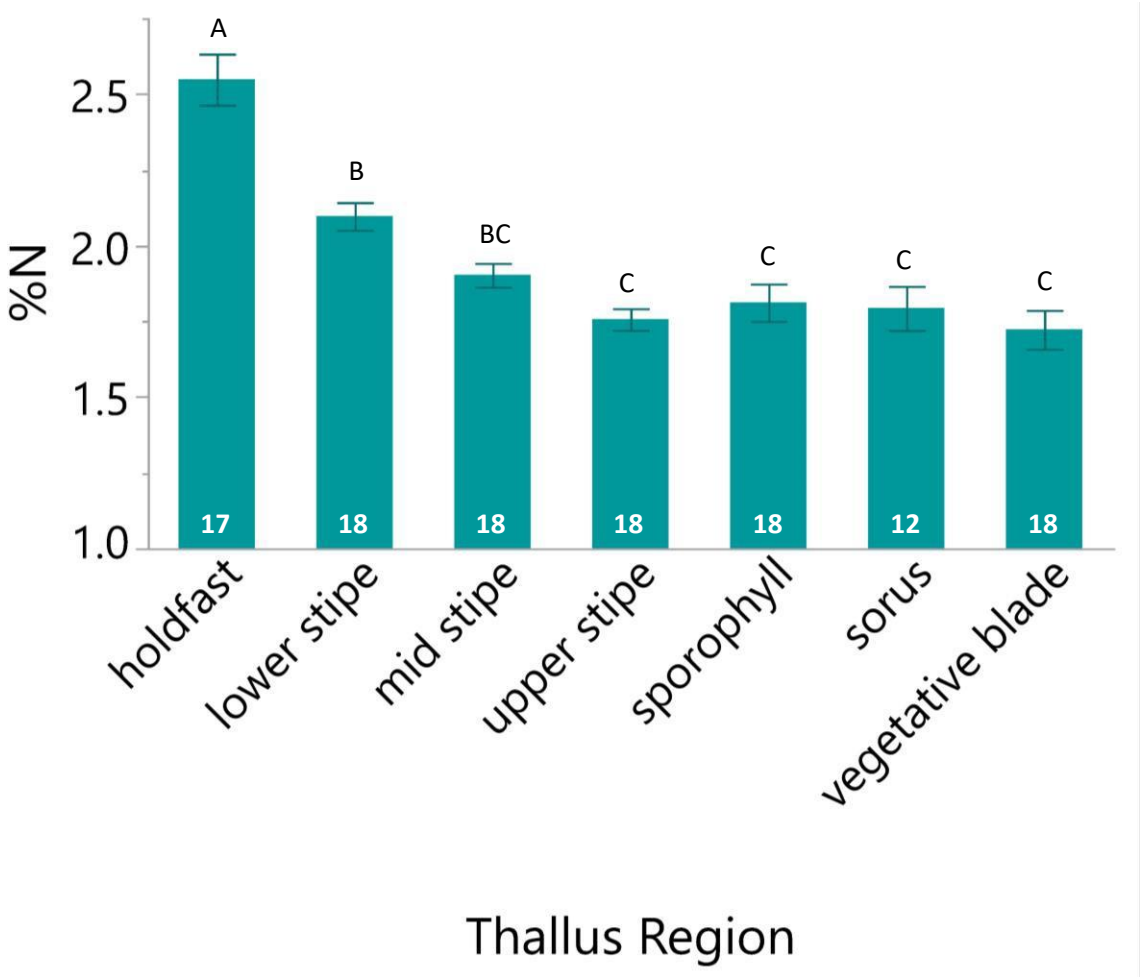

Figure 19: Mean %N among thallus regions of harvested control thalli for all sampling dates. Sample sizes are indicated by the number at the base of each bar. Letters indicate significant differences among thallus regions; thallus regions not connected by the same letter are significantly different. Error bars are ±SE.

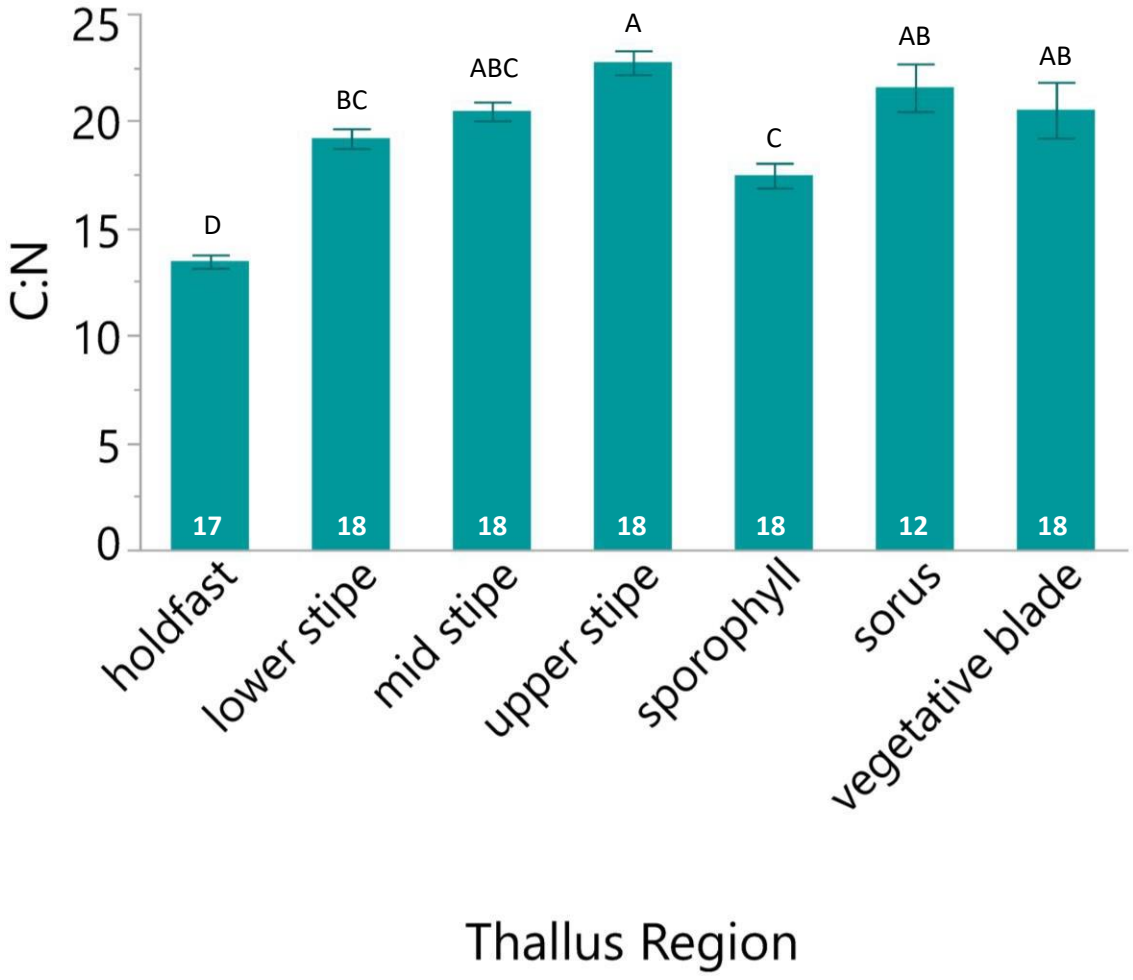

Figure 20: Mean C:N among thallus regions of harvested control thalli for all sampling dates. Sample sizes are indicated by the number at the base of each bar. Letters indicate significant differences among thallus regions; thallus regions not connected by the same letter are significantly different. Error bars are ±SE.

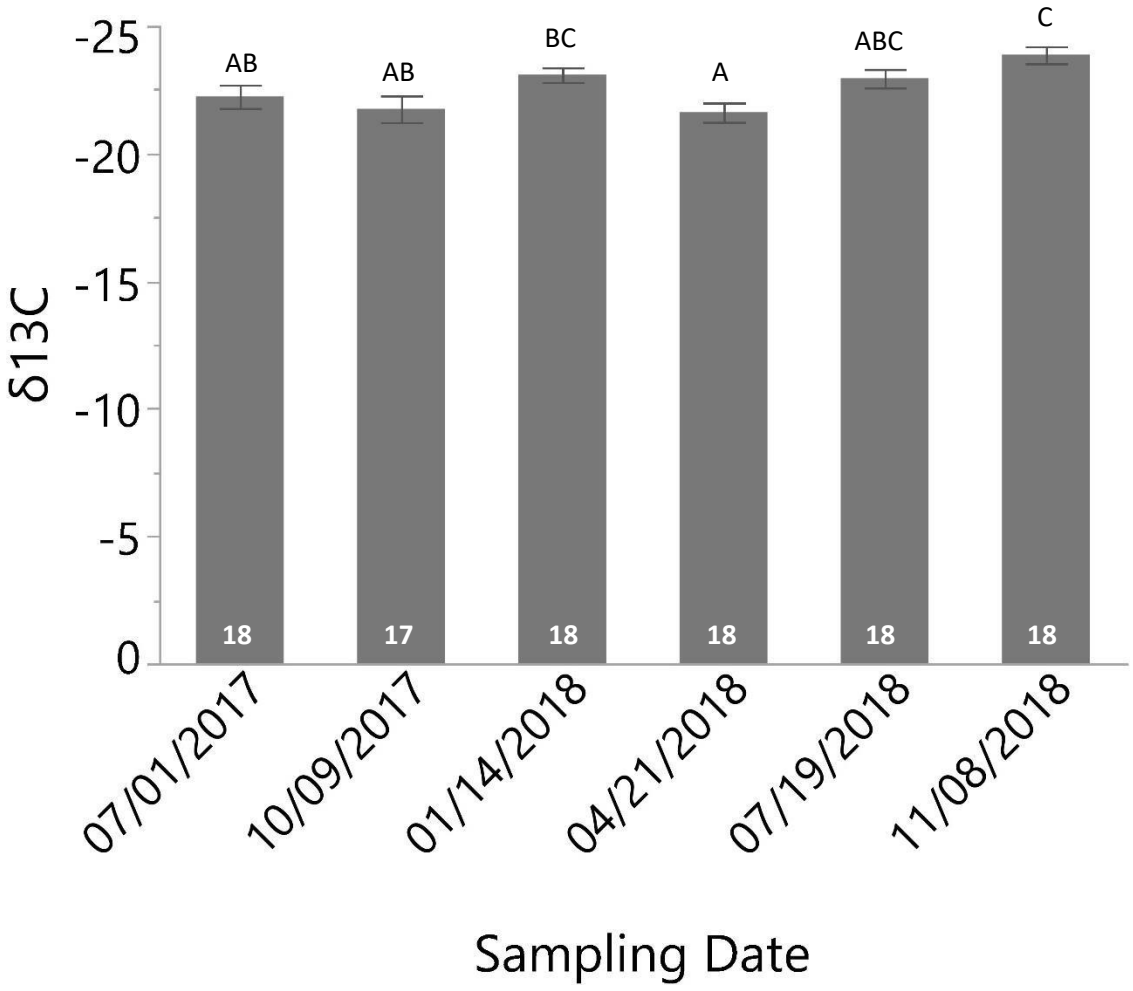

Figure 21: Mean $\delta^{13}C$ of harvested control thalli among sampling dates. "Sorus" thallus region was excluded from these data because it was not present on each sampling date. Sample sizes are indicated by the number at the base of each bar. Letters indicate significant differences among sampling dates; sampling dates not connected by the same letter are significantly different. Error bars are ±SE.

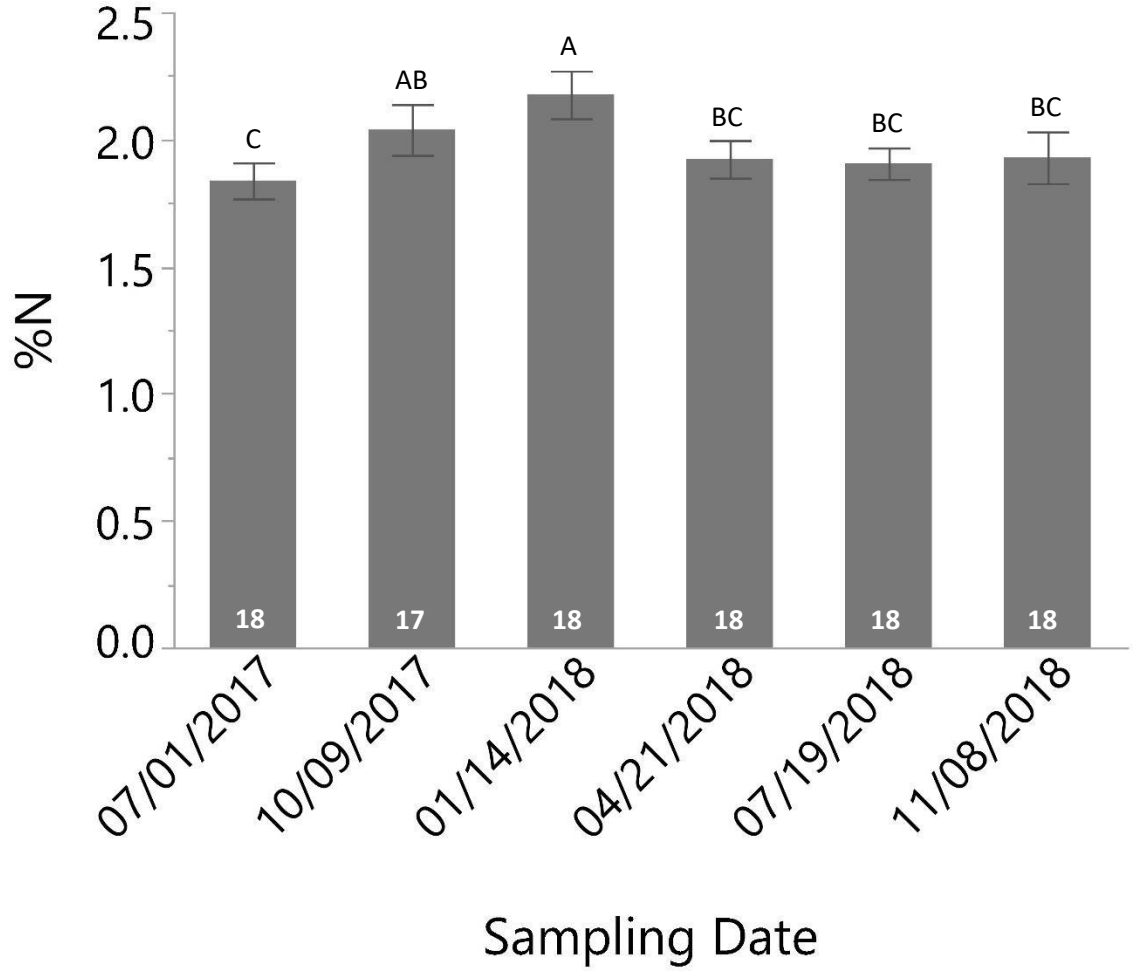

Figure 22: Mean %N of harvested control thalli among sampling dates. "Sorus" thallus region was excluded from these data because it was not present on each sampling date. Sample sizes are indicated by the number at the base of each bar. Letters indicate significant differences among sampling dates; sampling dates not connected by the same letter are significantly different. Error bars are ±SE.

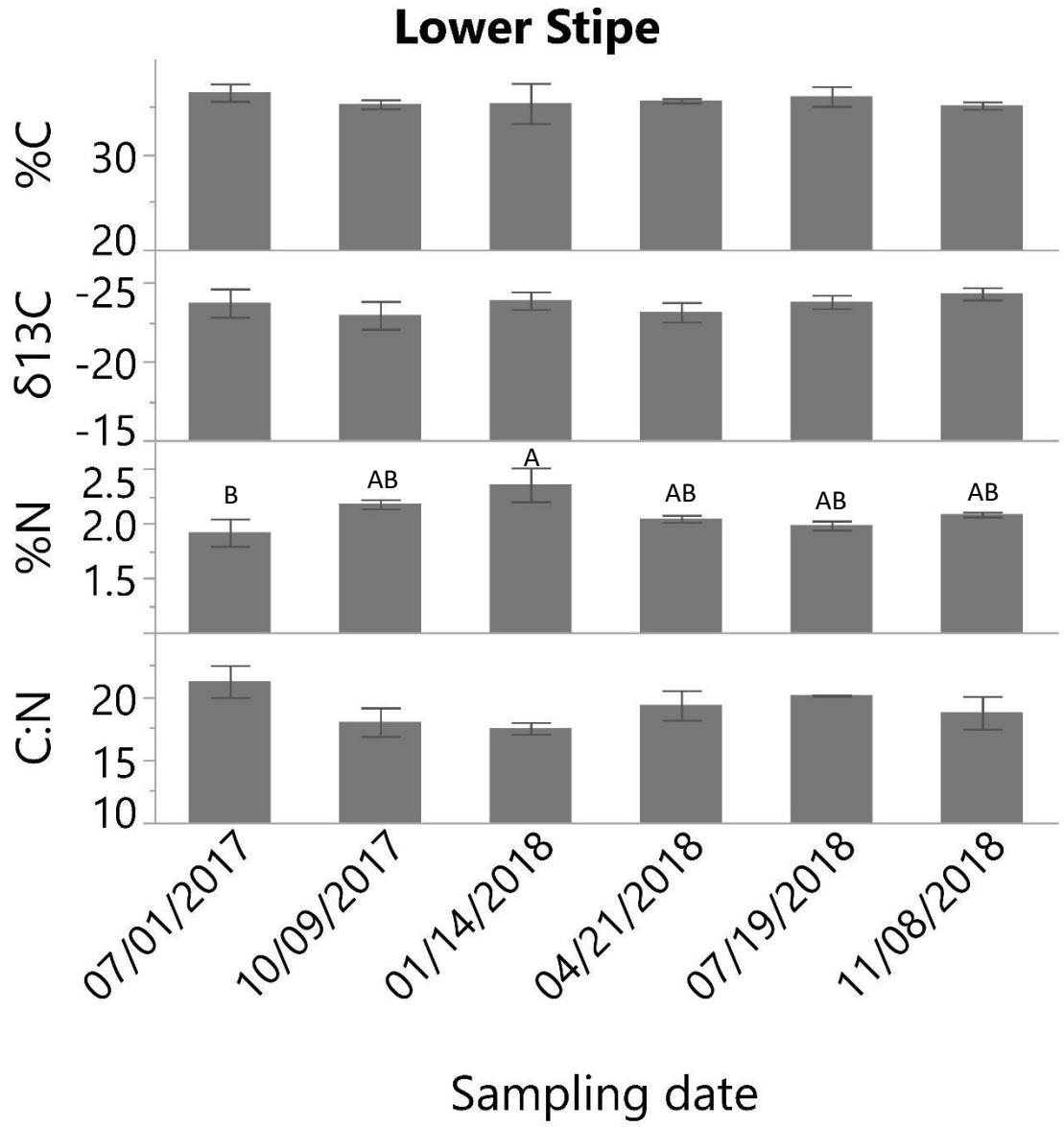

Figure 23: Mean %C, δ13C, %N, and C:N values for the lower stipe region of control thalli among all sampling dates. Sample size for each bar is n = 3. Letters indicate significant differences among sampling dates; sampling dates not connected by the same letter are significantly different. Error bars are ±SE.

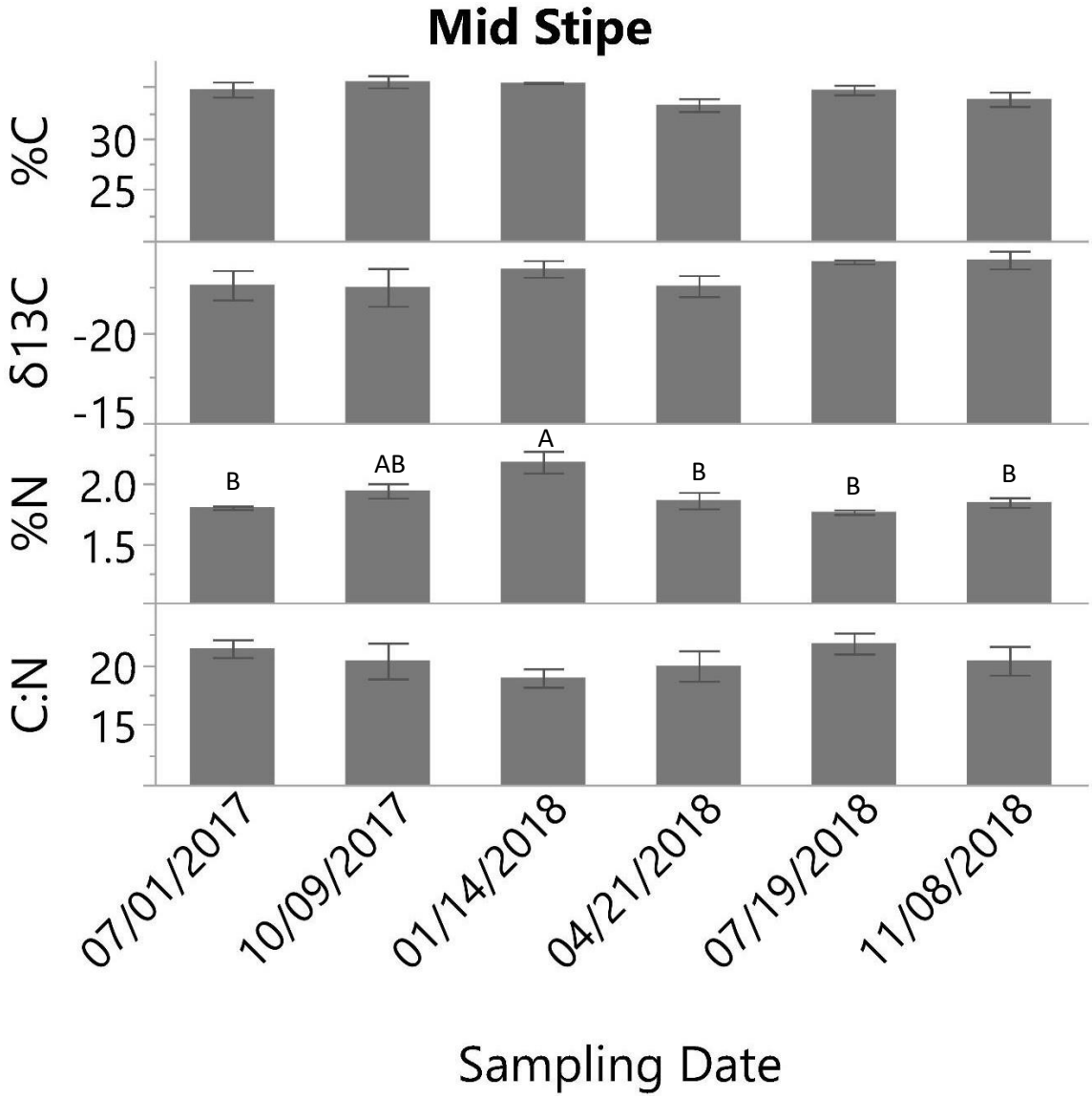

Figure 24: Mean %C, δ13C, %N, and C:N values for the mid stipe region of control thalli among all sampling dates. Sample size for each bar is n = 3. Letters indicate significant differences among sampling dates; sampling dates not connected by the same letter are significantly different. Error bars are ±SE.

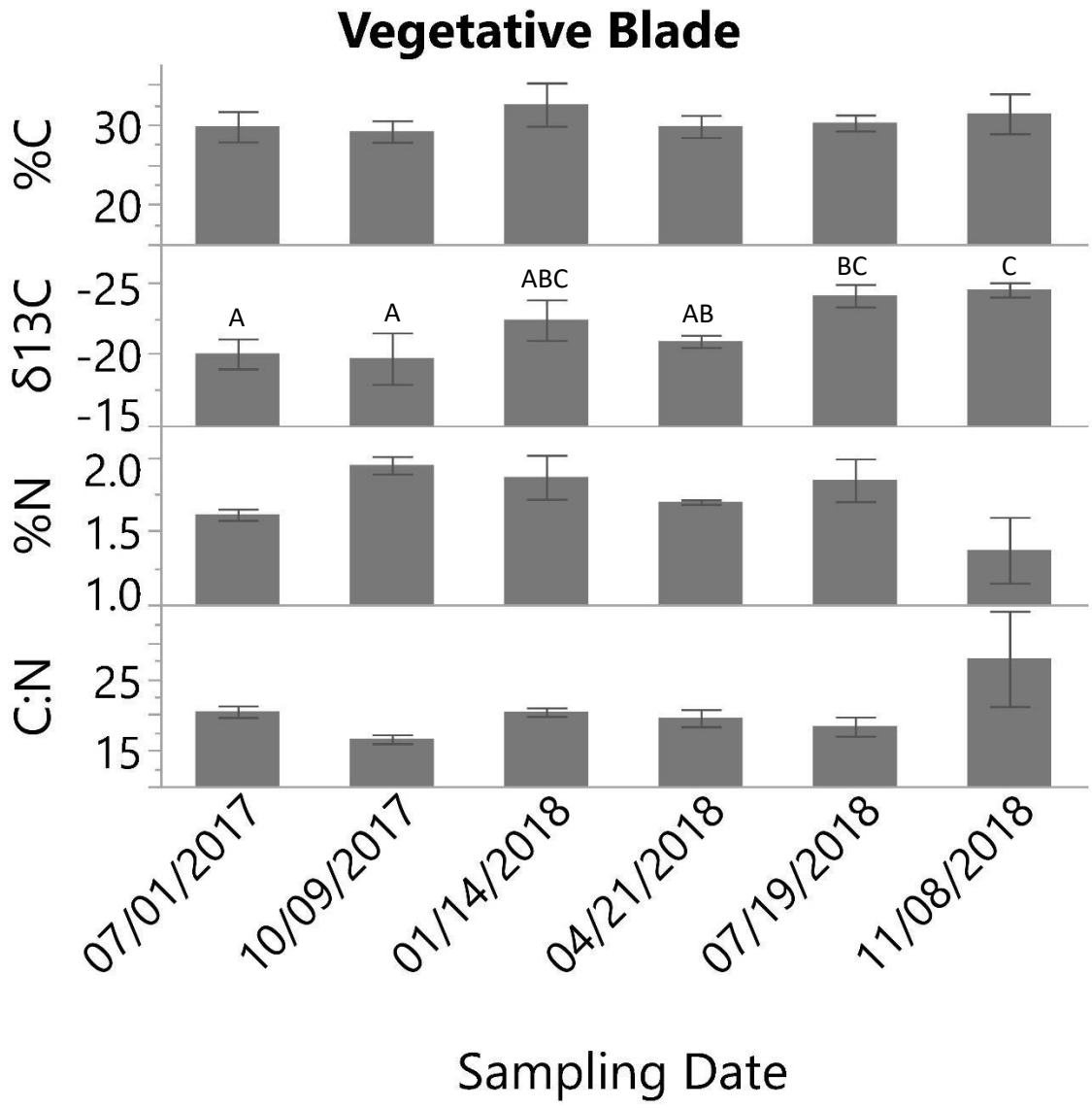

Figure 25: Mean %C, δ13C, %N, and C:N values for the vegetative blade region of control thalli among all sampling dates. Sample size for each bar is n = 3. Letters indicate significant differences among sampling dates; sampling dates not connected by the same letter are significantly different. Error bars are ±SE.

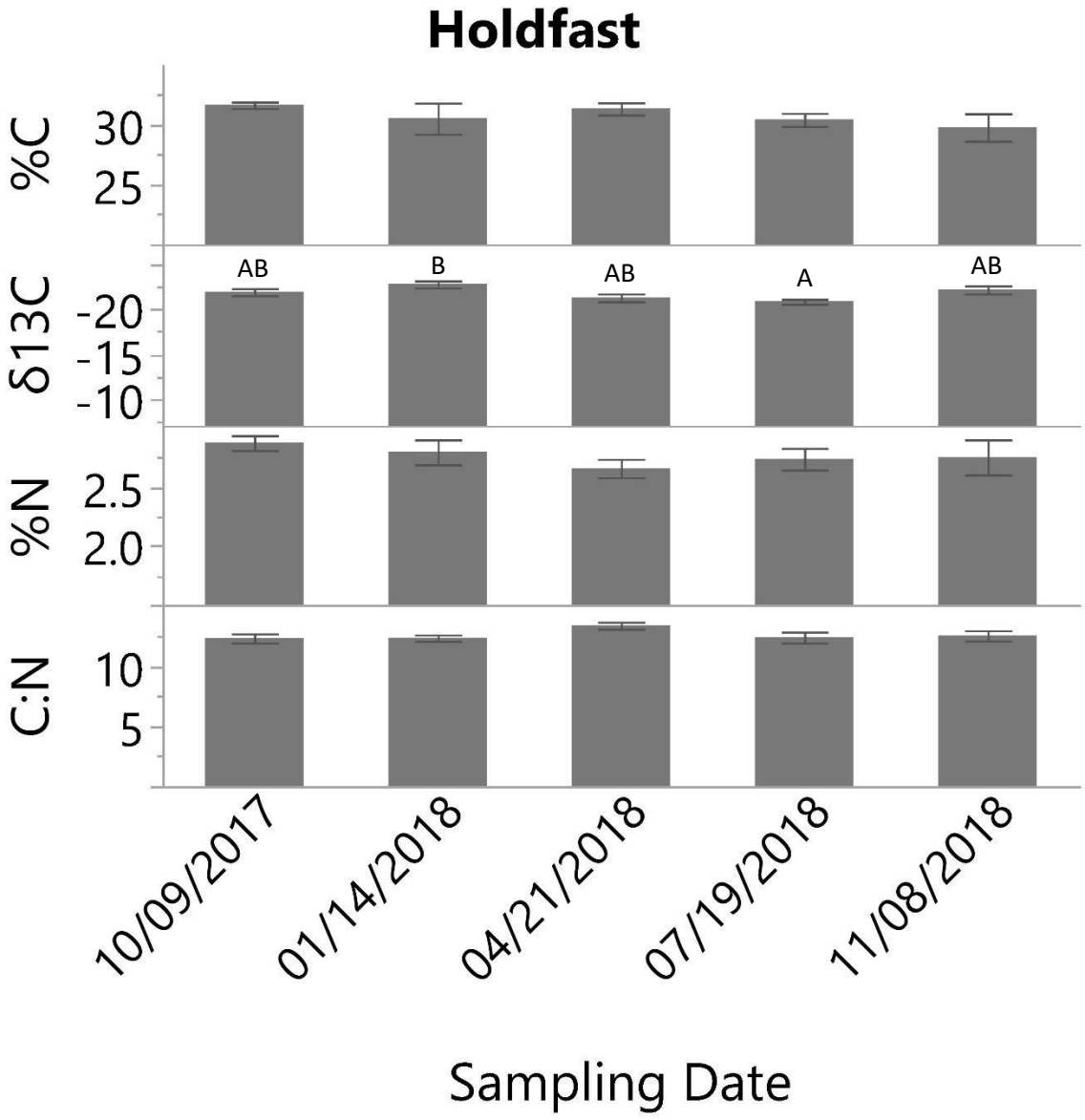

Figure 26: Mean %C, δ13C, %N, and C:N for holdfast region of control and experimental thalli among sampling dates. On 7/1/2017, only control thalli were harvested as it was the start of experimental manipulations, and thus data from that sampling date was excluded from this analysis. Sample size for each bar is n = 12, except those of 10/9/2017, for which n = 11. Letters indicate significant differences among sampling dates; sampling dates not connected by the same letter are significantly different. Error bars are ±SE.

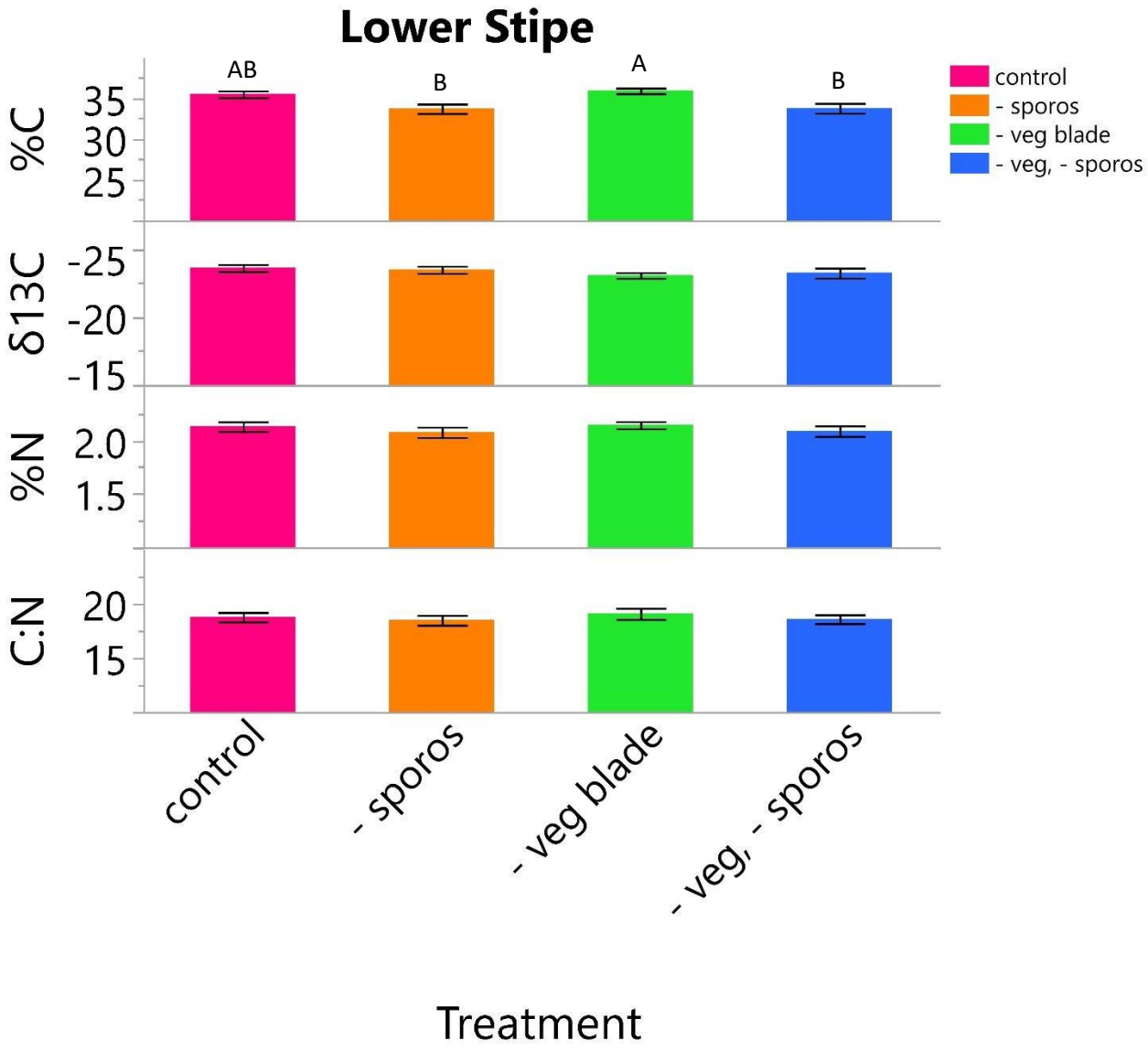

Figure 27: Mean %C, δ13C, %N, and C:N for lower stipe region of control and experimental thalli among all treatments. On 7/1/2017, only control thalli were harvested as it was the start of experimental manipulations, and thus data from that sampling date was excluded from this analysis. Sample size for each bar is n = 15. Letters indicate significant differences among treatments; treatments not connected by the same letter are significantly different. Error bars are ±SE.

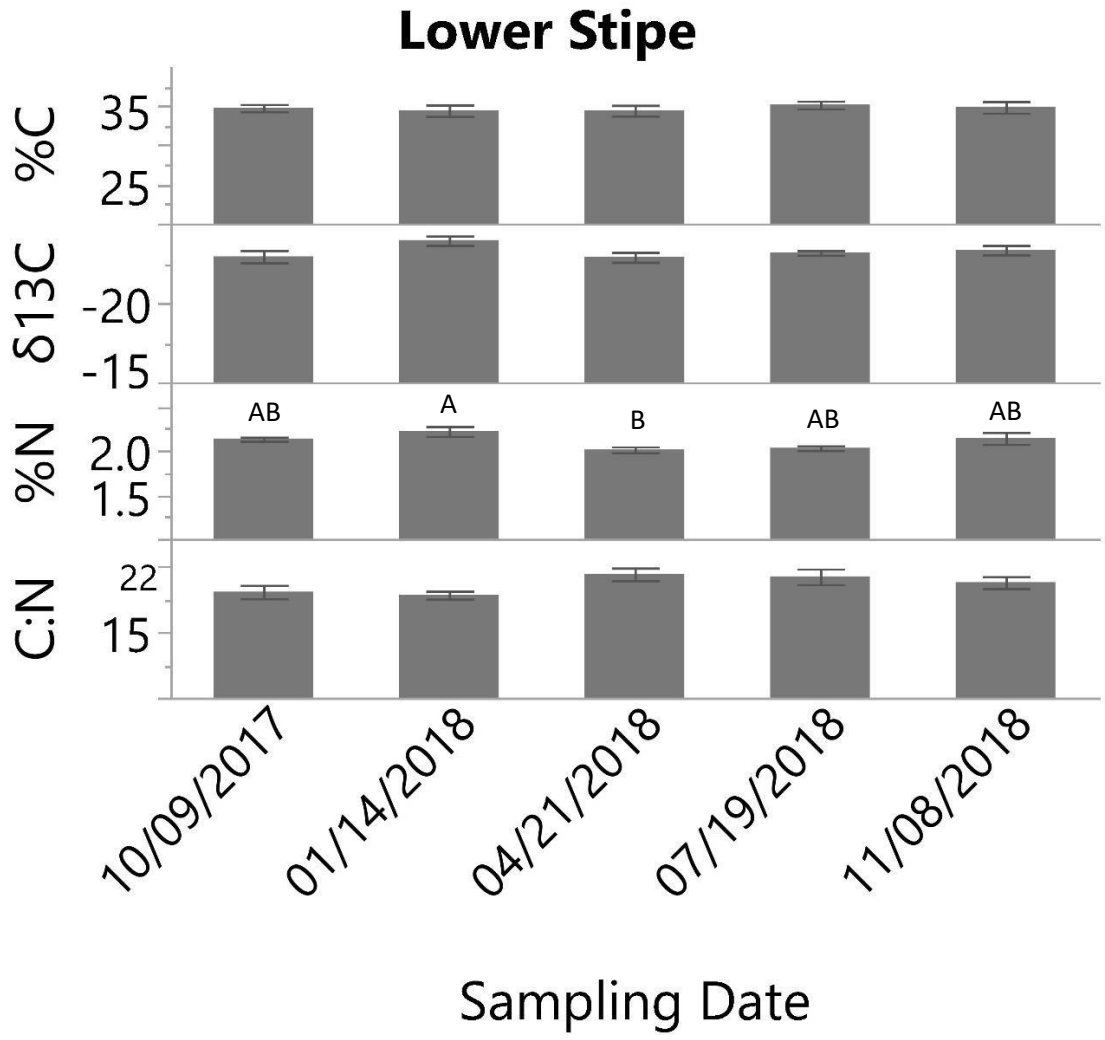

Figure 28: Mean %C, δ13C, %N, and C:N for lower stipe region of control and experimental thalli among sampling dates. On 7/1/2017, only control thalli were harvested as it was the start of experimental manipulations, and thus data from that sampling date was excluded from this analysis. Sample size for each bar is n = 12. Letters indicate significant differences sampling dates; sampling dates not connected by the same letter are significantly different. Error bars are ±SE.

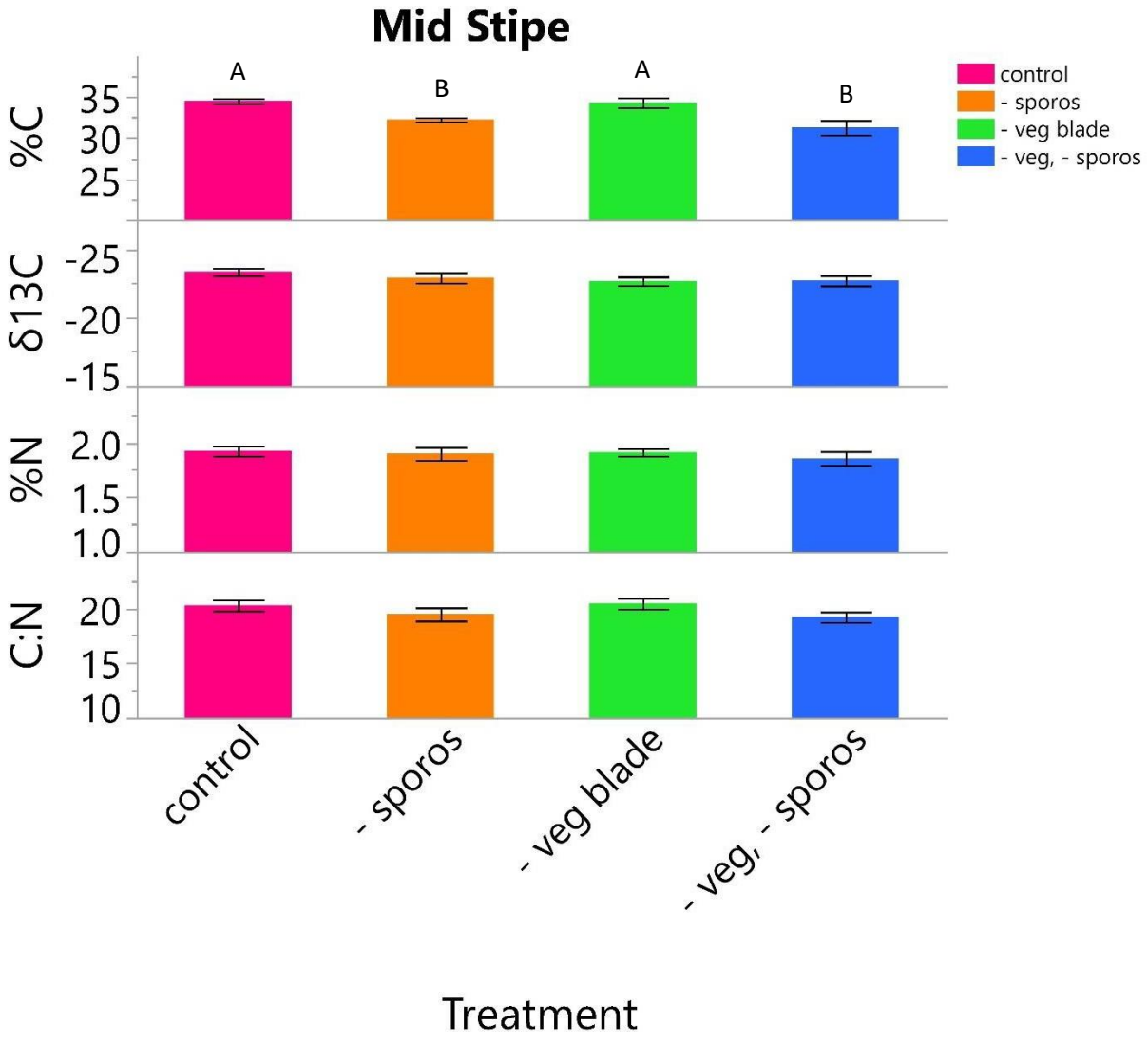

Figure 29: Mean %C, δ13C, %N, and C:N for mid stipe region of control and experimental thalli among all treatments. On 7/1/2017, only control thalli were harvested as it was the start of experimental manipulations, and thus data from that sampling date was excluded from this analysis. Sample size for each bar is n = 15. Letters indicate significant differences among treatments; treatments not connected by the same letter are significantly different. Error bars are ±SE.

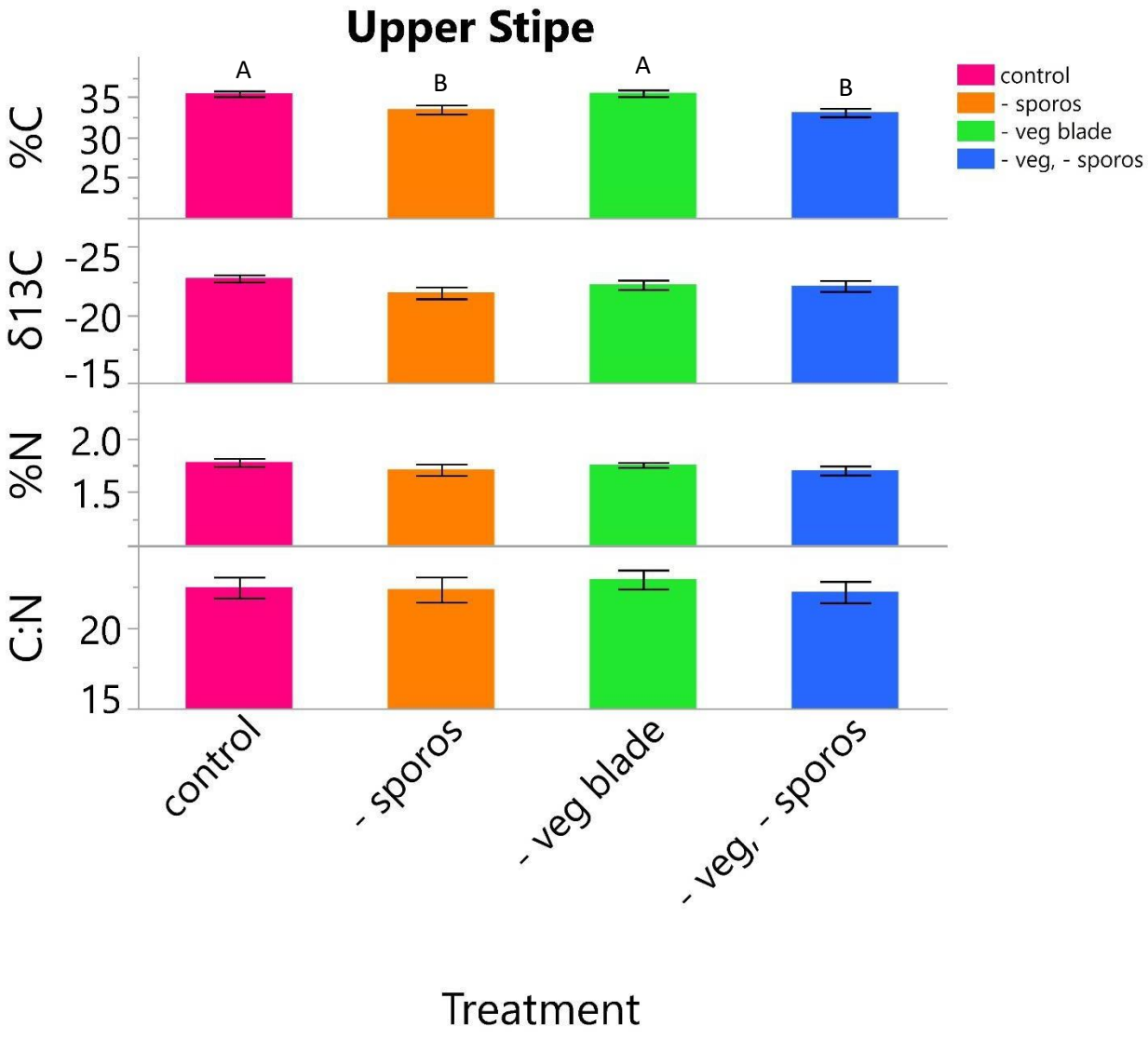

Figure 30: Mean %C, δ13C, %N, and C:N for upper stipe region of control and experimental thalli among all treatments. On 7/1/2017, only control thalli were harvested as it was the start of experimental manipulations, and thus data from that sampling date was excluded from this analysis. Sample size for each bar is n = 15, except those of minus sporos, for which n = 14. Letters indicate significant differences among treatments; treatments not connected by the same letter are significantly different. Error bars are ±SE.

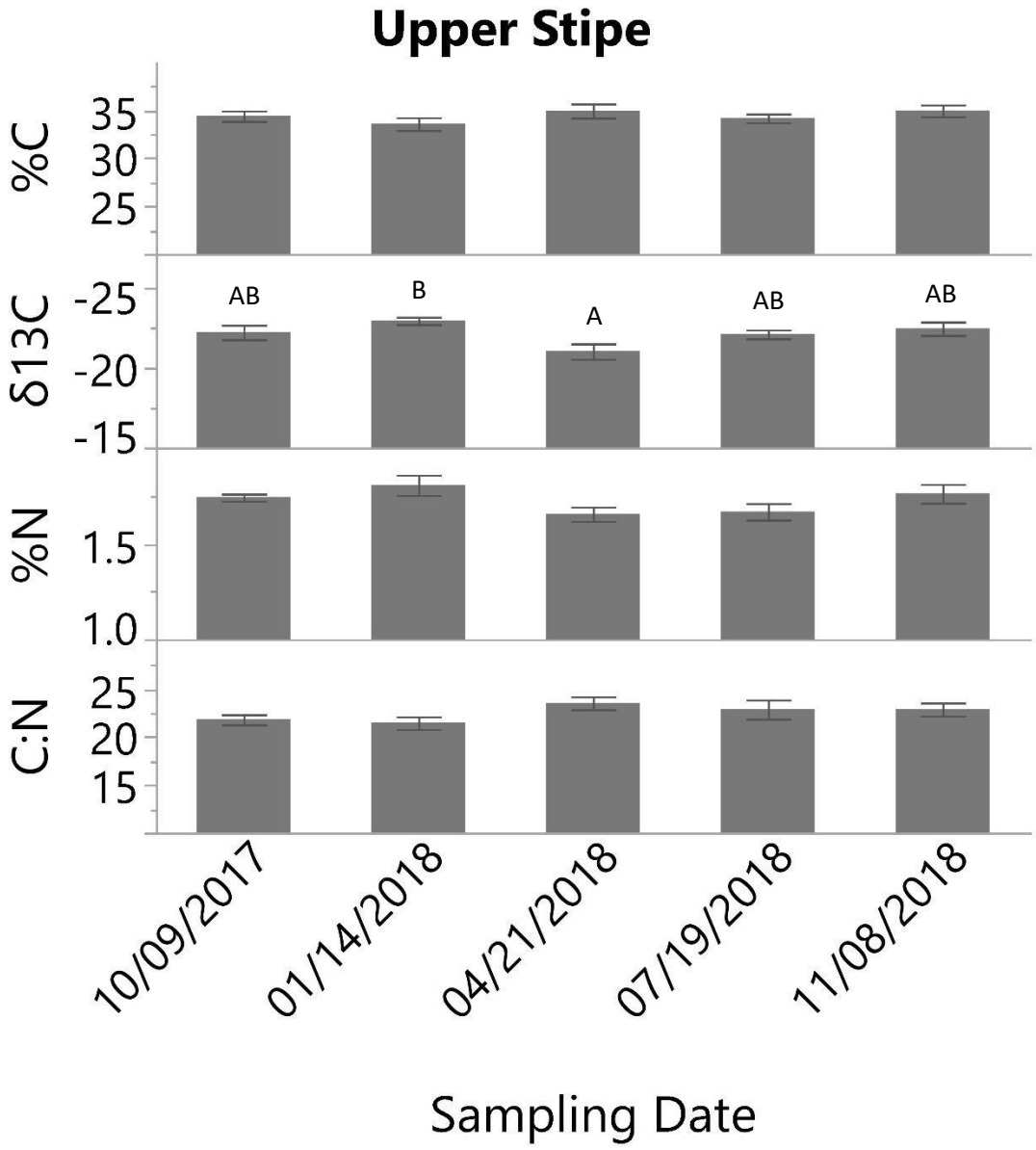

Figure 31: Mean %C, δ13C, %N, and C:N for upper stipe region of control and experimental thalli among all sampling dates. On 7/1/2017, only control thalli were harvested as it was the start of experimental manipulations, and thus data from that sampling date was excluded from this analysis. Sample size for each bar is n = 12, except those of 4/21/2018, for which n = 11. Letters indicate significant differences among treatments; treatments not connected by the same letter are significantly different. Error bars are ±SE.

TABLES

Table 1: One-way ANOVA testing the effect of seasonal variability on regional proportions of the total thallus biomass for control thalli.

A) Vegetative Blade % of total biomass

Source	DF	Sum of Squares	F Ratio	Prob > F
Date	5	16.822217	4.0059	0.0119*
Error	19	15.957524		

B) Sporophylls % of total biomass

Source	DF	Sum of Squares	F Ratio	Prob > F
Date	5	407.31838	1.1383	0.3745
Error	19	1359.7518		

C) Stipe % of total biomass

Source	DF	Sum of Squares	F Ratio	Prob > F
Date	5	232.93101	0.7337	0.6072
Error	19	1206.3417		

D) Holdfast % of total biomass

Source	DF	Sum of Squares	F Ratio	Prob > F
Date	5	170.31018	1.2821	0.3124
Error	19	504.76971		

Table 2: One-way ANOVA testing the effect of seasonal changes on the mean # of sporophylls per thallus, mean sporophyll length (cm), and mean total sporophyll wet weight (g) for control thalli.

A) # Sporophylls / thallus

Source	DF	Sum of Squares	F Ratio	Prob > F
Date	5	613.61000	3.4303	0.0224*
Error	19	679.7500		

B) Sporophyll length (cm)

Source	DF	Sum of Squares	F Ratio	Prob > F
Date	5	1402.9048	1.8211	0.1568
Error	19	2927.4352		

C) Sporophyll wet weight (g)

Source	DF	Sum of Squares	F Ratio	Prob > F
Date	5	729319.66	2.1545	0.1027
Error	19	1286342.8		

Table 3: One-way ANOVA testing the effect of seasonal variability on mean vegetative blade length (cm) and mean vegetative blade wet weight (g) for control thalli.

A) Vegetative blade length (cm)

Source	DF	Sum of Squares	F Ratio	Prob > F
Date	5	22250.506	13.5232	<.0001*
Error	19	6252.354		

B) Vegetative blade wet weight (g)

Source	DF	Sum of Squares	F Ratio	Prob > F
Date	5	3236.2242	10.3493	<.0001*
Error	19	1188.2558		

Table 4: Two-way ANOVA testing variability in mean # of sporophylls per thallus, mean sporophyll length (cm), & mean sporophyll wet weight (g) due to sampling date, treatment, and sampling date*treatment for thalli in the control & minus vegetative blade treatments.

A) # Sporophylls / thallus

Source	DF	Sum of Squares	F Ratio	Prob > F
Sampling date	4	775.31170	5.2147	0.0032*
Treatment	1	0.50676	0.0136	0.9079
Sampling date*Treatment	4	85.72196	0.5766	0.6821
Error	26	966.4167		

B) Sporophyll length (cm)

Source	DF	Sum of Squares	F Ratio	Prob > F
Sampling date	4	3387.9767	8.1939	0.0002*
Treatment	1	593.4933	5.7415	0.0238*
Sampling date*Treatment	4	792.3710	1.9164	0.1365
Error	27	2790.9631		

C) Sporophyll wet weight (g)

Source	DF	Sum of Squares	F Ratio	Prob > F
Sampling date	4	509912.93	1.6080	0.2010
Treatment	1	6485.29	0.0818	0.7771
Sampling date*Treatment	4	50934.05	0.1606	0.9564
Error	27	2140550.4		

Table 5: Two-way ANOVA testing variability in mean vegetative blade wet weight (g) and mean vegetative blade length (cm) due to sampling date, treatment, and sampling date*treatment for thalli in the control & minus sporophylls treatments. Data for both vegetative biomass and vegetative length was Log [x + 1] transformed.

A) Vegetative blade wet weight (g)

Source	DF	Sum of Squares	F Ratio	Prob > F
Sampling date	4	5.1688933	2.0929	0.1095
Treatment	1	8.8087149	14.2666	0.0008*
Sampling date*Treatment	4	5.6124290	2.2725	0.0875
Error	27	16.670807		

B) Vegetative blade length (cm)

Source	DF	Sum of Squares	F Ratio	Prob > F
Sampling date	4	2.4818573	0.7535	0.5645
Treatment	1	9.0884389	11.0370	0.0026*
Sampling date*Treatment	4	4.0699067	1.2356	0.3193
Error	27	22.233268		

Table 6: One-way ANOVA testing variability in mean %C, $\delta^{13}C$, %N, and C:N due to thallus region for control thalli. Data from all sampling dates was included in this analysis.

A) %C

Source	DF	Sum of Squares	F Ratio	Prob > F
Thallus region	6	958.73604	22.2351	<.0001*
Error	112	804.8708		

B) $\delta^{13}C$

Source	DF	Sum of Squares	F Ratio	Prob > F
Thallus region	6	52.711576	2.9937	0.0095*
Error	112	328.67177		

C) %N

Source	DF	Sum of Squares	F Ratio	Prob > F
Thallus region	6	8.7534803	24.9665	<.0001*
Error	112	6.544693		

D) C:N

Source	DF	Sum of Squares	F Ratio	Prob > F
Thallus region	6	966.04923	17.5575	<.0001*
Error	112	1027.0759		

Table 7: Two-way ANOVA testing variability in mean %C, $\delta^{13}C$, %N, and C:N among sampling date, thallus region, and sampling date*thallus region for control thalli. The "sorus" thallus region was not present for all dates, and therefore excluded from these analyses.

A) %C

Source	DF	Sum of Squares	F Ratio	Prob > F
Sampling date	5	21.80271	0.5356	0.7486
Thallus region	5	917.31638	22.5332	<.0001*
Sampling date*Thallus region	25	118.11787	0.5803	0.9354
Error	71	578.0753		

B) $\delta^{13}C$

Source	DF	Sum of Squares	F Ratio	Prob > F
Sampling date	5	67.098772	6.0015	0.0001*
Thallus region	5	51.860272	4.6385	0.0010*
Sampling date*Thallus region	25	67.665541	1.2104	0.2616
Error	71	158.76137		

C) %N

Source	DF	Sum of Squares	F Ratio	Prob > F
Sampling date	5	1.4371420	5.8356	0.0001*
Thallus region	5	8.6133350	34.9751	<.0001*
Sampling date*Thallus region	25	0.9422912	0.7652	0.7698
Error	71	3.497039		

D) C:N

Source	DF	Sum of Squares	F Ratio	Prob > F
Sampling date	5	69.95839	1.8383	0.1163
Thallus region	5	885.29727	23.2633	<.0001*
Sampling date*Thallus region	25	248.92493	1.3082	0.1890
Error	71	540.3893		

Table 8: One-way ANOVA testing variability in mean %C, $\delta^{13}C$, %N, and C:N in the "holdfast" region among sampling dates for control thalli.

A) %C

Source	DF	Sum of Squares	F Ratio	Prob > F
Sampling date	5	42.592719	0.8727	0.5296
Error	11	107.36812		

B) $\delta^{13}C$

Source	DF	Sum of Squares	F Ratio	Prob > F
Sampling date	5	12.406292	1.0089	0.4569
Error	11	27.053961		

C) %N

Source	DF	Sum of Squares	F Ratio	Prob > F
Sampling date	5	0.63206461	1.0666	0.4290
Error	11	1.3037412		

D) C:N

Source	DF	Sum of Squares	F Ratio	Prob > F
Sampling date	5	1.9202080	0.1693	0.9687
Error	11	24.947336		

Table 9: One-way ANOVA testing variability in mean %C, $\delta^{13}C$, %N, and C:N in the "lower stipe" region among sampling dates for control thalli.

A) %C

Source	DF	Sum of Squares	F Ratio	Prob > F
Sampling date	5	4.2679740	0.2531	0.9302
Error	12	40.476807		

B) $\delta^{13}C$

Source	DF	Sum of Squares	F Ratio	Prob > F
Sampling date	5	3.8569954	0.5847	0.7118
Error	12	15.830540		

C) %N

Source	DF	Sum of Squares	F Ratio	Prob > F
Sampling date	5	0.36747841	3.2696	0.0430*
Error	12	0.26973954		

D) C:N

Source	DF	Sum of Squares	F Ratio	Prob > F
Sampling date	5	28.548845	1.8256	0.1822
Error	12	37.532230		

Table 10: One-way ANOVA testing variability in mean %C, $\delta^{13}C$, %N, and C:N in the "mid stipe" region among sampling dates for control thalli.

A) %C

Source	DF	Sum of Squares	F Ratio	Prob > F
Sampling date	5	11.839766	2.3984	0.0996
Error	12	11.847662		

B) $\delta^{13}C$

Source	DF	Sum of Squares	F Ratio	Prob > F
Sampling date	5	7.5444265	1.1749	0.3765
Error	12	15.411068		

C) %N

Source	DF	Sum of Squares	F Ratio	Prob > F
Sampling date	5	0.34914831	7.3290	0.0023*
Error	12	0.11433380		

D) C:N

Source	DF	Sum of Squares	F Ratio	Prob > F
Sampling date	5	15.962666	0.8880	0.5186
Error	12	43.114566		

Table 11: One-way ANOVA testing variability in mean %C, $\delta^{13}C$, %N, and C:N in the "upper stipe" region among sampling dates for control thalli.

A) %C

Source	DF	Sum of Squares	F Ratio	Prob > F
Sampling date	5	9.4304717	0.7803	0.5827
Error	12	29.006140		

B) $\delta^{13}C$

Source	DF	Sum of Squares	F Ratio	Prob > F
Sampling date	5	2.8054153	0.4725	0.7899
Error	12	14.249206		

C) %N

Source	DF	Sum of Squares	F Ratio	Prob > F
Sampling date	5	0.14449415	1.4257	0.2838
Error	12	0.24323279		

D) C:N

Source	DF	Sum of Squares	F Ratio	Prob > F
Sampling date	5	8.5410402	0.2377	0.9382
Error	12	86.235124		

Table 12: One-way ANOVA testing variability in mean %C, $\delta^{13}C$, %N, and C:N in the "sporophyll" region among sampling dates for control thalli.

A) %C

Source	DF	Sum of Squares	F Ratio	Prob > F
Sampling date	5	49.697329	0.4639	0.7959
Error	12	257.08333		

B) $\delta^{13}C$

Source	DF	Sum of Squares	F Ratio	Prob > F
Sampling date	5	46.594241	2.6573	0.0768
Error	12	42.081929		

C) %N

Source	DF	Sum of Squares	F Ratio	Prob > F
Sampling date	5	0.18715081	0.4579	0.8001
Error	12	0.9810036		

D) C:N

Source	DF	Sum of Squares	F Ratio	Prob > F
Sampling date	5	45.718617	1.9375	0.1614
Error	12	56.63271		

Table 13: One-way ANOVA testing variability in mean %C, δ13C, %N, and C:N in the "vegetative blade" region among sampling dates for control thalli.

A) %C

Source	DF	Sum of Squares	F Ratio	Prob > F
Sampling date	5	23.714312	0.4302	0.8191
Error	12	132.29322		

B) $\delta^{13}C$

Source	DF	Sum of Squares	F Ratio	Prob > F
Sampling date	5	63.202167	3.4369	0.0370*
Error	12	44.13467		

C) %N

Source	DF	Sum of Squares	F Ratio	Prob > F
Sampling date	5	0.66614426	2.7330	0.0713
Error	12	0.5849882		

D) C:N

Source	DF	Sum of Squares	F Ratio	Prob > F
Sampling date	5	222.34823	1.8282	0.1817
Error	12	291.89734		

Table 14: Two-way ANOVA testing variability in mean %C, $\delta^{13}C$, %N, and C:N in the "holdfast" region due to sampling date, treatment, and sampling date*treatment for thalli in the control and experimental treatments. Data from sampling date 7/1/2017 were excluded from these analyses since it was the start of manipulations, and all samples taken on this date were from control thalli.

A) %C

Source	DF	Sum of Squares	F Ratio	Prob > F
Sampling date	4	27.645945	0.6496	0.6306
Treatment	3	12.944017	0.4055	0.7499
Sampling date*Treatment	12	56.704419	0.4441	0.9344
Error	39	414.97135		

B) $\delta^{13}C$

Source	DF	Sum of Squares	F Ratio	Prob > F
Sampling date	4	27.558627	3.2695	0.0210*
Treatment	3	4.041117	0.6392	0.5943
Sampling date*Treatment	12	13.773876	0.5447	0.8714
Error	39	82.18356		

C) %N

Source	DF	Sum of Squares	F Ratio	Prob > F
Sampling date	4	0.2779159	0.5416	0.7061
Treatment	3	0.5694745	1.4798	0.2350
Sampling date*Treatment	12	1.1061541	0.7186	0.7244
Error	39	5.0027033		

D) C:N

Source	DF	Sum of Squares	F Ratio	Prob > F
Sampling date	4	9.286240	1.3191	0.2799
Treatment	3	12.869228	2.4373	0.0791
Sampling date*Treatment	12	7.791449	0.3689	0.9669
Error	39	68.640506		

Table 15: Two-way ANOVA testing variability in mean %C, δ13C, %N, and C:N in the "lower stipe" region due to sampling date, treatment, and sampling date*treatment for thalli in the control and experimental treatments. Data from sampling date 7/1/2017 were excluded from these analyses since it was the start of manipulations, and all samples taken on this date were from control thalli.

A) %C

Source	DF	Sum of Squares	F Ratio	Prob > F
Sampling date	4	4.746362	0.2463	0.9102
Treatment	3	59.872255	4.1432	0.0120*
Sampling date*Treatment	12	10.634690	0.1840	0.9985
Error	40	192.67561		

B) $\delta^{13}C$

Source	DF	Sum of Squares	F Ratio	Prob > F
Sampling date	4	8.913089	1.8923	0.1307
Treatment	3	2.592792	0.7339	0.5379
Sampling date*Treatment	12	11.302640	0.7999	0.6483
Error	40	47.102493		

C) %N

Source	DF	Sum of Squares	F Ratio	Prob > F
Sampling date	4	0.36063836	3.1023	0.0258*
Treatment	3	0.04822125	0.5531	0.6491
Sampling date*Treatment	12	0.14616272	0.4191	0.9469
Error	40	1.1625048		

D) C:N

Source	DF	Sum of Squares	F Ratio	Prob > F
Sampling date	4	23.653891	1.8170	0.1445
Treatment	3	3.110348	0.3186	0.8119
Sampling date*Treatment	12	18.140975	0.4645	0.9236
Error	40	130.17747		

Table 16: Two-way ANOVA testing variability in mean %C, δ13C, %N, and C:N in the "mid stipe" region due to sampling date, treatment, and sampling date*treatment for thalli in the control and experimental treatments. Data from sampling date 7/1/2017 were excluded from these analyses since it was the start of manipulations, and all samples taken on this date were from control thalli.

A) %C

Source	DF	Sum of Squares	F Ratio	Prob > F
Sampling date	4	28.56232	1.7445	0.1593
Treatment	3	114.14771	9.2957	<.0001*
Sampling date*Treatment	12	88.08347	1.7933	0.0829
Error	40	163.72792		

B) δ13C

Source	DF	Sum of Squares	F Ratio	Prob > F
Sampling date	4	13.449021	1.8253	0.1429
Treatment	3	4.543557	0.8222	0.4894
Sampling date*Treatment	12	9.575281	0.4332	0.9402
Error	40	73.68169		

C) %N

Source	DF	Sum of Squares	F Ratio	Prob > F
Sampling date	4	0.19069689	1.1810	0.3338
Treatment	3	0.04131723	0.3412	0.7956
Sampling date*Treatment	12	0.48197865	0.9950	0.4707
Error	40	1.6146554		

D) C:N

Source	DF	Sum of Squares	F Ratio	Prob > F
Sampling date	4	22.973154	1.1954	0.3277
Treatment	3	16.052767	1.1137	0.3549
Sampling date*Treatment	12	18.503561	0.3209	0.9812
Error	40	192.18085		

Table 17: Two-way ANOVA testing variability in mean %C, δ13C, %N, and C:N in the "upper stipe" region due to sampling date, treatment, and sampling date*treatment for thalli in the control and experimental treatments. Data from sampling date 7/1/2017 were excluded from these analyses since it was the start of manipulations, and all samples taken on this date were from control thalli.

A) %C

Source	DF	Sum of Squares	F Ratio	Prob > F
Sampling date	4	15.084289	1.0953	0.3724
Treatment	3	69.440186	6.7230	0.0009*
Sampling date*Treatment	12	29.988750	0.7259	0.7177
Error	39	134.27302		

B) δ13C

Source	DF	Sum of Squares	F Ratio	Prob > F
Sampling date	4	25.232046	3.4090	0.0175*
Treatment	3	10.386903	1.8711	0.1504
Sampling date*Treatment	12	10.760713	0.4846	0.9115
Error	39	72.16457		

C) %N

Source	DF	Sum of Squares	F Ratio	Prob > F
Sampling date	4	0.20216451	2.3677	0.0693
Treatment	3	0.06303702	0.9844	0.4101
Sampling date*Treatment	12	0.25578549	0.9986	0.4681
Error	39	0.8324823		

D) C:N

Source	DF	Sum of Squares	F Ratio	Prob > F
Sampling date	4	32.646299	1.1168	0.3625
Treatment	3	4.992616	0.2277	0.8765
Sampling date*Treatment	12	47.620980	0.5430	0.8726
Error	39	285.01336		

APPENDIX – A: Results for $\delta^{15}N$

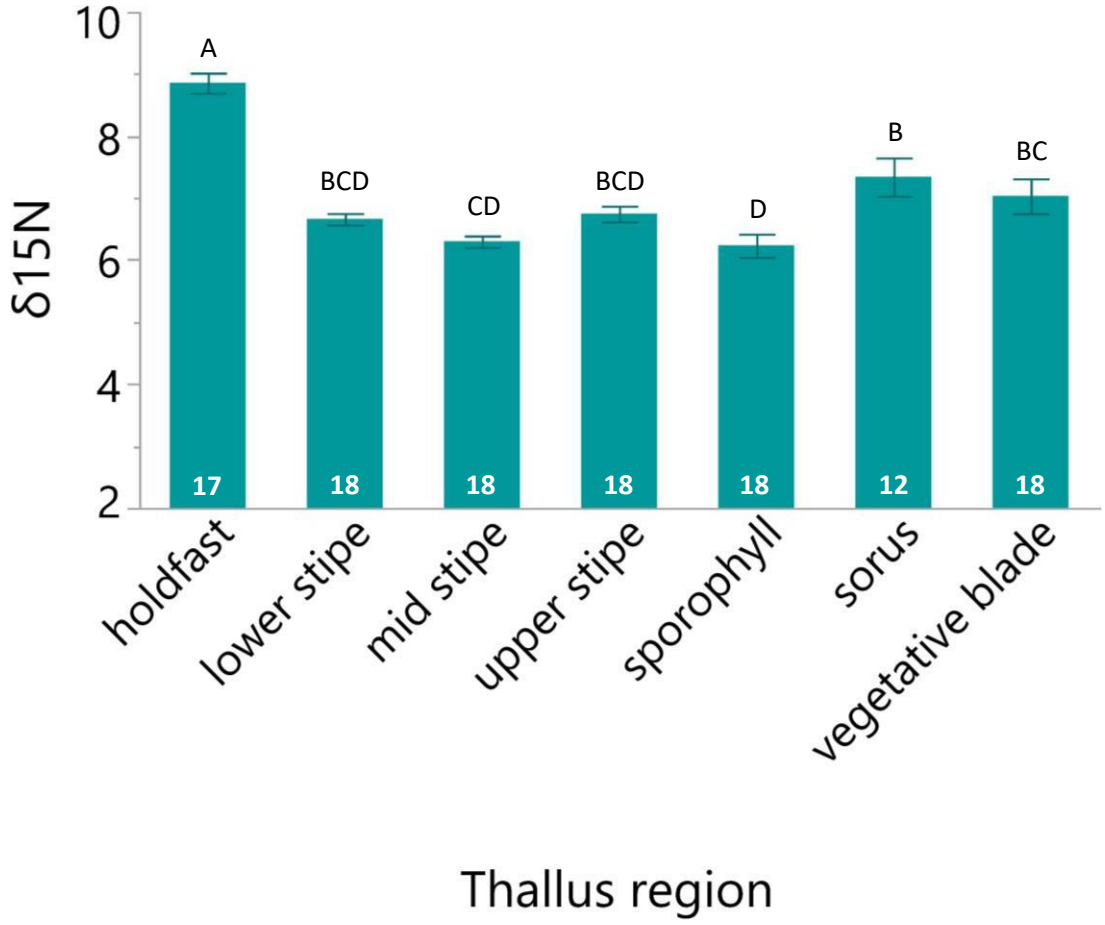

Figure A1: Mean $\delta^{15}N$ for control thalli among thallus regions. Sample sizes are indicated by the number at the base of each bar. Letters indicate significant differences among thallus regions; thallus regions not connected by the same letter are significantly different. Error bars are ±SE.

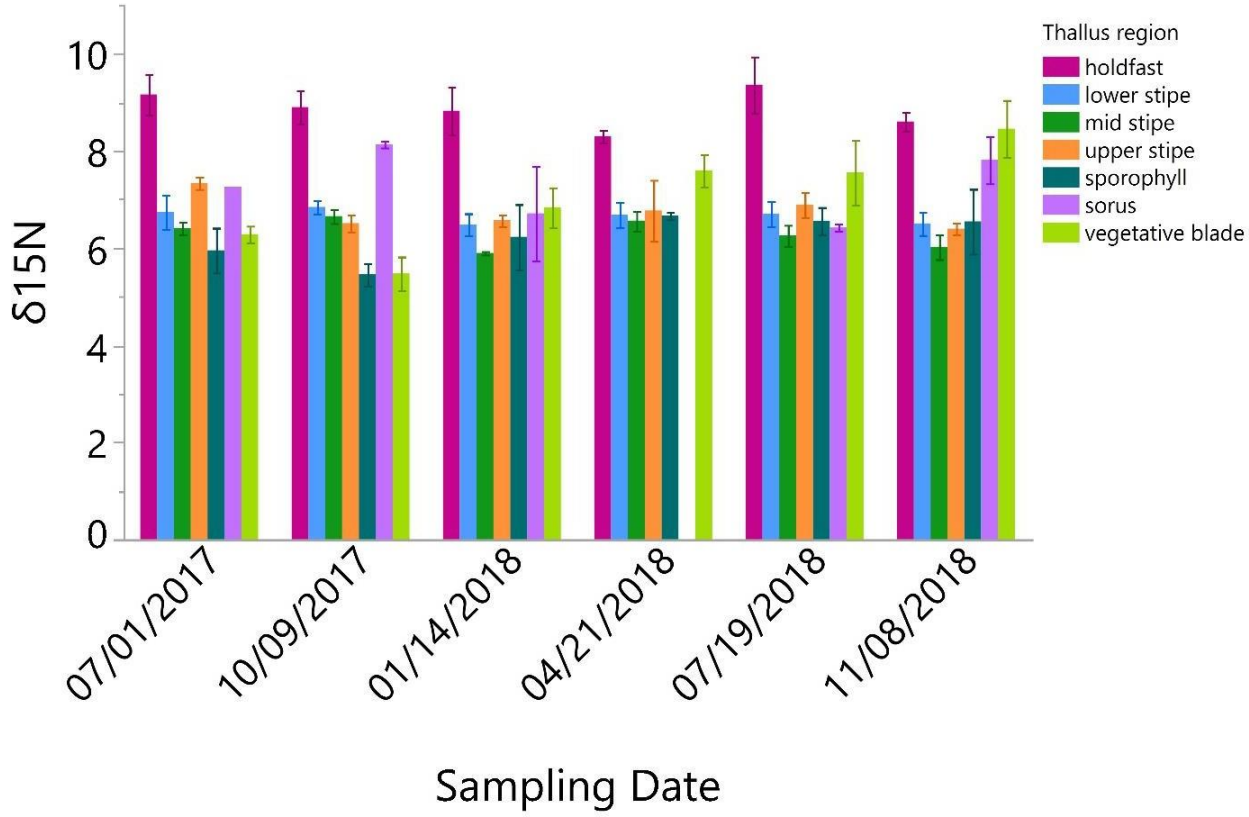

Figure A2: Mean $\delta^{15}N$ for control thalli among sampling dates and thallus regions. Error bars are ±SE. See Table A2 for significance.

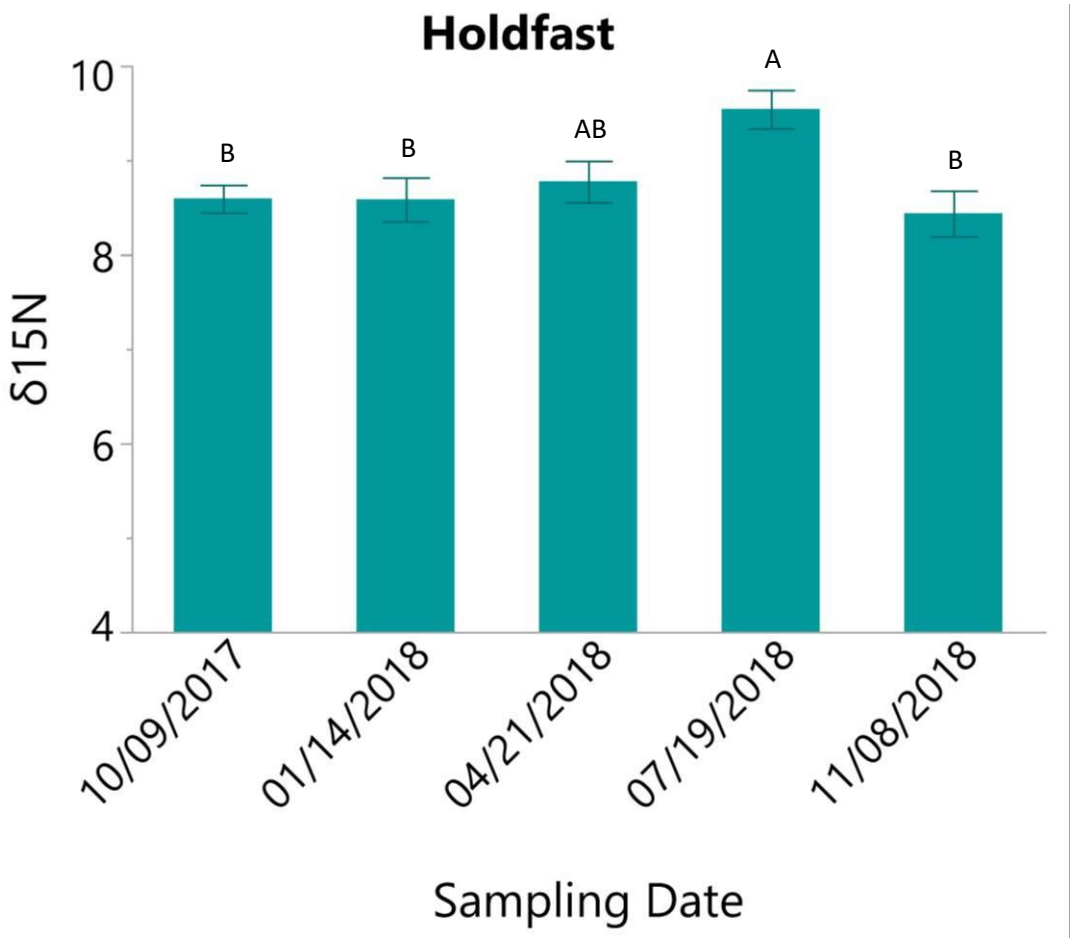

Figure A3: Mean $\delta^{15}N$ in the "holdfast" region for control & experimental thalli among sampling dates. Letters indicate significant differences among sampling dates; sampling dates not connected by the same letter are significantly different. Error bars are ±SE.

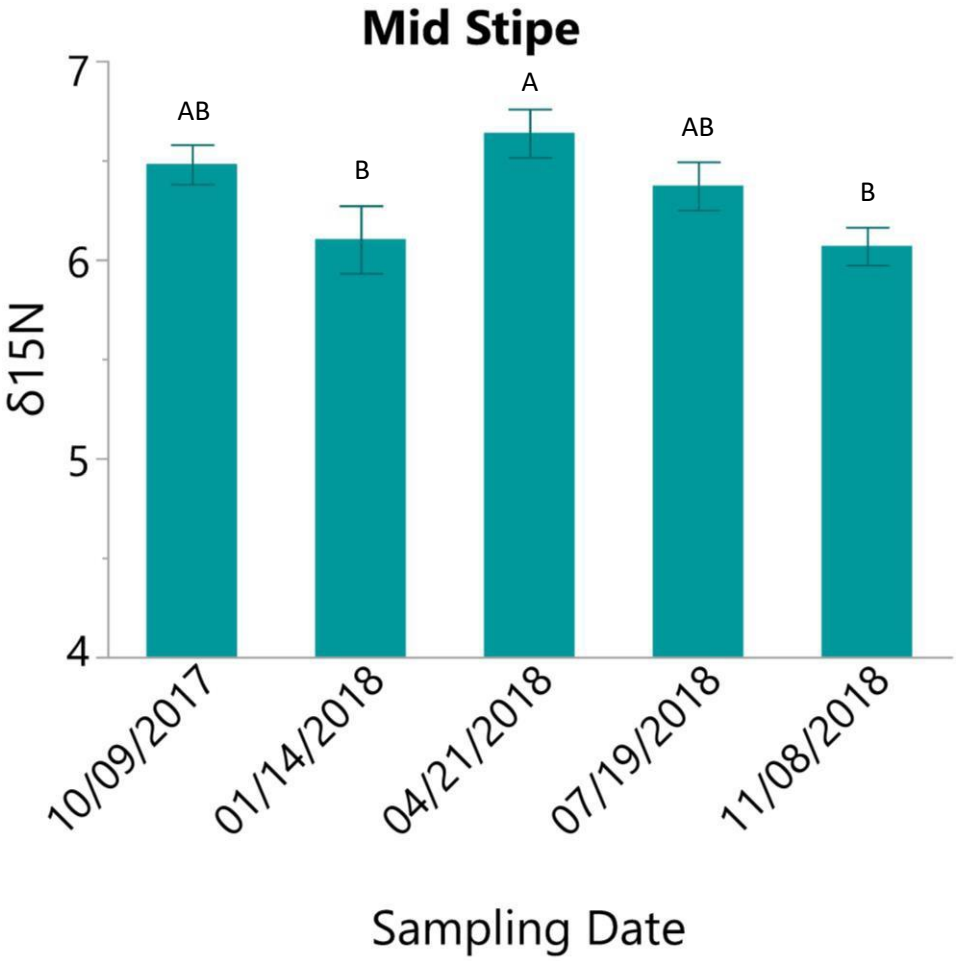

Figure A4: Mean $\delta^{15}N$ in the "mid stipe" region for control & experimental thalli among sampling dates. Letters indicate significant differences among sampling dates; sampling dates not connected by the same letter are significantly different. Error bars are ±SE.

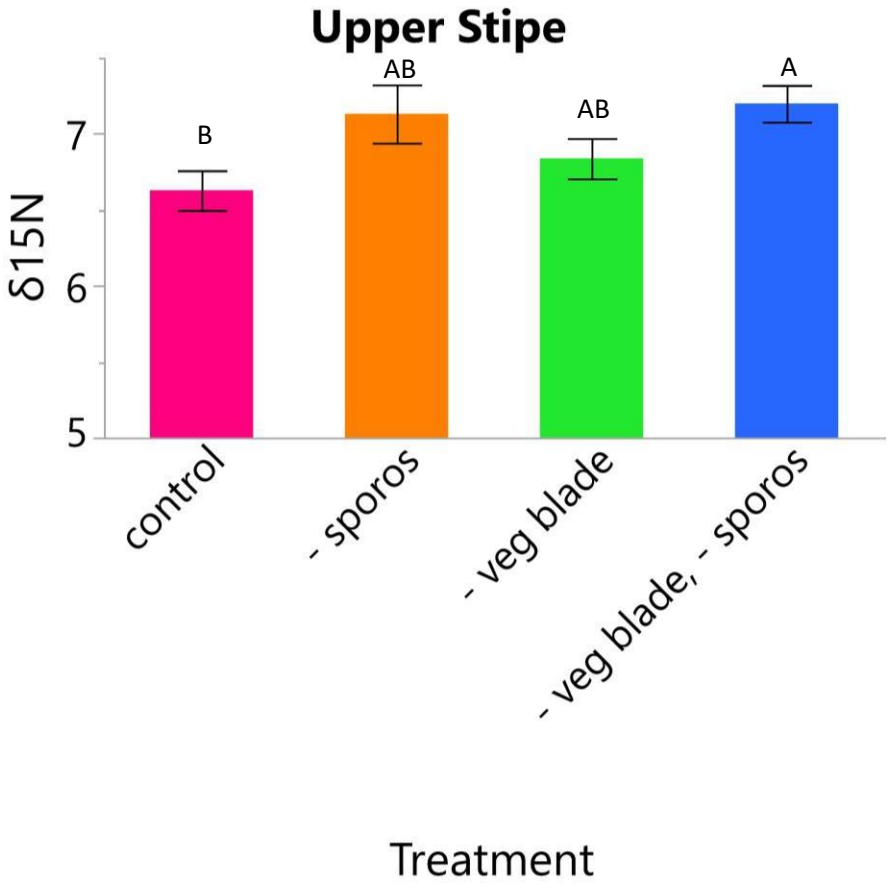

Figure A5: Mean $\delta^{15}N$ in the "upper stipe" region for control & experimental thalli among treatments. Letters indicate significant differences among treatments; treatments not connected by the same letter are significantly different. Error bars are ±SE.

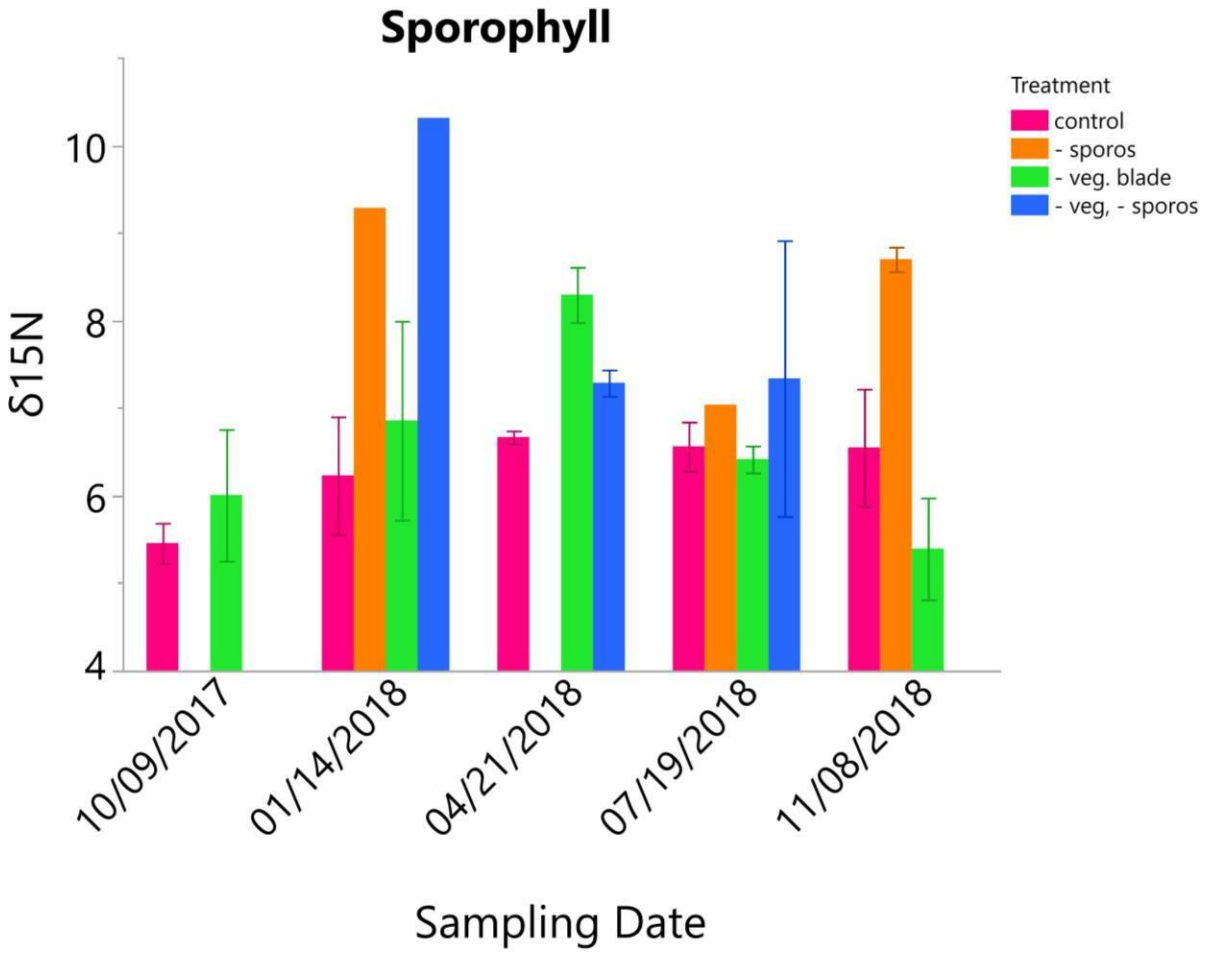

Figure A6: Mean $\delta^{15}N$ in the "sporophyll" region for control & experimental thalli among sampling dates & treatments. Sporophyll tissue was not present on harvested thalli from the minus sporophylls treatment on 10/9/2017 and 4/21/2018. It was also missing from the minus both treatment on 10/9/2017 and 11/8/2018. Bars with no error bars denote that there was one data point.

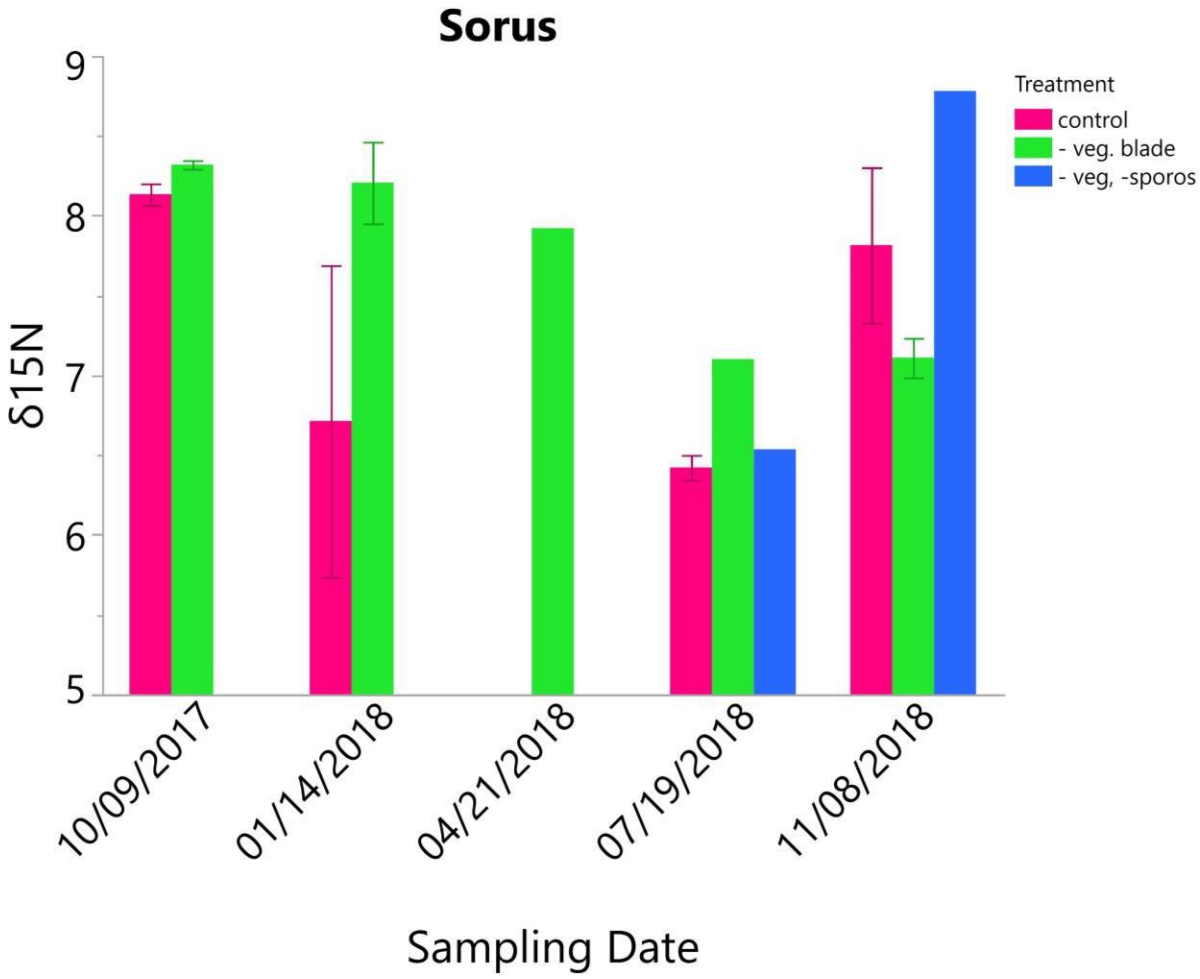

Figure A7: Mean $\delta^{15}N$ in the "sorus" region for control & experimental thalli among sampling dates & treatments. Soral tissue was not present on any harvested thalli from the minus sporophylls treatment for all dates. It was also missing from the control thalli on 4/21/2018, and from the minus both treatment on 10/9/2017, 1/14/2018, and 4/21/2018. Bars with no standard error bars denote that there was one data point.

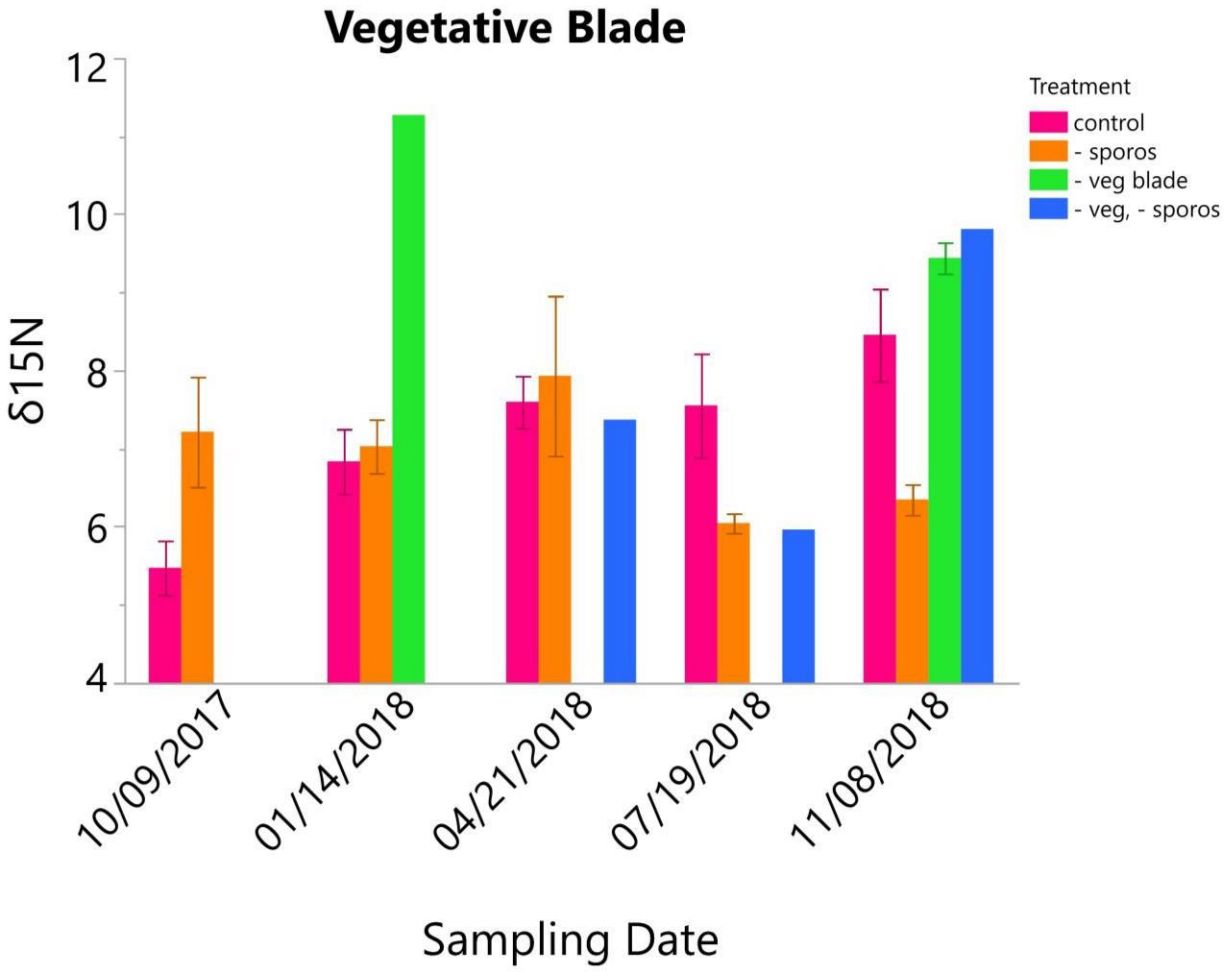

Figure A8: Mean $\delta^{15}N$ in the "vegetative blade" region for control & experimental thalli among sampling dates & treatments. Vegetative blade tissue was not present on any harvested thalli from the minus vegetative blade treatment on 10/9/2017, 4/21/2018, and 7/19/2018. It was also missing from thalli in the minus both treatment on 10/9/2017 and 1/14/2018. Bars with no standard error bars denote that there was one data point.

Table A1: One-way ANOVA testing variability in mean $\delta^{15}N$ due to thallus region for control thalli. Data from all sampling dates was included in this analysis.

Source	DF	Sum of Squares	F Ratio	Prob > F
Thallus region	6	82.546037	23.7412	<.0001*
Error	112	64.90227		

Table A2: Two-way ANOVA testing variability in mean $\delta^{15}N$ among sampling date, thallus region, and sampling date*thallus region for control thalli. The "sorus" thallus region was not present for all dates, and therefore excluded from these analyses.

Source	DF	Sum of Squares	F Ratio	Prob > F
Sampling date	5	3.974640	2.1266	0.0721
Thallus region	5	79.690737	42.6385	<.0001*
Sampling date*Thallus region	25	21.447513	2.2951	0.0034*
Error	71	26.53958		

Table A3: Two-way ANOVA testing variability in mean $\delta^{15}N$ by thallus region due to sampling date, treatment, and sampling date*treatment for thalli in the control and experimental treatments. Data from sampling date 7/1/2017 were excluded from these analyses since it was the start of manipulations, and all samples taken on this date were from control thalli. Sporophyll, sorus, and vegetative blade regions were not present for each sampling date or treatment and therefore, were unable to be analyzed statistically.

A) Holdfast

Source	DF	Sum of Squares	F Ratio	Prob > F
Sampling date	4	10.762719	4.7694	0.0031*
Treatment	3	0.169146	0.0999	0.9596
Sampling date*Treatment	12	7.995115	1.1810	0.3290
Error	40	22.566166		

B) Lower stipe

Source	DF	Sum of Squares	F Ratio	Prob > F
Sampling date	4	1.7602255	2.1293	0.0950
Treatment	3	0.9230664	1.4888	0.2322
Sampling date*Treatment	12	0.9399670	0.3790	0.9635
Error	40	8.266589		

C) Mid stipe

Source	DF	Sum of Squares	F Ratio	Prob > F
Sampling date	4	2.8699573	3.7036	0.0117*
Treatment	3	0.1087638	0.1871	0.9045
Sampling date*Treatment	12	2.3484022	1.0102	0.4579
Error	40	7.749107		

D) Upper stipe

Source	DF	Sum of Squares	F Ratio	Prob > F
Sampling date	4	2.5022175	1.9898	0.1151
Treatment	3	3.2561753	3.4524	0.0256*
Sampling date*Treatment	12	2.2725425	0.6024	0.8267
Error	39	12.261088		

APPENDIX – B: Results for %C, $\delta^{13}C$, %N, and C:N in the sporophyll, sorus, and vegetative blade regions of control and experimental thalli

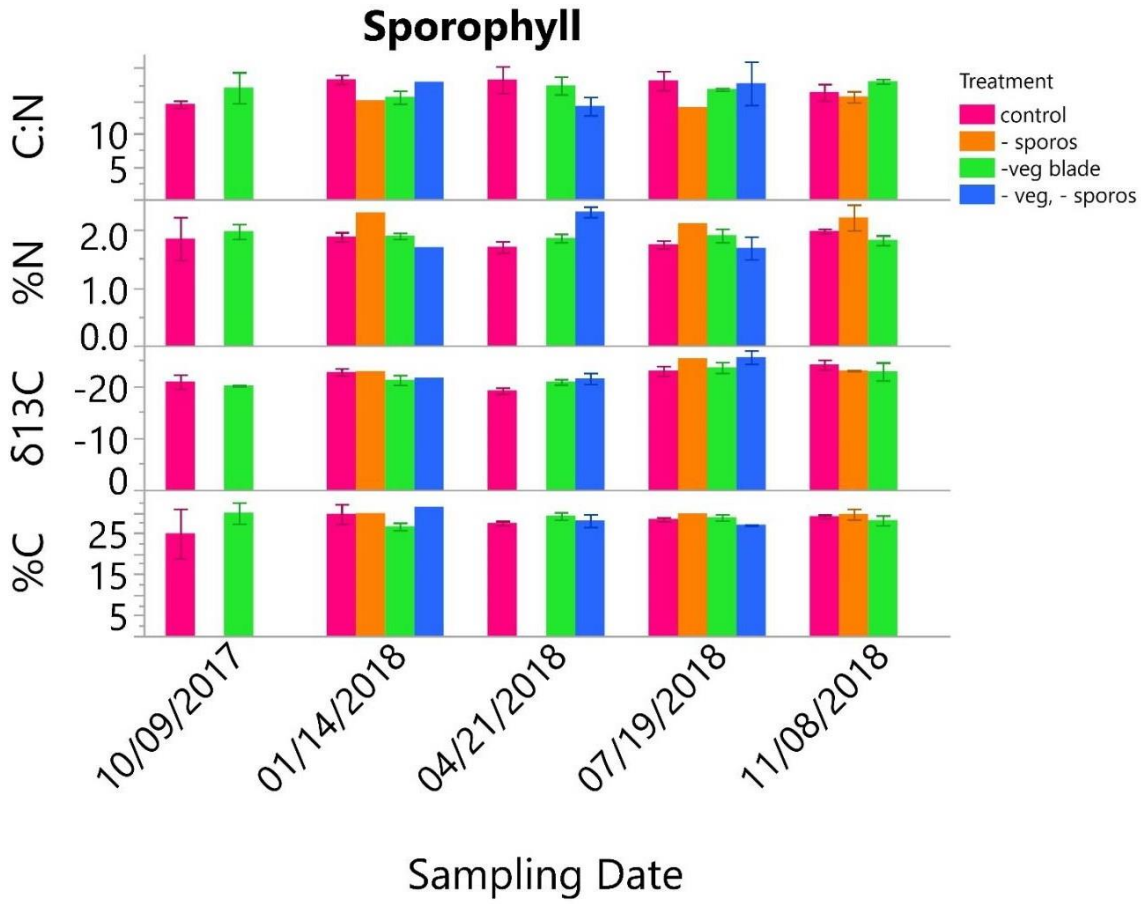

Figure B1: Mean %C, δ13C, %N, and C:N values for the "sporophyll" region among sampling dates and treatments. Sporophyll tissue was not present on harvested thalli from the minus sporophylls treatment on 10/9/2017 and 4/21/2018. It was also missing from the minus both treatment on 10/9/2017 and 11/8/2018. Bars with no standard error bars denote that there was one data point.

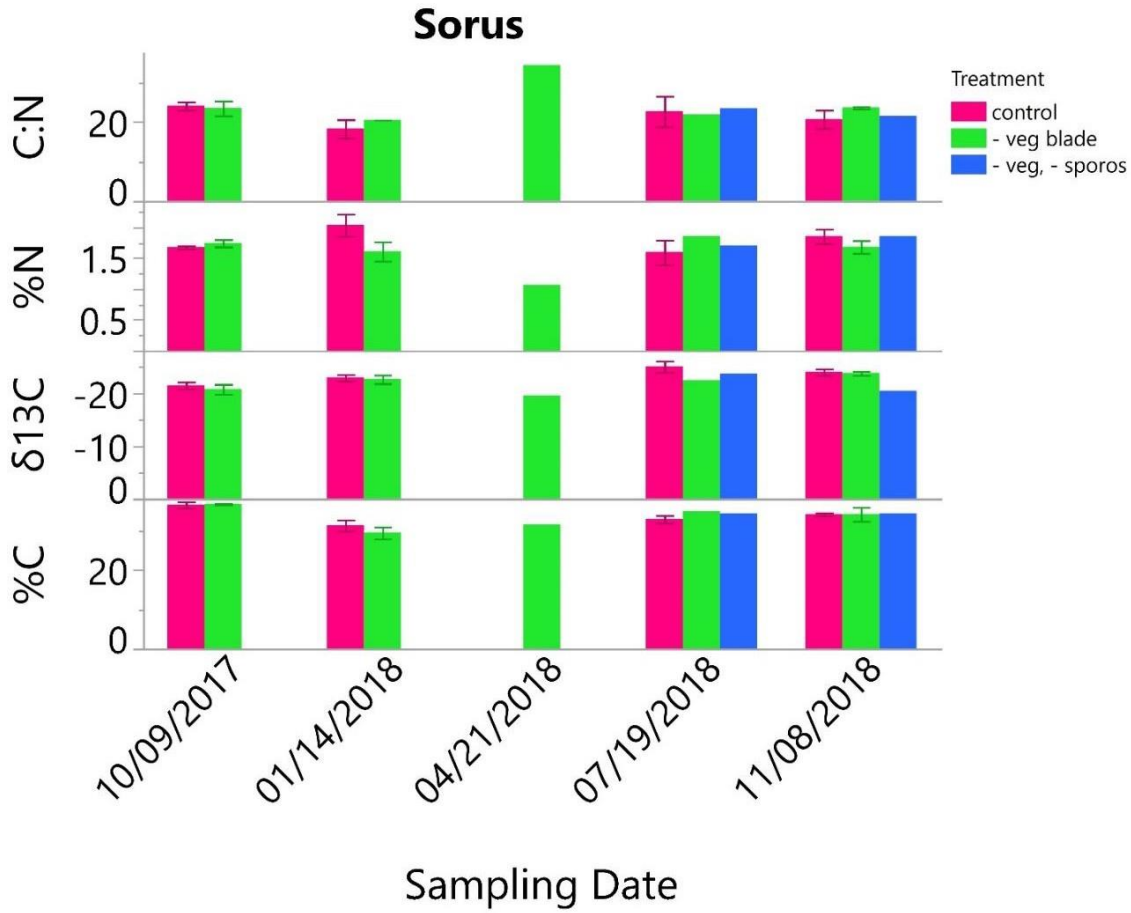

Figure B2: Mean %C, δ13C, %N, and C:N values for the "sorus" region across sampling dates and treatments. Soral tissue was not present on any harvested thalli from the minus sporophylls treatment for all dates. It was also missing from the control thalli on 4/21/2018, and from the minus both treatment on 10/9/2017, 1/14/2018, and 4/21/2018. Bars with no standard error bars denote that there was one data point.

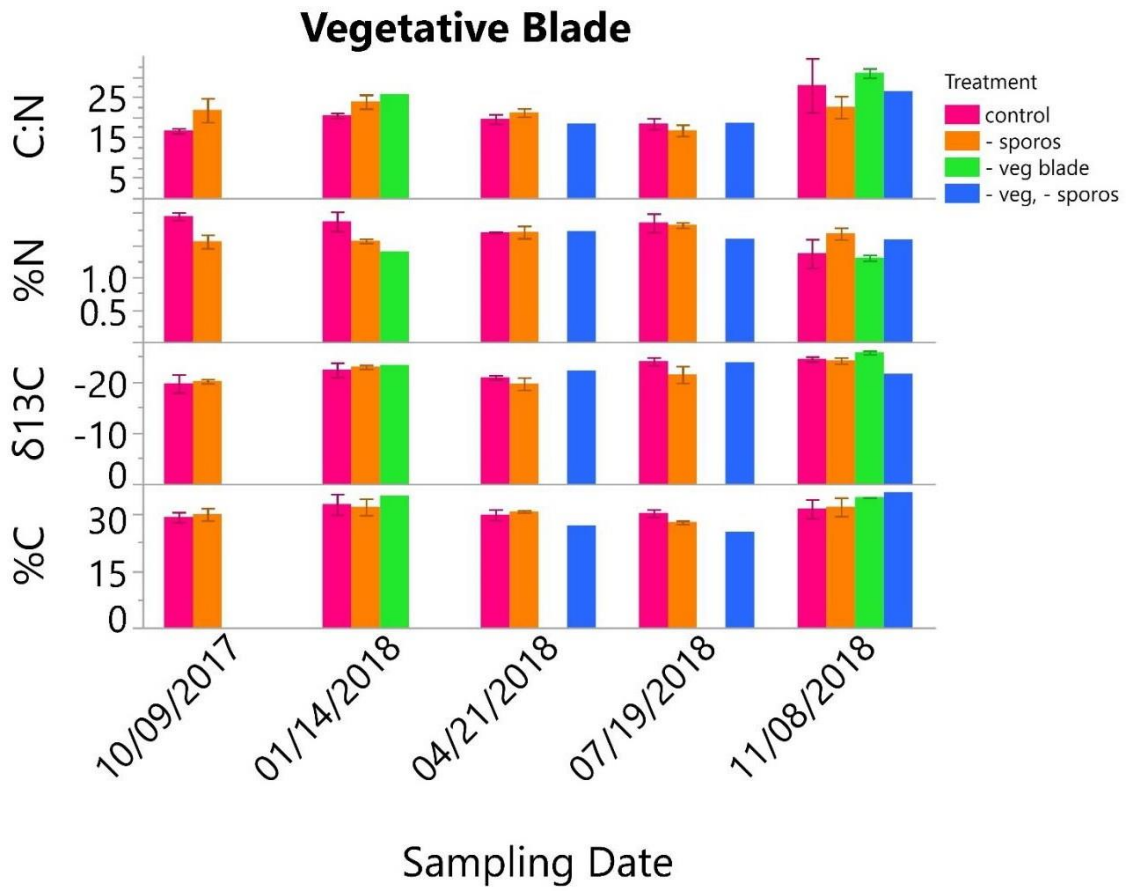

Figure B3: Mean %C, δ13C, %N, and C:N values for the "vegetative blade" region across sampling dates and treatments. Vegetative blade tissue was not present on any harvested thalli from the minus vegetative blade treatment on 10/9/2017, 4/21/2018, and 7/19/2018. It was also missing from thalli in the minus both treatment on 10/9/2017 and 1/14/2018. Bars with no standard error bars denote that there was one data point.